Aus der Klinik für Plastische, Ästhetische und Handchirurgie
der Medizinischen Fakultät
der Otto-von-Guericke-Universität Magdeburg

Untersuchungen zur Sphäroidbildung von Schilddrüsenkarzinomzellen in simulierter Mikrogravitation

Dissertation

zur Erlangung des Doktorgrades

Dr. rer. medic.

(doctor rerum medicarum)

an der Medizinischen Fakultät
der Otto-von-Guericke-Universität Magdeburg

vorgelegt von **Elisabeth Gerda Warnke**
aus **Schönebeck (Elbe)**
Magdeburg **2017**

Angefertigt von **Februar 2013 bis März 2017** in der Klinik für Plastische, Ästhetische und Handchirurgie, Arbeitsgruppe von Professor Daniela Grimm.

Klinikdirektor:	**Herr Professor Dr. med. Manfred Infanger**
Betreuer:	**Frau Professor Dr. med. Daniela Grimm**
	Frau Privatdozentin Dr. rer. nat. Ruth Hemmersbach
	Herr Professor Dr. med. Manfred Infanger

Bibliographische Beschreibung:

Warnke, Elisabeth:
Untersuchungen zur Sphäroidbildung von Schilddrüsenkarzinomzellen in simulierter Mikrogravitation – 2017. – 115 Bl., 4 Abb., 0 Tab., 5 Anlagen

Kurzreferat

Die Zellkulturtechnik ist eine wichtige Forschungsmethode im Bereich der Zellbiologie und Biomedizin. Wesentliche Unterschiede zwischen den Zellen *in vivo* und Zellen *in vitro* sind jedoch deren Wachstumsbedingungen. Während in Laboren Schilddrüsenzellen als adhärenter Zellrasen am Boden von Kulturflaschen wachsen, zeigen sie im Körper ein dreidimensionales (3D)-Wachstum. Bilden sich Tumore im Körper, so kann das Ablösen aus dem Zellverband in Form von multizellulären Aggregaten (z.B. Metastasen) beobachtet werden. Sphäroide gleichen Metastasen in hohem Maße, da auch sie ein 3D-Wachstum und das Ablösen als Zellaggregate unter Laborbedingungen zeigen. Eine Möglichkeit diese Sphäroide künstlich zu erzeugen ist die Nutzung von Bodenanlagen (Ground-based Facilities - GBF-Anlagen) zur Simulation von Mikrogravitation auf der Erde im Laboratorium. Dazu werden im Rahmen dieser Arbeit die Random Positioning Machine (RPM) und der zweidimensionale (2D)-Klinostat (CN) genutzt. Ein Vergleich beider Versuchsmethoden an der Zelllinie FTC-133 wurde in der Arbeit „*Thyroid cells exposed to simulated microgravity conditions – comparison of the fast rotating clionstat and the random positioning machine*“ publiziert. In der Veröffentlichung „*Common effects of cancer cells exerted by a random positioning machine and a 2D clinostat*“ wurden für die Zelllinien ML-1 und RO82-W-1 ebenfalls vergleichende Untersuchungen auf diesen Bodenanlagen vorgenommen. Mechanismen für die Bildung von Sphäroiden wurden in den Arbeiten „*Spheroid formation of human thyroid cancer cells under simulated microgravity: a possible role of CTGF and CAV1*“ und „*Cytokine release and focal adhesion proteins in normal thyroid cells cultured on the random positioning machine*” untersucht. Diese Studien wurden durch die European Space Agency (ESA) und durch das Deutsche Zentrum für Luft- und Raumfahrt (DLR) unterstützt.

Schlüsselwörter
Multizelluläre Sphäroide; Schilddrüsenzellen; Random Positioning Machine; 2D-Klinostat; simulierte Mikrogravitation; adhärentes Wachstum

Die vorliegende Doktorarbeit basiert auf den folgenden chronologisch aufgeführten Publikationen:

1) **Warnke E**, Pietsch J, Wehland M, Bauer J, Infanger M, Görög M, Hemmersbach R, Braun M, Ma X, Sahana J, Grimm D: Spheroid formation of human thyroid cancer cells under simulated microgravity: a possible role of CTGF and CAV1. Cell Commun. Signal. 12. 32 (2014)

2) Svejgaard B, Wehland M, Ma X, Kopp S, Sahana J, **Warnke E,** Aleshcheva G, Hemmersbach R, Hauslage J, Grosse J, Bauer J, Corydon TJ, Islam T, Infanger M, Grimm D: Common effects on cancer cells exerted by a random positioning machine and a 2D clinostat. PLoS One. 10. e0135157 (2015)

3) **Warnke E**, Kopp S, Wehland M, Hemmersbach R, Bauer J, Pietsch J, Infanger M, Grimm D: Thyroid cells exposed to simulated microgravity conditions – comparison of the fast rotating clinostat and the random positioning machine. Microgravity Sci. Technol. 28. 247-260 (2016)

4) **Warnke E,** Pietsch, J, Kopp S, Bauer J, Sahana J, Wehland M, Krüger M, Hemmersbach R, Infanger M, Lützenberg R, Grimm D: Cytokine release and focal adhesion proteins in normal thyroid cells cultured on the random positioning machine. Cell. Physiol. Biochem. 43. 257-270 (2017)

Die veröffentlichten Publikationstexte sind im Anhang dieser Dissertation aufgeführt.

Inhaltsverzeichnis

Abkürzungsverzeichnis

2D	Zweidimensional
3D	Dreidimensional
AD	Adhärente Zellen
ADS	Airbus Defense and Space
BDNF	Brain-derived neutrophic factor
CAV1	Caveolin-1 Gen
CCL2	Monocyte chemotactic protein-1 Gen
CN	Klinostat
CO_2	Kohlenstoffdioxid
CORA	Continuously Open Research Announcement
CTGF	Connective tissue growth factor
CTGF	Connective tissue growth factor Gen
CXCL8	Interleukin-8 Gen
d	Tag
DGLRM	Deutsche Gesellschaft für Luft- und Raumfahrtmedizin
DLR	Deutsches Zentrum für Luft- und Raumfahrt
DTC	Differenzierte Schilddrüsenkarzinome
ELISA	Enzyme-Linked Immunosorbent Assay
ESA	European Space Agency
F-Aktin	Filamentöses Aktin
FLUMIAS	Fluoreszenzmikroskopisches Analysesystem für biologische und biomedizinische Forschung im Weltraum
FN1	Fibronectin
FN1	Fibronectin Gen
FTC	Follikuläres Schilddrüsenkarzinom
g	Schwerkraft, Gravitation
GBF	Ground-Based Facilities, Bodenanlagen
GC-A	Guanylylzyklase A
GM-CSF	Granulocyte-macrophage colony-stimulating factor
h	Stunden
ICAM1	Intercellular adhesion molecule 1
IL	Interleukin
IL	Interleukin Gen
ISS	International Space Station
ITBG1	Integrin β_1 Gen

LAMA1	Laminin Gen
MAP	Multi-Analyte Profiling
MCP-1	Monocyte chemotactic protein-1
MCS	Multizelluläre Sphäroide
MeCoSa	Mentoring und Coaching Programm Sachsen-Anhalt
MIP	Macrophage inflammatory protein
MMP	Matrix metalloproteinase
NASA	National Aeronautics and Space Administration
PBS	Phosphate-buffered saline
PCR	Polymerase-Kettenreaktion
PFC	Parabelflugkampagne
PTC	Papilläre Schilddrüsenkarzinome
RBM	Rules-Based Medicine
r-µ*g*	Reale Mikrogravitation
RPM	Random Positioning Machine
rpm	Revolutions per minute, Umdrehungen pro Minute
RT-qPCR	Quantitative real time PCR
RWV	Rotating Wall Vessel
SCF	Stem cell factor
SD	Standard deviation
s-µ*g*	Simulierte Mikrogravitation
SV40	Simian Virus 40
Tg	Thyreoglobulin
TIMP-1	Tissue inhibitor of metalloproteinase
TIMP1	Tissue inhibitor of metalloproteinase Gen
TLN1	Talin-1 Gen
TSH	Thyreoidea-stimulierendes Hormon
VEGF	Vascular endothelial growth factor
VEGF	Vascular endothelial growth factor Gen
WB	Western Blot

1. Vorwort

Die vorliegende Arbeit wurde von Februar 2013 bis März 2017 am Universitätsklinikum, Klinik für Plastische, Ästhetische und Handchirurgie, der Otto-von-Guericke Universität Magdeburg in der Arbeitsgruppe von Frau Prof. Grimm Gravitationsbiologie und Translationale Regenerative Medizin angefertigt. Von Februar 2015 bis April 2016 wurde die Arbeit auf Grund von Mutterschutz und Elternzeit unterbrochen.

Die Experimente auf der RPM wurden in der Gruppe Weltraummedizin bei Frau Prof. Grimm am Institut für Biomedizin, Universität Aarhus, in Dänemark durchgeführt. Vorversuche auf dem Klinostaten fanden am Deutschen Zentrum für Luft- und Raumfahrt (DLR), Institut für Luft- und Raumfahrtmedizin, Köln in der Abteilung Gravitationsbiologie, geleitet von Frau PD Dr. Hemmersbach, statt. Durch die Teilnahme an der Helmholtz Space Life Science Research School des DLR im Institut für Luft- und Raumfahrtmedizin, dem Mentoring und Coaching Programm Sachsen-Anhalt (MeCoSa) sowie der Graduiertenschule der Otto-von-Guericke-Universität Magdeburg, konnten diverse interdisziplinäre Vorträge und Workshops wahrgenommen werden.

Betreuer der Doktorarbeit

Professor Dr. med. Daniela Grimm
Professorin für Weltraummedizin
Institut für Biomedizin, Pharmakologie, Universität Aarhus,
8000 Aarhus, Dänemark

und

Gastprofessorin für Gravitationsbiologie und Translationale Regenerative Medizin,
Universitätsklinikum Magdeburg, Otto-von-Guericke-Universität,
39112 Magdeburg, Deutschland

Professor Dr. med. Manfred Infanger
Leiter der Klinik für Plastische, Ästhetische und Handchirurgie
Universitätsklinik Magdeburg
39112 Magdeburg, Deutschland

Privatdozentin Dr. rer. nat. Ruth Hemmersbach
Stellvertretende Institutsdirektorin
Leiterin der Abteilung Gravitationsbiologie
Institut für Luft- und Raumfahrtmedizin
Deutsches Zentrum für Luft- und Raumfahrt (DLR)
Linder Höhe
51147 Köln, Deutschland

2. Preface

The present doctoral thesis was prepared from February 2013 until March 2017 at the University hospital, Clinic for Plastic, Aesthetic and Hand Surgery, of the Otto-von-Guericke University Magdeburg, in the group Gravitational Biology and Translational Regenerative Medicine of Prof. Grimm. The work was interrupted from February 2015 until April 2016 due to parental leave.

The experiments on the RPM were performed in the group Space Medicine of Prof. Grimm, Institute for Biomedicine, Aarhus University, Denmark. Preliminary tests on the clinostat were performed at the German Aerospace Center, Institute of Aerospace Medicine in the division Gravitational Biology of PD Dr. Hemmersbach. The participation in the Helmholtz Space Life Science Research School of the German Aerospace Center, the mentoring and coaching program of Saxony-Anhalt (MeCoSa) as well as the Graduate School of the Otto-von-Guericke University Magdeburg enabled participation in various interdisciplinary lectures and workshops.

Supervisors:

Professor Daniela Grimm, MD
Professor for Space Medicine
Institute for Biomedicine, Pharmacology, Aarhus University,
8000 Aarhus, Denmark

and

Guest Professor for Gravitational Biology and Translational Regenerative Medicine
Otto-von-Guericke-University,
39112 Magdeburg, Germany

Professor Manfred Infanger, MD
Director of the Clinic for Plastic, Aesthetic and Hand Surgery
University Hospital, Otto-von-Guericke-University Magdeburg,
39112 Magdeburg, Germany

PD Ruth Hemmersbach, PhD
Deputy director
Division head Gravitational Biology
Institute of Aerospace Medicine
German Aerospace Centre (DLR)
Linder Höhe
51147 Cologne, Germany

3. Zielsetzung

Die Arbeitsgruppe von Frau Prof. Grimm beschäftigt sich seit vielen Jahren mit Schilddrüsenzellen und dem Einfluss von realer und simulierter Mikrogravitation auf humane Zellen. Ein bedeutender Meilenstein dieser Forschung war die erste Weltraummission SimBox/Shenzhou-8 im Jahr 2011. Schilddrüsenkarzinomzellen waren für 10 Tage der realen Mikrogravitation (r-µ*g*) ausgesetzt und zeigten die eindeutige Bildung von Sphäroiden.

Das wesentliche Fundament der Weltraumforschung ist die Vorarbeit und die Validierung der Ergebnisse durch Versuche auf der Erde. In Bodenanlagen (GBF-Anlagen) sollen dabei Bedingungen, wie sie in r-µ*g* auftreten, simuliert werden. Der Ansatz, gezielt simulierte Mikrogravitation (s-µ*g*) für die Sphäroidbildung zu nutzen, ist eine wertvolle Ergänzung und in Zukunft möglicherweise eine Alternative zu Experimenten in r-µ*g*, die diverse Vorteile gegenüber herkömmlicher Methoden bieten. Diese werden in dieser Arbeit diskutiert.

Das Ziel dieser Dissertation ist es:
1. Die Eignung der beiden GBF-Anlagen (3D-RPM und 2D-Klinostat) für die Induktion der Bildung von Sphäroiden aus adhärent wachsenden Schilddrüsenzellen zu untersuchen und zu vergleichen.
2. Gene und Proteine zu identifizieren, die eine Rolle bei der Sphäroidbildung spielen.

Im Rahmen der vorliegenden Doktorarbeit soll die Hypothese geprüft werden, ob die Kultivierung von Schilddrüsenzellen sowohl auf der Random Positioning Maschine als auch auf dem Klinostaten zu Sphäroidbildung führt. Im Weiteren soll die Beteiligung der Interleukine IL-6 und IL-8, des Wachstumsfaktors CTGF und Caveolin-1 an der Sphäroidbildung untersucht werden.

4. Einleitender Textteil zum Stand der Forschung

Während der deutsch-chinesischen Raumfahrtmission SimBox/Shenzhou-8 wurden Schilddrüsenkarzinomzellen der Linie FTC-133 für 10 Tage (d) der realen Mikrogravitation ausgesetzt und unter diesen Bedingungen kultiviert (Pietsch *et al*. 2013, Ma *et al*. 2014). Nach Rückkehr und Analyse der Proben wurden in den Kulturkammern multizelluläre Aggregate, sogenannte multizelluläre Sphäroide (MCS) gefunden, welche sich neben der adhärent wachsenden Kultur gebildet hatten. Dieses Verhalten ist besonders interessant, da die besagte Zelllinie unter normalen Schwerkraftbedingungen (1*g*) auf der Erde nur ein adhärentes Wachstumsverhalten am Boden der Zellkulturflasche zeigt. Bereits in früheren Studien wurde diese besondere Eigenschaft auch für andere Zelllinien wie Chondrozyten beschrieben (Freed *et al*. 1997, Stamenkovic *et al.* 2010, Aleshcheva *et al.* 2013). Die genaue Ursache sowie die Mechanismen, welche für den Übergang von einem 2D- in ein 3D-Wachstum verantwortlich sind, blieben jedoch ungeklärt.
Das Auftreten von Sphäroiden konnte für FTC-133 Zellen in früheren Studien mittels der Bodenanlage RPM induziert werden (Grosse *et al.* 2012, Pietsch *et al.* 2011a), vergleichende Messungen mit anderen Simulationsmethoden existieren jedoch nicht. Eine nähere Betrachtung der verschiedenen Methoden zur Simulation von Mikrogravitation auf der Erde, die Bedeutung von Sphäroiden für die Medizin, sowie die Entscheidung für Schilddrüsenzellen als Modelsystem, werden in den nachfolgenden Punkten 4.1 bis 4.3. näher erläutert.

4.1 Bodenanlagen – Simulation von Schwerelosigkeit auf der Erde

Die Schwerkraft oder Gravitationskraft ist eine fundamentale Kraft unseres Universums. Sie beruht auf der gegenseitigen Anziehung von Massen, beispielsweise zwischen der Erde und einem beliebigen Objekt auf ihr.

Der Zustand „ohne mechanische Unterstützung der Masse“ wird als sogenannte „Mikrogravitation“ bezeichnet (Briegleb 1992, Herranz *et al.* 2013). So ist die Schwerkraft auf der Erde zwar allgegenwärtig, kurze Perioden realer Mikrogravitation in Form von „freiem Fall“ können dennoch durchaus erreicht werden. In Fallturmexperimenten können etwa 5 Sekunden r-µ*g* erreicht werden, in Parabelflügen befinden sich Experimentatoren und Experimente in 31 Parabeln für jeweils 22 Sekunden im „freien Fall“. Auf Höhenforschungsraketen können je nach Steighöhe 6 bis 12 Minuten Mikrogravitation erreicht werden. Gemeinsam sind all diesen Experimenten die Phasen in denen die Massen der Körper frei von mechanischer Unterstützung sind und somit frei im Raum schweben (Grimm *et al.* 2013).

Durch die Nutzung von Satelliten werden auch längere Phasen der r-µ*g* von 1 bis 3 Monaten, bei Experimenten auf Raumschiffen und Raumstationen wie der Internationalen Raumstation (ISS) oder der chinesischen Tiangong für mehrere Tage bis Monate oder gar Jahre möglich. Selbst auf einer „stillstehenden" ISS würde eine Erdanziehung von 90% der hier auf der Erde spürbaren Anziehungskraft auf Raumstation und Astronauten wirken. Erst durch das kontinuierliche „Fallen" um die Erde herum erfahren die Astronauten einen scheinbaren Zustand von Mikrogravitation. Man spricht von Mikrogravitation, wenn die absolute Summe aller massenabhängigen Beschleunigungen ein sehr kleines Hintergrundrauschen im Idealfall von etwa 10^{-5} bis 10^{-6}*g* nicht überschreitet (Herranz *et al.* 2013, Albrecht-Buehler 1992).

Das Ausmaß des Schwerkraftvektors auf der Erde kann nicht verändert werden, wohl aber sein Einfluss auf einen Modellorganismus (Briegleb 1992, Herranz *et al*. 2013). Genutzt werden dafür Bodenanlagen, die im Wesentlichen auf dem gleichen Grundsatz beruhen: einer Randomisierung, also Änderung, des Einflusses des Schwerkraftvektors durch Bewegung einer Probe um ein oder zwei Achsen.

Der 2D-Klinostat beruht auf dem Prinzip einer Zentrifuge, besitzt also nur eine Achse (Brown 1992). Geändert wurde hier die Rotationsachse, die nicht vertikal, sondern horizontal ausgerichtet wurde und somit im rechten Winkel zur Richtung des Schwerkraftvektors verläuft. In der Arbeit von Eiermann *et al.* 2013 wurde die Nutzung des 2D-Klinostaten für adhärente Zellen beschrieben. Bei einer Rotationsgeschwindigkeit von 60 rpm und einer maximalen Entfernung zur Achse von etwa 3 mm werden somit Schwerkraftqualitäten von ≤ 0,012 *g* erreicht (Eiermann *et al.* 2013).
Diese Versuchsbedingungen wurden für sämtliche Versuche dieser Arbeit übernommen. Das Prinzip der Simulation von Mikrogravitation wird in Abbildung 1 verdeutlicht.

Bei der RPM werden zwei unabhängig voneinander rotierende Rahmen genutzt und somit zwei Rotationsachsen erzeugt. Permanente Richtungsänderungen und eine Verteilung der Schwerkraftwirkung auf alle drei Raumachsen werden so ermöglicht (van Loon 2007). Ein Computerprogramm steuert dabei die maximal zufällige Bewegung der zwei Rahmen. Durch eine maximale Entfernung von 7 cm zum Drehzentrum wird eine Beschleunigung von 10^{-4} bis 10^{-2} *g* bei 60°/sec erreicht (van Loon 2007). Die beschriebenen Arbeitsbedingungen von 60°/sec, zufällige Richtungsänderungen beider Rahmen und eine maximale Entfernung der Proben von 7 cm vom Drehzentrum wurden ebenfalls in allen vorgelegten Arbeiten übernommen.

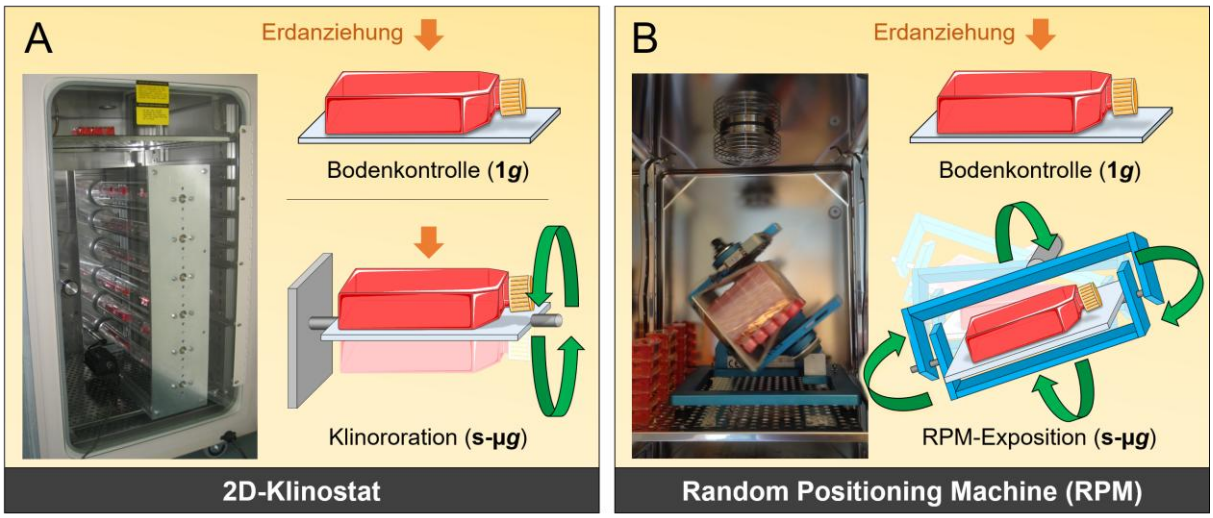

Abb. 1: Verdeutlichung des Prinzips der simulierten Mikrogravitation
A: 2D-Klinostat (DLR Köln, Deutschland) im Inkubator mit zeitgleich angesetzten Bodenkontrollen auf dem Zwischenboden, oben im Bild. Schematische Darstellung der Wirkung der Schwerkraft auf die Kulturflasche. Die statischen Bodenkontrollen (1*g*) sind der konstanten Wirkung der Schwerkraft in eine Richtung ausgesetzt. Proben auf dem 2D-Klinostaten werden permanent und konstant um die horizontale Achse rotiert. Die Richtung des Schwerkraftvektors in Bezug zum Flaschenboden ändert sich somit kontinuierlich.
B: Random Positioning Machine (RPM, Airbus Defense and Space, früher Dutch Space, Niederlande) im Inkubator mit parallel angesetzten Bodenkontrollen, links im Bild. Die Proben werden permanent und zufällig um zwei Achsen rotiert, permanente Richtungsänderungen finden statt. Die Richtung des Schwerkraftvektors im Verhältnis zum Flaschenboden ist somit gänzlich zufällig und über alle Richtungen verteilt.

Neben der Klinorotation und der Random Rotation auf der RPM gibt es weitere Möglichkeiten zur Simulation von Mikrogravitation, die zur Vollständigkeit kurz erwähnt werden sollen. Die Rotating Wall Vessel (RWV) und auch die Diamagnetische Levitation werden zusätzlich in einem vergleichenden Review von Herranz *et al.* 2013 näher betrachtet. Die RWV beruht ebenfalls auf einer Randomisierung des Schwerkraftvektors und wurde ursprünglich von der National Aeronautics and Space Administration (NASA) entwickelt. Zellen in Suspension oder auf Mikroträgern befinden sich dabei in stetigem „freien Fall“, da das kreisförmige Kulturgefäß im 90° Winkel zum Schwerkraftvektor rotiert wird (Schwarz *et al.* 1992). Die Sedimentation kann somit verhindert werden. Für meine Versuche mit adhärenten Zellen (AD) erschien die RWV nur bedingt geeignet. Bei Experimenten mit AD müssten Mikroträgerperlen verwendet werden, auf denen die Zellen zunächst anwachsen müssten, um ihnen dann den „freien Fall“ im Medium zu ermöglichen, oder die Zellen wären adhärent am Kulturgefäß angewachsen und dann gedreht worden, was wiederum zu einem erhöhten Abstand zur Rotationsachse geführt und somit erhöhte Scherkräfte zur Folge gehabt hätte. Insgesamt erschien diese Methode somit wenig geeignet und wurde folglich nicht eingesetzt.

Bei der Diamagnetischen Levitation wird der Schwerkraft ein Magnetfeld entgegengesetzt, das die Zellen zwar in der Schwebe hält, wiederum aber einen starken Einfluss auf die Zellen zeigt (Hemmersbach *et al.* 2014). In Mausfibroblasten C3H10T1/2 wurden beim Anlegen eines

Magnetfeldes mit und ohne Levitation, Veränderungen des Zytoskeletts festgestellt, die demzufolge nicht auf eine Änderung des Schwerkrafteinflusses zurückgeführt werden konnten, sondern als Nebenwirkungen des Magnetfeldes einzustufen waren (Herranz *et al.* 2013). Darüber hinaus wird auch in den Arbeiten von Maret und Dransfeld 1985 beschrieben, dass verschiedene Biomoleküle wie Tubulin, Aktin und auch DNA in Lösungen durch starke magnetische Felder ausgerichtet werden können. Aufgrund der Kritikpunkte wurde diese Methode für das gewählte Modellsystem, humane Schilddrüsenzellen, als wenig geeignet eingestuft.

Für adhärente Zellen bleiben somit CN und RPM als Mittel der Wahl zur Simulation von Mikrogravitation bestehen. Nebeneffekte wie Zentrifugalbeschleunigungen, Scherkräfte und Vibrationen sollten bei der Ernte und Interpretation der Ergebnisse berücksichtigt werden (Herranz *et al.* 2013). Abschließend ist zu sagen, dass Bodenanlagen eine kontinuierliche Forschung, allein stehende Studien, aber auch die kosteneffiziente Vorbereitung von Raumflügen ermöglichen. Sie können daher eine wertvolle Ergänzung bieten, jedoch nicht als Ersatz für Forschung unter realer Mikrogravitation gesehen werden (Herranz *et al.* 2013).

Darüber hinaus haben die letzten Jahrzehnte der Forschung gezeigt, dass Zellwachstum sowohl unter realer als auch unter simulierter Mikrogravitation biologische Prozesse beeinflusst, die möglicherweise auch für die Krebsforschung von entscheidender Bedeutung sein können (Becker und Souza 2013). Auf molekularer Ebene konnten Veränderungen der Protein- und Genexpression, erhöhte Apoptose, verlangsamtes Zellwachstum sowie Veränderungen im Zytoskelett und die Ausbildung von Sphäroiden in Schilddrüsenzellen beobachtet werden (Svejgaard *et al.* 2015, Pietsch *et al.* 2011b, Grimm *et al.* 2002).

4.2 Sphäroidbildung – Methoden und Bedeutung in der Medizin

In der herkömmlichen Zellkultur wachsen die meisten Zelllinien adhärent als Monolayer am Flaschenboden und besitzen daher weniger Zell-Zellkontakte (Becker und Souza 2013). Schon auf Grund dieser Tatsache zeigen sie nicht vollständig die charakteristischen Merkmale eines soliden 3D-Tumors (Santini und Rainaldi 1999). Zu diesem Zweck wurden verschiedene Methoden zur Erzeugung von multizellulären Sphäroiden (MCS) entwickelt. Diese stellen ein intermediäres Modell zwischen 2D-Kultur und *in vivo* Tumoren dar. Die Kultur von MCS bietet daher eine deutlich bessere Möglichkeit für Studien zur Untersuchung von Metastasen, Gefäßneubildungen in Tumoren und pharmazeutischen Tests (Grimm *et al.* 2014, Becker und Souza 2013).

Die grundlegende Fähigkeit von diversen Zelllinien, 3D-Tumorsphäroide zu bilden, wurde von Santini und Rainaldi 1999 beschrieben. Die Autoren weisen darauf hin, das sich die Zeitdauer und die erreichbare Größe zwischen verschiedenen Zelllinien stark unterscheiden kann. Diese Beobachtungen

stimmen mit unseren Erfahrungen an Schilddrüsenzellen überein. Während maligne FTC-133 Schilddrüsenkarzinomzellen dazu neigen sehr schnell große Sphäroide (bis zu 200 µm im Durchmesser nach 7 d) zu bilden, wurde für benigne Nthy-ori 3-1 Schilddrüsenzellen ein eher verhaltenes Wachstum beobachtet (≤ 100 µm im Durchmesser nach 7d) (Kopp *et al.* 2015).

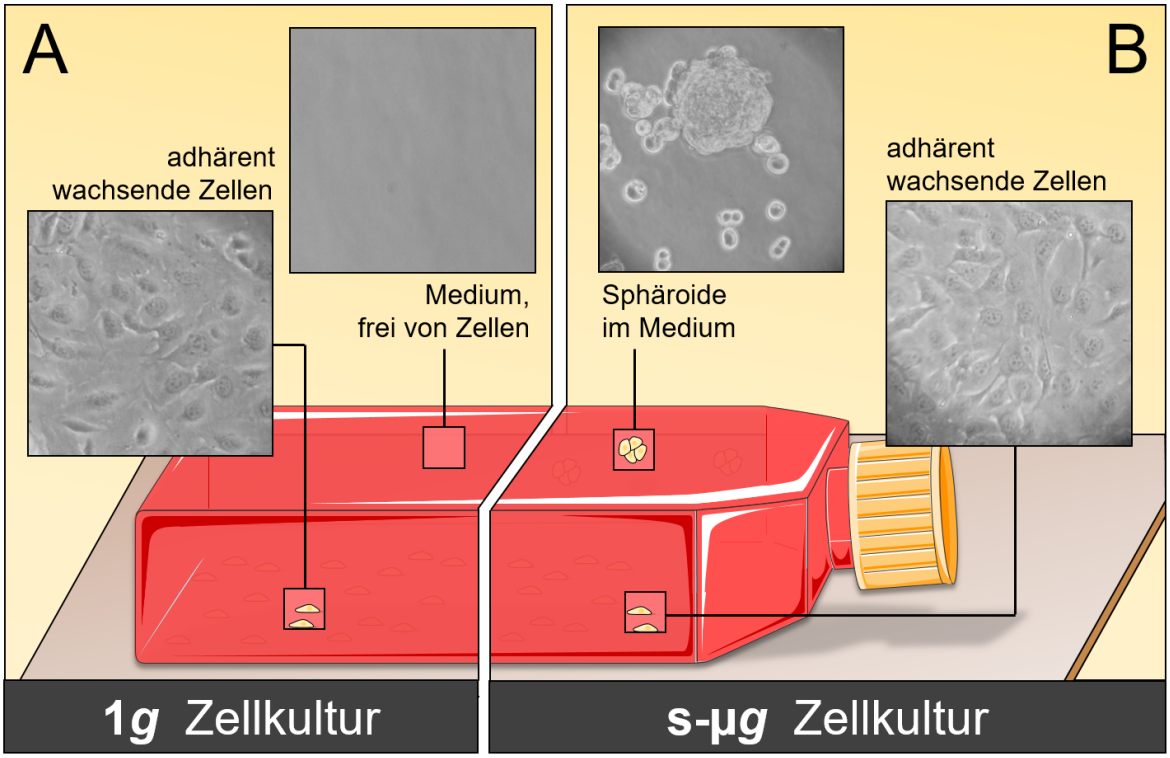

Abb. 2: **Zellwachstum bei 1*g* Bedingungen und unter simulierter Mikrogravitation (s-µ*g*)** erzeugt durch permanente Klinorotation. Gezeigt sind humane Schilddrüsenkarzinomzellen FTC-133. **A:** Unter 1*g* Bedingungen sind adhärent am Boden der Kulturflasche wachsende Zellen zu sehen. Das Medium ist frei von Zellen. **B:** Werden Zellen während des Wachstums durch permanente Klinorotation einer Randomisierung des Schwerkrafteinflusses ausgesetzt, spricht man von simulierter Mikrogravitation (s-µ*g*). Dabei wird angenommen, dass sich Betrag und Richtung des Gravitationsvektors für das Modellsystem über die Zeit zu annähernd Null mitteln. Nach 24 h sind sowohl adhärent am Kulturflaschenboden wachsende Zellen, als auch im Medium frei schwebende Zellaggregate, so genannte Sphäroide (MCS), erkennbar.

Verschiedene Ansätze stehen für die Erzeugung von MCS zur Verfügung. Bei der weit verbreiteten Liquid-Overlay-Technik wird eine definierte Menge an Einzelzellen auf eine nicht-adhäsive Oberfläche pipettiert. Ein Beispiel ist eine mit Agarose beschichtete 96-Wellplatte oder eine normale Kulturflasche mit einem Überzug aus Agar oder Agarose (Santini and Rainaldi 1999, Carlsson und Yuhas 1984). Da die Zellen so nicht anwachsen können, formen sie Zellaggregate. Einzelne Zellen und unregelmäßig geformte Aggregate werden entsorgt und lediglich gleichmäßige, runde Zellaggregate werden umgesetzt und auf frisch überzogenen Agaroseplatten weiter gezüchtet (Santini and Rainaldi 1999). Ein wesentlicher Nachteil dieser Methode ist der direkte Kontakt der Zellen mit der Agarose, der zu einer Veränderung der Oberflächeneigenschaften führen kann. Darüber hinaus kann keine Umwandlung von 2D- in 3D-Wachstum untersucht werden, da vornehmlich adhärent

wachsende Zellen in Suspension eingesetzt werden müssen. Eindeutiger Vorteil dieser Methode ist der geringe Materialaufwand und die gute Vergleichbarkeit der Sphäroide durch den Einsatz einer definierten Zellzahl für jedes Sphäroid. Aus diesem Grund wurde auch die Liquid-Overlay-Technik für die nähere Untersuchung des Einflusses der Interleukine IL-6 und IL-8 auf die Sphäroidbildung genutzt. Die Ergebnisse sind in Svejgaard *et al.* 2015 bzw. im Punkt 5.2 näher beschrieben.
Bei der Spinner flask-Technik wird ein Magnetrührer eingesetzt. Die Zellen werden dafür in einer Phase des exponentiellen Wachstums mithilfe von Trypsin in eine Einzelzellsuspension überführt. Eine definierte Zellzahl wird in das Medium in der Spinner flask gegeben. Durch das permanente Rühren mit etwa 190 rpm wird ein Anheften der Zellen verhindert und Aggregate werden geformt (Sutherland und Duran 1984*).* Bei dieser Technik ist ebenfalls von Nachteil, dass adhärent wachsende Zellen durch das Trypsinieren abgelöst und als Suspension in die Spinner flask pipettiert werden und somit kein Übergang vom 2D- in das 3D-Wachstum beobachtet werden kann. Darüber hinaus unterliegen die Zellen einem ständigen mechanischen Reiz durch den Rührer, was als zusätzlicher Zellstress die Ergebnisse beeinflusst.

Bei der Hanging Drop-Technik wird ein Tropfen des Zellkulturmediums mit einer definierten Zellzahl an der inneren Oberseite eines Zellkulturgefäßes aufgetragen. Im unteren Teil des Gefäßes befindet sich PBS um eine ausreichende Feuchtigkeit im Gefäß zu gewährleisten und das Austrocknen der Tropfen zu verhindern. Die Zellen sedimentieren auf dem Boden des Tropfens und bilden Sphäroide aus (Foty 2011). Klarer Vorteil dieser Methode ist, dass nur Medium und keine künstlichen Oberflächen oder Ähnliches zum Ausbilden der Zellen benötigt werden. Die Zellen sind somit keinem zusätzlichen Stress durch Rührbewegungen ausgesetzt. Ein Nachteil ist auch hier, dass die Zellen zuvor trypsiniert werden müssen, um sie in Form einer Suspension einsetzen zu können. Somit kann hier ebenfalls kein Übergang zwischen den Wachstumsformen beobachtet werden.

Um den tatsächlichen Übergang aus einem 2D-wachsenden Zellphänotyp zu einem dreidimensionalen MCS Phänotyp zu induzieren, bieten sich simulierte Mikrogravitation mit Hilfe der Random Positioning Machine oder dem Klinostaten an (Abb. 2 und 3, Kapitel 4.1). Zeitverläufe und Dokumentationen zum Sphäroidwachstum sind in Abb.4 Kapitel 5.2 gezeigt.

4.3 Schilddrüse – gesunde Zellen und das Karzinom

Die Schilddrüse ist die größte endokrine Drüse des menschlichen Körpers (Heinrich *et al*. 2014). Das Schilddrüsenkarzinom ist allerdings auch der am meisten verbreitete endokrine Tumor (Agate *et al.* 2012). Hierbei ist zu erwähnen, dass das papilläre Schilddrüsenkarzinom (PTC) und das follikuläre Schilddrüsenkarzinom (FTC) als differenzierte Schilddrüsenkarzinome (DTC) klassifiziert werden (Liao und Shindo 2012). Die DTC machen etwa 90% der Schilddrüsentumorerkrankungen aus und

haben bei entsprechender Behandlung eine exzellente Prognose (Sherman 2003, Schmidbauer *et al.* 2017). Die 10-Jahres Überlebensrate liegt beim minimal invasiven FTC bei 80-90% (O‘ Neill *et al.* 2010, Grosse *et al.* 2013).

Die Behandlung der DTC umfasst die teilweise oder vollständige Thyroidektomie, also eine operative Entfernung der Schilddrüse, sowie Radiojodtherapien. Bei unzureichender Radiojodaufnahme oder dem erneuten postoperativen Auftreten von Tumoren, ist die Bestrahlung induziert. Schreitet der Tumor trotz Radiojodtherapie fort, ist dies häufig in einer zunehmenden Dedifferenzierung begründet und verschlechtert damit die 10-Jahres Überlebensrate erheblich auf weniger als 15 % (Durante *et al.* 2006, Grosse *et al.* 2013). Der Einsatz üblicher Zytostatika zeigt bei diesen Arten von dedifferenzierten Schilddrüsentumoren eine sehr geringe Resonanz von 0-22% bei gleichzeitig hoher Toxizität (Baudine und Schlumberger 2007, Grosse *et al.* 2013).

Für die vorliegende Arbeit wurden sowohl Zellen aus gesundem Schilddrüsengewebe (Nthy-ori 3-1, HTU-5) als auch aus malignem Karzinomen (FTC-133, ML-1, RO82-W-1) untersucht, um ein möglichst umfassendes Bild zu erzeugen, und allgemeingültige Effekte aufdecken zu können.
Die Zelllinie Nthy-ori 3-1 stammt von einer 35-jährigen weiblichen Patientin. Es handelt sich um gesunde Schilddrüsenfollikelepithelzellen mit einem Plasmid mit SV Genom zur Immortalisierung (Lemoine *et al.* 1989). Sie zeigen keine Kanzerogenität im Mausmodell. Normale Schilddrüsenepithelfunktionen wie Jodaufnahme und Thyreoglobulinproduktion sind weiterhin vorhanden (Lemoine *et al*. 1989).
Die HTU-5 Zelllinie stammt ebenfalls von gesundem follikulären Schilddrüsengewebe eines Organspenders. Die Zellen produzieren weiterhin Thyreoglobulin (Curcio *et al.* 1994).
Aus einer Lymphknotenmetastase eines 42-jährigen männlichen Patienten entstammt die Zelllinie FTC-133 (Goretzki *et al.* 1990). Sie wird als niedrigdifferenzierte follikuläre Schilddrüsenkarzinomzelllinie eingestuft. Die Zellen zeigen Immunreaktivität gegenüber Thyreoglobulin und dem Thyreotropin bzw. Thyreoidea-stimulierendes Hormon (TSH) (Goretzki *et al.* 1990).
Aus einem dedifferenzierten follikulären Schilddrüsenkarzinomrezidiv einer 50-jährigen weiblichen Patientin (Schönberger *et al.* 2000) entstammt die Zelllinie ML-1. Trotz operativer Entfernung der Schilddrüse (Thyreoidektomie) und zweifacher Radiojodtherapie, traten erneut Tumore auf. Die Zelllinie ML-1 zeigt Tumorigenität im Mausmodell und die Produktion von Thyreoglobulin, Thyroxin und Tryiiodthyronin (Schönberger *et al.* 2000).
Aus der Metastase eines follikulären Karzinoms einer weiblichen Patientin stammt die RO82-W-1 Zelllinie. Die Zellen zeigen Tumorigenität im Mausmodell und sind weiterhin in der Lage Thyreoglobulin zu synthetisieren (Estour *et al.* 1989)

Die Studien mit gesunden und malignen Schilddrüsenzellen sind in der Arbeitsgruppe von Frau Prof. Grimm sehr gut etabliert. Diverse Vorstudien standen als Grundlage für diese Arbeit zur Verfügung. Als Vergleichsdaten konnte auf Experimente zum zellulären Verhalten unter Hypergravitation oder Vibration und über Zellversuche unter realer Schwerelosigkeit zurück gegriffen werden (Pietsch *et al.* 2013, Ma *et al.* 2013, Wehland *et al.* 2016), was eine Einordnung und Bewertung der Daten deutlich erleichterte.

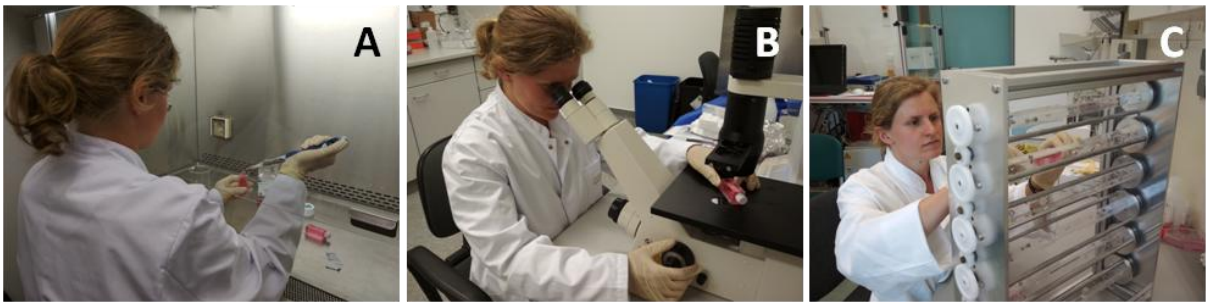

Abb. 3: Arbeit in der Zellkultur
A: Luftblasenfreies Füllen der Flasketten für Versuche auf dem Klinostaten (CN)
B: Überprüfung des adhärenten Anwachsens der Zellen am Flaskettenboden
C: Befestigung der Flasketten auf dem Klinostaten (DLR, Köln Deutschland)

5. Ergebnisse und Diskussion der zugrundeliegenden Publikationen

Die Daten der vorliegenden Doktorarbeit habe ich in drei Publikationen als Erstautorin (Warnke *et al.* 2014, Warnke *et al.* 2016 und Warnke *et al.* 2017) publiziert. Darüber hinaus war ich Mitautorin an der Publikation von Svejgaard *et al.* 2015. In den folgenden vier Abschnitten 5.1. bis 5.4. wird auf die genutzten Untersuchungsmethoden eingegangen und die wichtigsten Ergebnisse der Originalarbeiten zusammengefasst und diskutiert.

5.1 Sphäroidbildung von humanen Schilddrüsenkarzinomzellen in simulierter Mikrogravitation: eine mögliche Rolle von CTGF und CAV1

Die Bildung von Schilddrüsentumorzellsphäroiden durch Kultivierung der Zellen auf der RPM ist bereits seit längerem bekannt (Grosse *et al.* 2012) und erscheint zunächst vergleichbar mit dem Entstehen von Sphäroiden unter realer Mikrogravitation. Es fehlten jedoch vergleichende Studien auf anderen GBF-Anlagen, um diese Ergebnisse zu belegen. Zu diesem Zweck wurde die humane Schilddrüsenkarzinomzelllinie FTC-133 für 4 h, 24 h und 3 d sowohl auf dem CN als auch auf der RPM kultiviert und die Ergebnisse untereinander sowie mit korrespondierenden 1*g* Kontrollen verglichen. Als Untersuchungsmethoden wurden die Phasenkontrastmikroskopie zur Bestimmung eines eventuellen Auftretens von Sphäroiden, die quantitative real time Polymerase-Kettenreaktion

(RT-qPCR) zur Ermittlung von Änderungen der Genexpression sowie die Multi-Analyte Profiling (MAP) Technologie zur Untersuchung des Zytokingehalts der gewonnenen Zellüberstände genutzt. Die Ergebnisse sind in der Publikation „***Warnke E, Pietsch J, Wehland M, Bauer J, Infanger M, Görög M, Hemmersbach R, Braun M, Ma X, Sahana J, Grimm D: Spheroid formation of human thyroid cancer cells under simulated microgravity: a possible role of CTGF and CAV1. Cell Commun Signal. 12. 32 (2014)“*** veröffentlicht worden.

Die Bildung von Sphäroiden konnte innerhalb von 3 d sowohl in den auf dem CN als auch auf der RPM kultivierten Proben beobachtet werden, wobei weiterhin ein Teil der Zellpopulation ein adhärentes Wachstum am Flaschenboden zeigte. Parallel dazu gezüchtete Bodenkontrollen (1*g*), welche stets im gleichen Inkubator wie die GBF-Anlagen gelagert waren, zeigten ein ausschließlich adhärentes Wachstum am Boden des Kulturgefäßes. Rein morphologisch haben also beide GBF-Anlagen die gleiche Auswirkung auf das Zellwachstum und induzieren die Bildung von Sphäroiden.

Auf Grundlage früherer Studien (Grosse *et al.* 2012) wurden anschließend diverse Zielgene mit Hilfe der RT-qPCR untersucht. Die ausgewählten Gene kodieren für verschiedene biologische Bereiche wie das Zytoskelett, Wachstumsfaktoren, Apoptose, Angiogenese und Signaltransduktion, welche möglicherweise mit der Bildung von Sphäroiden in Verbindung stehen können (Grosse *et al.* 2012).
Als vielversprechender Ansatz zeigte sich hier der Connective Tissue Growth Factor (CTGF). Bereits nach 4 h konnte eine signifikant erhöhte *CTGF*-Expression in adhärenten Zellen für beide GBF-Anlagen im Vergleich zur entsprechenden 1*g* Kontrolle beobachtet werden. Die Tendenz blieb auch nach 3 Tagen bestehen, wobei hier interessanterweise in den MCS Proben eine signifikante Verringerung zu beobachten war. Eine Überexpression von *CTGF* wurde in papillären Schilddrüsenkarzinomen beschrieben und korrelierte dort mit Metastasierung und Größe des Karzinoms (Cui *et al.* 2011).
Auch für das Caveolin-1 Gen (*CAV1*) konnte ein ähnliches Expressionsverhalten auf beiden GBF-Anlagen beobachtet werden. Zwar zeigte sich für die AD Zellen keine Änderung, bei den MCS war ebenfalls nach 3 d eine signifikant verringerte Expression von *CAV1* sowohl bei CN als auch bei RPM Proben auffällig. Das integrale Membranprotein Caveolin-1 ist wesentlich an der Regulierung der Zellproliferation, Differenzierung und Apoptose beteiligt (Mo *et al.* 2011). Darüber hinaus ist die Verringerung von Caveolin-1 für die Fähigkeit von Zellen sich in Gewebe zu integrieren verantwortlich (Lu *et al.* 2003). Insgesamt zeigten die meisten Gene ein unterschiedliches Expressionsverhalten, abhängig von der gewählten GBF-Anlage.

Im nächsten Schritt wurde die Sekretion von Zytokinen und Wachstumsfaktoren der Tumorzellen in den Zellüberstand durch MAP-Analysen gemessen. Diese Untersuchungen wurden von der Firma Myriad-Rouldes Based Medicine (RBM) in Austin, TX, USA durchgeführt. Das Ergebnis war

überraschend. Lediglich die Tendenz der Zellen vermehrt Eotaxin-1 und weniger Vascular endothelial growth factor (VEGF) zu sezernieren wurde für beide GBF-Anlagen übereinstimmend festgestellt. Im Vergleich zu den 1*g* Kontrollen wurden jedoch in den RPM Proben nach3 d signifikant höhere Werte für Granulocyte-macrophage colony-stimulating factor (GM-CSF), Interleukin-(IL-) 6, IL-8, Brain-derived neutrophic factor (BDNF), Eotaxin-1, Intercellular adhesion molecule 1 **(**ICAM1), IL-1α, IL-1β, IL-1Ra, IL-12p40, IL-15, IL-17, IL-23, Matrix metalloproteinase 3 (MMP-3) und Stem cell factor (SCF) gefunden.
Proben, die auf dem CN kultiviert wurden, zeigten im Überstand hingegen signifikant geringere Werte für GM-CSF, IL-6, IL-8, Macrophage inflammatory protein (MIP)-1α, MIP-1β und BDNF als in ihren korrespondierenden 1*g* Kontrollen.
Das Ergebnis zeigt, dass zwar beide GBF-Anlagen in der Lage sind, ein Sphäroidwachstum bei FTC-133 Zellen zu induzieren, es aber offensichtlich bei der Zytokinsekretion der Zellen zu deutlichen Unterschieden kommt. Dies unterstreicht erneut die Bedeutung von Vergleichsstudien, sowie die Notwendigkeit, die Ergebnisse mit Daten aus realer Mikrogravitation zu vergleichen. Dabei sollten Zeitrahmen, verwendete Hardware und Prozeduren angeglichen werden, um einen Einfluss von externen Faktoren auf das Ergebnis zu minimieren.

Bereits kleine Unterschiede können enorme Auswirkungen haben. Dies zeigt die Arbeit von Eiermann *et al.* 2013. Die Autoren beschreiben in ihrer Veröffentlichung, dass im Klinostaten bei 60 rpm Restbeschleunigungen von 0,012*g* im Bereich von ±3 mm um die Rotationsachse herrschen und bis zu 0.036*g* in ±9 mm Entfernung. Bei ihren Untersuchungen zur Expression von Guanylylzyklase A (GC-A) in gering metastasenbildenden humanen 1F6 Melanomzellen zeigten sich signifikante Expressionsunterschiede zwischen Zellen, die aus den jeweiligen Bereichen der Flaskette geerntet wurden. Die Gegenwart von funktionellen natriuretischen peptidsensitiven membrangebundenen GC-Isoformen in Melanomzellen wurde in früheren Studien bereits mit der Bildung von Metastasen in Verbindung gebracht (Ivanova *et al.* 2001, Kong *et al*. 2008, Eiermann *et al*. 2013).

Während sich die adhärenten Zellen bei der Ernte aus CN Proben für die RT-qPCR relativ leicht separieren lassen, können die Überstände nur für das gesamte Kulturgefäß geerntet werden, was wiederum bei der Betrachtung der Ergebnisse der MAP Analyse berücksichtigt werden muss.

Insgesamt zeigt diese erste Studie auf Grund der unterschiedlichen Ergebnisse, die bei CN- und RPM-Kulturen erzielt wurden, die Notwenigkeit von vergleichenden Studien mit unterschiedlichen GBF-Anlagen. Grundsätzlich sind sowohl CN als auch RPM geeignet, um die Bildung von Sphäroiden zu induzieren. Zur Untersuchung des Übergangs von 2D-Wachstum in 3D-Wachstum bieten somit beide Tools einen wertvollen Ansatz. Gerätespezifische Einflüsse müssen jedoch stets berücksichtigt werden. Eine genauere Betrachtung möglicher gerätespezifischer Unterschiede wird in Kapitel 5.3 diskutiert.

5.2 Kultivierung auf der Random Positioning Maschine und dem 2D-Klinostaten: Gemeinsame Auswirkungen auf Karzinomzellen

Es handelt es sich bei den untersuchten Zelllinien ML-1 und RO82-W-1 um humane niedrig differenzierte follikuläre Schilddrüsenkarzinomzellen. Biologische Veränderungen nach jeweils drei und sieben Tagen Kultivierung im CN oder in der RPM wurden in der Publikation „***Svejgaard B, Wehland M, Ma X, Kopp S, Sahana J, Warnke E, Aleshcheva G, Hemmersbach R, Hauslage J, Grosse J, Bauer J, Corydon TJ, Islam T, Infanger M, Grimm D: Common effects on cancer cells exerted by a random positioning machine and a 2D clinostat. PLoS One. 10:e0135157 (2015)*** veröffentlicht. Als Untersuchungsmethoden wurden Phasenkontrastmikroskopie, Western Blot Analyse, F-Aktinfärbung sowie Zytokinmessung mittels MAP und Enzyme-linked Immunosorbent Assay (ELISA) vorgenommen. Darüber hinaus wurden Sphäroide beider Zelllinien mit Hilfe der Liquid-Overlay-Technik gezüchtet, um die Effekte einer zusätzlichen IL-6 und IL-8 Applikation zu untersuchen.

Auch bei den Schilddrüsentumorzelllinien ML-1 und RO82-W-1 konnten bereits nach dreitägiger Kultivierung, sowohl im CN als auch in der RPM die Bildung von multizellulären Sphäroiden beobachtet werden. Die 1*g* Kontrollproben zeigten ausschließlich ein adhärentes Wachstum. Hinsichtlich der Sphäroidanzahl wurden keine signifikanten Unterschiede beobachtet. Es wurde eine maximale Größe von etwa 0,4 mm bei den MCS festgestellt, wobei kleine und größere MCS stets gemischt auftraten (Abb. 4).

Bei den Zytokinuntersuchungen wurden nach sieben Tagen in den Überständen von ML-1 Zellen, im Vergleich zu den korrespondierenden 1*g* Kontrollen, sowohl nach RPM- als auch nach CN-Exposition signifikant erhöhte Werte von IL-6 und MCP-1 gemessen. In Immunohistochemischen Färbungen von papillären Schilddrüsenkarzinomzellen korrelierte eine hohe MCP-1 Expression mit der Lymphknotenmetastasierung und dem Wiederauftreten von Tumoren (Tanaka *et al.* 2009).

Im Gegensatz dazu zeigten sich bei den RO82-W-1 Zellen signifikant verringerte Werte für MCP-1 nach s-µ*g*. Für die Zytokine IL-6 und auch IL-8 fand sich hingegen eine Erhöhung der Werte im Vergleich zur 1*g* Kontrolle, die jedoch nur für die RPM-Proben eine Signifikanz aufwiesen. IL-8 spielt eine Rolle bei rheumatischen Erkrankungen (Deleuran *et al.* 1994) und ist bekannt für die Tumorprogression und für Lebermetastasen in kolorektalen Tumoren (Terada *et al.* 2005). Da sowohl IL-6 als auch IL-8 bereits in früheren Studien mit der Bildung von MCS in Verbindung gebracht wurden (Grosse *et al.* 2012), sollte dies noch näher untersucht werden.

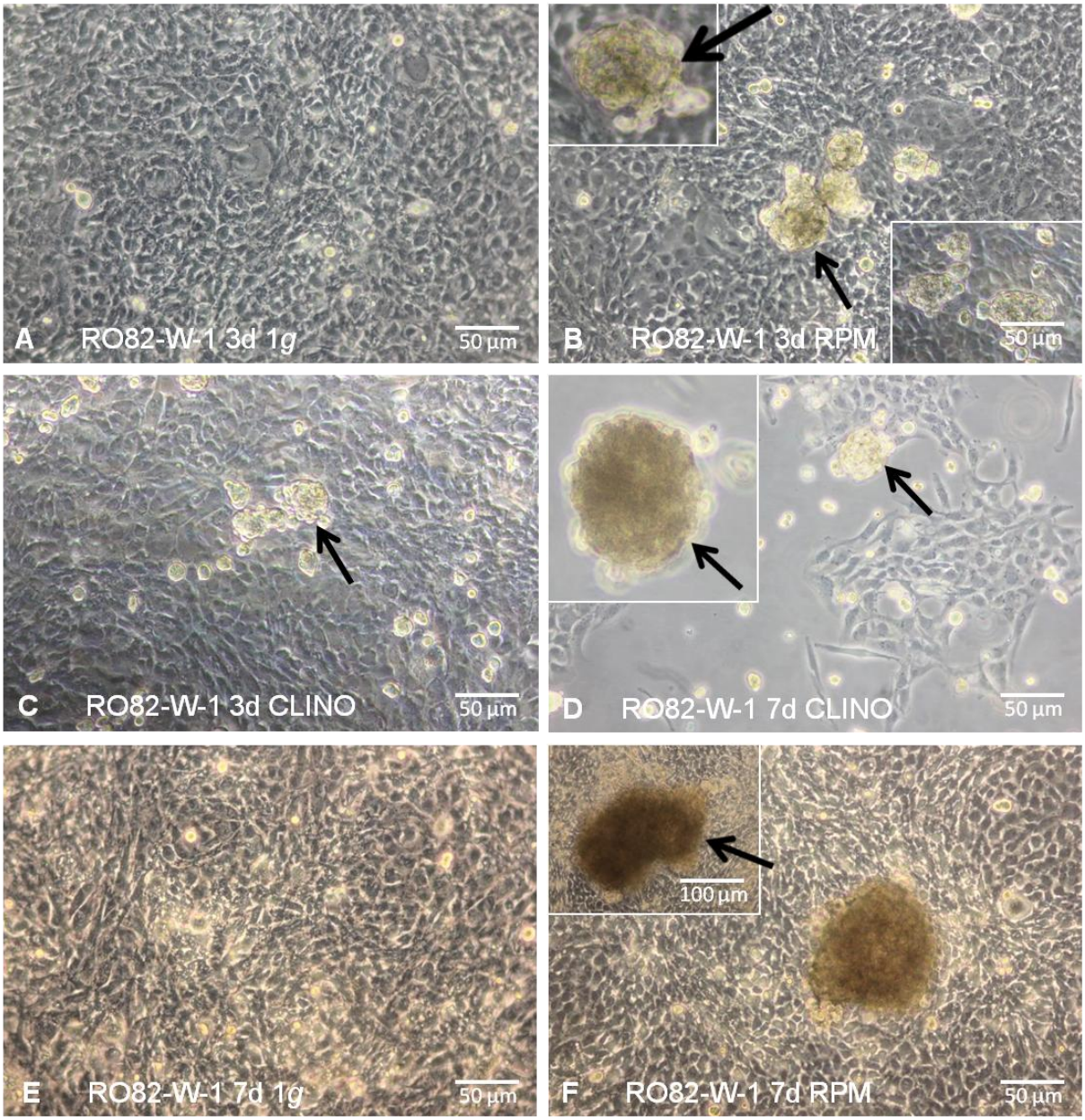

Abb. 4: **Phasenkontrastmikroskopie von RO82-W-1 nach 1*g* und s-µ*g***
A: Follikuläre Schilddrüsenkarzinomzellen RO82-W-1, nach 3 d Kultivierung unter statischen 1*g*-Bedingungen, zeigen ein Zellwachstum im adhärenten Monolayer. **B:** RO82-W-1 nach 3 d Kultivierung auf der RPM. Zusätzlich wird ein MCS im Zellkulturüberstand gezeigt. **C:** MCS nach 3 d auf dem Klinostaten (CN) **D:** RO82-W-1 Zellen nach 7 d auf dem CN. Zusätzlich wird ein MCS im Zellkulturüberstand gezeigt. **E:** RO82-W-1 nach 7 d unter statischen 1*g*-Bedingungen, im konfluenten Monolayer. **F:** RO82-W-1 nach 7d RPM-Exposition, adhärentes und MCS Wachstum ist sichtbar. 3D-Aggregate werden durch Pfeile verdeutlicht (Multizelluläre Sphäroide; MCS). (Svejgaard *et al.* 2015)

Mit Hilfe der Liquid-Overlay-Technik wurden zu diesem Zweck Sphäroide unter 1*g* Bedingungen gezüchtet. 96-Multiwell-Testplatten wurden dafür mit Agarose überzogen und 200 µl einer Zellsuspension in Kulturmedium mit 200 Zellen/µl aufgetragen. Zusätzlich wurden verschiedene Konzentrationen von IL-6 (1 ng/mL, 10 ng/mL, 100 ng/mL) oder IL-8 (1 ng/mL, 10 ng/mL, 45 ng/mL) zugegeben. Bei allen Versuchen zeigte sich ein positiver Effekt der Interleukinapplikation auf

die Sphäroidbildung. Während die ML-1 Zellen ohne Interleukingabe lediglich lose Zellaggregate bildeten, entstanden mit IL-Gabe nach drei und sieben Tagen MCS, die optisch vergleichbar zu den Sphäroiden nach s-µ*g* Exposition waren. Auch RO82-W-1 Zellen wiesen im Gegensatz zu den irregulären Aggregaten ohne IL deutlich kompaktere MCS nach Zusatz von IL-6 oder IL-8 auf.

Im nächsten Schritt wurde der Einfluss einer zusätzlichen Interleukingabe auf die Bildung der Proteine β-Aktin, β_1-Integrin, Talin-1 und Ki-67 mittels Western Blot Analysen untersucht. Als zusätzliche Konzentrationen wurden 0,03 ng/mL IL-6 ausgewählt, da dies die maximale Konzentration darstellte, welche in s-µ*g* Proben von ML-1 Zellen sezerniert wurde. Für IL-8 wurden in s-µ*g* maximal 45 ng/mL in den Kulturüberständen von ML-1 Proben gemessen. Die Versuche zeigten, dass sowohl IL-6 als auch IL-8 vor allem in physiologischen Bereichen (0,03 ng/mL und 45 ng/mL) die Mengen an β-Aktin, β_1-Integrin, sowie KI-67 innerhalb von drei bzw. sieben Tagen erhöhten. In Studien von Gopinathan *et al*. 2015 wurde IL-6 als ein wichtiger Faktor, der für Tumorzellwachstum, Metastasierung und Angiogenese verantwortlich ist, vorgeschlagen.

Auch Zellen ohne zusätzliche Interleukingabe, aber mit s-µ*g*-Exposition, wurden in Bezug auf Änderungen ihres Proteingehalts untersucht. Eine signifikante Reduktion von β-Aktin zeigte sich in ML-1 Zellen nach CN-Exposition, die Werte von RPM-Proben blieben unverändert. Bei den RO82-W-1 Zellen ergaben sich generell keine Änderungen im β-Aktingehalt unter s-µ*g*. β-Aktin ist ein wichtiger Bestandteil des Zytoskeletts und damit verantwortlich für Stabilität, Beweglichkeit und Struktur der Zelle. Über eine Überexpression wurde in den Arbeiten von Xu *et al.* 2013 bei der Metastasierung von gastrointestinalen Karzinomen berichtet.

Der Gehalt an β_1-Integrin war in beiden Zelllinien nach s-µ*g*-Exposition signifikant vermindert, unabhängig von der genutzten GBF-Anlage. Die geringsten Werte waren hier jeweils in MCS zu finden. β_1-Integrin gehört zur Familie der Adhäsionsmoleküle und ist somit maßgeblich an der Bindung an die Basalmembran, der Freisetzung von Adhäsionsmolekülen und der Invasivität von Tumoren in umgebendes Gewebe beteiligt. Sowohl follikuläre als auch papilläre Schiddrüsenkarzinome zeigten in Studien von Ensinger *et al.* 1998 und Demeure *et al*. 1992 erhöhte Werte von β_1-Integrin.

Weiterhin wurde der Einfluss von s-µ*g* auf die Struktur des Zytoskeletts der Zellen näher untersucht. Die Zellen wurden nach einer dreitägigen Exposition auf RPM oder CN mit einer Rhodamin-Phalloidin-Färbung zur Darstellung des F-Aktins gefärbt und mit den entsprechenden 1*g*-Kontrollen verglichen. Es fand sich eine vermehrte Ablagerung von F-Aktin um die äußere Zellmembran bei adhärenten Zellen in CN- und RPM-Proben. Diese wurde auch für sich bildende Sphäroide beobachtet. Diese Befunde passen sehr gut zu früheren Studien, die von einem großen Einfluss der Mikrogravitation auf zytoskelettale Proteine berichteten (Buravkova und Romanov 2001, Aleshcheva

et al. 2015, Ulbrich *et al.* 2011). Zum Teil konnten während eines Parabelflugs bereits nach der ersten Parabel mit 22s dauernder r-µ*g*-Phase eine Neuordnung des F-Aktinnetzwerkes mit perinuklearer Ansammlung bei ML-1 Zellen beobachtet werden (Ulbrich *et al.* 2011).

Zusammenfassend ist zu sagen, dass in dieser Studie oft ähnliche Effekte für den Gehalt an ausgesuchten Proteinen und die Zytokinausschüttung nach CN- und RPM-Exposition beobachtet werden konnten. In den Zelllinien ML-1 und RO82-W-1 induzierte die Kultivierung auf beiden GBF-Anlagen die Bildungen von Sphäroiden. Darüber hinaus fanden sich nach s-µ*g*-Exposition Veränderungen des F-Aktin-Zytoskeletts mit vermehrter Ablagerung um die Zellmembran. Unterschiede beim Gehalt an Proteinen oder der Sekretion zwischen den Zelllinien sind möglicherweise auf die unterschiedliche Herkunft und Charakteristik der Zelllinien zurückzuführen. Ein eindeutig positiver Effekt der IL-6 und IL-8 auf die Sphäroidbildung konnte mittels Liquid-Overlay-Technik in dieser Studie nachgewiesen werden.

5.3 Schilddrüsenzellen in simulierter Mikrogravitation – Vergleich von Klinostat und Random Positioning Maschine

Das Verhalten von Schilddrüsenkarzinomzellen und gesunden Schilddrüsenzellen unter s-µ*g* mit Fokus auf Wachstumsverhalten, Gen- und Proteinexpressionsmuster sowie Sekretionsverhalten der Zellen wurde in der Publikation "***Warnke E, Kopp S, Wehland M, Hemmersbach R, Bauer J, Pietsch J, Infanger M, Grimm D: Thyroid cells exposed to simulated microgravity conditions – comparison of the fast rotating clinostat and the random positioning machine. Microgravity Sci. Technol. 28.247-260 (2016)"*** zusammengefasst. Ergänzend wurden die Proteingehalte von β-Aktin und β-Tubulin mittels Western Blot Analysen für FTC-133 und Nthy-ori 3-1 nach 7 d RPM-Exposition erhoben. Verschiedene Aspekte, die bei der Nutzung der GBF-Anlagen CN und RPM auftreten können, wurden diskutiert.

Die Experimente wurden durch das CORA-ESA-GBF Projekt-2011-005 (Akronym „Device Comparison") sowie das ESA-CORA-GBF-2013-001 (Akronym „Thyroid III") gefördert. Langfristige Ziele der Forschung waren dabei neben dem grundlegenden Verständnis der Zellbiologie, die Vorbereitung von zukünftigen Weltraumflügen sowie die Identifizierung möglicher Ansätze für die Therapie von Schilddrüsenkarzinomen. GBF-Anlagen ermöglichten sowohl eigenständige Studien als auch effiziente Vorbereitung späterer Mikrogravitationsexperimente.

Diverse frühere Studien haben gezeigt, dass Schilddrüsenzellen sowohl *in vitro* als auch *in vivo* auf veränderte Schwerkraftbedingungen reagieren (Kossmehl *et al*. 2002, 2003, Meli *et al.* 1998, Martin *et al.* 2000, Masini *et al.* 2012). Die Sphäroidbildung ist dabei von besonderem Interesse, da sie sowohl

in r-µ*g* als auch in s-µ*g* ohne die Nutzung von Trägermaterial induziert werden konnte. Vor allem für die Gewebezüchtungen könnte somit die Nutzung von s-µ*g* zur Züchtung größerer Gewebestücke einen vielversprechenden Ansatz bieten (Grimm *et al.* 2014). In einer Proteomanalyse zur Sphäroidbildung von FTC-133 Zellen konnte gezeigt werden, dass verschiedene Proteine in fokalen Adhäsionskomplexen den 3D-Zusammenhalt von Zellen fördern (Pietsch *et al.* 2011a). Diese Proteine sind vor allem für die Gewebezüchtung, aber auch für weitere Studien zur Metastasierung von Tumorzellen und pharmakologische Studien von Bedeutung.

In einem weiteren Punkt wurde das Zytoskelett als möglicher Gravitationssensor betrachtet (Häder *et al.* 2017). Als dynamische Struktur verleiht es den Zellen mechanischen Halt, ist formgebend, ermöglicht aber auch die Anpassung der Zelle an externe Faktoren. Die genauen molekularen Mechanismen sind weiterhin unklar. Vorselen *et al*. 2014 schlagen vor, dass die physikalische Kraft der Gravitation in ein biochemisches Signal umgewandelt werden muss und dass dies mit Hilfe des Gravitationssensors Zytoskelett geschehen könnte.
Ulbrich *et al*. 2011 zeigten frühe Veränderungen des Zytoskeletts an follikulären Schilddrüsenkarzinomzellen nach der ersten Parabel mit 22 s r-µ*g* während eines Parabelflugs. Auch Boonstra 1999 unterstützt die These vom Zytoskelett als Gravitationssensor. Er fand in A431 Epidermoidkarzinomzellen nach ca. 7 Min Aufenthalt in der r-µ*g* erhöhte F-Aktinwerte.

Die von mir erhobenen Western Blot Daten für Nthy-ori 3-1 Schilddrüsenzellen nach 7 d RPM-Exposition ergaben eine signifikante Erhöhung des β-Aktin- und β-Tubulinproteins in Zellen, die auf der RPM inkubiert wurden, im Vergleich zu den korrespondierenden 1*g*-Kulturen.
Bei den FTC-133 Schilddrüsenkarzinomzellen zeigt sich keine signifikante Änderung für β-Aktin und lediglich signifikant erhöhte β-Tubulinwerte in MCS Zellen von RPM-Proben.

Diese Unterschiede könnten im Adaptationsverhalten der jeweiligen Zelllinien an die veränderten Gravitationsbedingungen begründet sein. Die Differenzierung und die Herkunft der Zellen könnten ebenfalls eine Rolle spielen. So handelt es sich beispielsweise bei Nthy-ori 3-1 um normale benigne Schilddrüsenzellen, während die FTC-133 einem niedrig differenzierten follikulären Schilddrüsenkarzinom entstammen. Untersuchungen zum Zytoskelett wurden bisher hauptsächlich an fixierten Zellen nach Abschluss der Experimente durchgeführt. Neue vielversprechende Erkenntnisse werden von dem DLR Projekt mit dem fluoreszenzmikroskopischen Analysesystem für biologische und biomedizinische Forschung im Weltraum (FLUMIAS, Airbus Defense and Space, Bremen) erwartet. Dies soll die online-in-time-Visualisierung der Dynamik und Adaptation des Zytoskeletts an lebenden Zellen unter r-µ*g* im Weltall ermöglichen.

Insgesamt konnte beobachtet werden, dass Mikrogravitation eine Vielzahl an Veränderungen sowohl in gesunden als auch in malignen Schilddrüsenzellen bewirkt. Neben Anzeichen für Apoptose,

konnten verändertes Wachstumsverhalten, ein Einfluss auf Migration, Differenzierung, Zelladhäsion und Zytokinsekretion beobachtet werden (Pietsch *et al.* 2011b).

Die Rolle von CN und RPM zur Vorbereitung von Weltraumstudien wurde bestätigt. Eventuelle Nebeneffekte wie Zentrifugalbeschleunigung, Scherkräfte und Vibrationen müssen berücksichtigt und näher untersucht werden (Herranz *et al.* 2013).

Es besteht eine komplexe Wechselwirkung zwischen Rotationsgeschwindigkeit, daraus resultierenden Beschleunigungen und der Reaktionszeit des Modellorganismus auf veränderte Gravitationsbedingungen (Hauslage *et al.* 2017). Wird zum Beispiel die Rotationsgeschwindigkeit verringert, könnten zwar geringere Restbeschleunigungen erreicht werden, gleichzeitig erhöht sich die Expositionszeit des Reizes, zum Beispiel der Schwerkraftwirkung in eine bestimmte Richtung, was für die Zelle zu permanenten Stress führen könnte (Horn *et al*. 2011). Auch die Effekte von Vibration und Hypergravitation werden häufig diskutiert. Frühere Studien mit der Schilddrüsenkarzinomzelllinie ML-1 zeigten, dass Mikrogravitationseffekte während einer Parabelflugkampagne stärker waren als Vibrations- und Hypergravitationseffekte (Ulbrich *et al.* 2011). Studien von Wehland *et al*. 2016 mit den gesunden Schilddrüsenzellen Nthy-ori 3-1 zeigten allerdings auch einen Einfluss von Hypergravitation und Vibration auf Gene und Proteine der Extrazellulären Matrix, des Zytoskeletts, der Apoptose, des Zellwachstums und verschiedener Signalprozesse. Dabei führte Vibration stets zu einer Reduktion der Expression, wohin gegen Hypergravitation ein breiter verteiltes Expressionsspektrum zeigte. Um diese Nebeneffekte so gut es geht zu minimieren und zu kontrollieren, wurden alle 1*g* Kontrollen in meinen Studien im gleichen Inkubator mit den GBF-Anlagen kultiviert. Zellen, die der s-µ*g* auf dem CN ausgesetzt wurden, wurden wie von Eiermann *et al.*2013 vorgeschlagen, nur im Bereich von ±3 mm um die Rotationsachse geerntet. Zellkulturflaschen auf der RPM wurden wie von van Loon *et al.*2007 empfohlen in einem maximalen Abstand von 7 cm zum Rotationszentrum angebracht. Darüber hinaus wurden die Zellkulturflaschen luftblasenfrei gefüllt, um zusätzliche Turbulenzen zu minimieren. Trotz allem scheint die Anfälligkeit der verschiedenen Zelllinien für diese Faktoren sehr unterschiedlich zu sein, sodass Ergebnisse unter s-µ*g* stets mit Ergebnissen von r-µ*g* validiert werden sollten, um einen wirklichen µ*g* Effekt zu belegen (Herranz *et al*. 2013).

5.4 Zytokinsekretion und Veränderungen fokaler Adhäsionsproteine von auf der Random Positioning Machine kultivierten Schilddrüsenzellen

Wie an Schilddrüsentumorzellen bereits gezeigt wurde, scheinen Zytokinsekretion und fokale Adhäsionsproteine bei der Sphäroidbildung eine entscheidende Rolle zu spielen. Dieser Sachverhalt wurde nun an normalen Nthy-ori 3-1 Schilddrüsenzellen näher untersucht. Wachstumsfaktoren, die

Zellen in den Zellkulturüberstand abgeben, sowie Komponenten der Zellmembran wurden vergleichend nach 4 h, 24 h und 3 d RPM-Exposition der Zellen betrachtet. Die Ergebnisse wurden in der Arbeit „***Warnke E, Pietsch, J, Kopp S, Bauer J, Sahana J, Wehland M, Krüger M, Hemmersbach R, Infanger M, Lützenberg R, Grimm D: Cytokine release and focal adhesion proteins in normal thyroid cells cultured on the random positioning machine. Cell. Physiol. Biochem. 43. 257-270 (2017)“*** veröffentlicht. Als Untersuchungsmethoden wurden Phasenkontrastmikroskopie, RT-qPCR, Western Blot, MAP- und zusätzlich Pathway-Analysen mittels Pathway Studio v.11 (Elsevier Research Solutions, Amsterdam, Niederlande) zur Analyse der Interaktionen eingesetzt.

Die Schilddrüsenzellen Nthy-ori 3-1 zeigten nach Inkubation auf der RPM die Koexistenz von AD und MCS Zellen nach etwa 24 h. Im weiteren Zeitverlauf erhöhte sich die Anzahl an MCS, wohingegen die Zahl der AD leicht abnahm. MAP-Analysen wurden durchgeführt, um Wachstumsfaktoren und Zytokine im Überstand zu bestimmen. Die Versuche wurden von der Firma Myriad-RBM in Austin, Texas, USA durchgeführt. Die Zytokine wurden mit dem Human CytokineMAP A und dem KidneyMAP® bestimmt, wobei nur 7 der 29 untersuchten Zytokine detektiert werden konnten. Obwohl nach 4 h noch alle Zellen adhärent wuchsen, konnten signifikant geringere Werte von Cystatin c und TIMP-1 in RPM-exponierten Kulturüberständen im Vergleich zu Kontrollüberständen nachgewiesen werden. Interessanterweise waren nach 3 d in den RPM-Kulturüberständen IL-6, IL-8 sowie TIMP-1 in signifikant erhöhten Konzentrationen zu finden.

Die Genexpression von *IL6* und *IL8* sowie des *MCP1* verlief umgekehrt. Sie blieb bei 1*g* weitgehend stabil. Die Genexpression war aber in allen drei Fällen in Zellen der RPM-Kulturen nach 4 h maximal, nach 24 h minimal und nach 3 d wieder deutlich erhöht. Beide Versuchsreihen zeigten eindeutig, dass simulierte Mikrogravitation einen Einfluss auf die Bildung und Abgabe bestimmter Wachstumsfaktoren hat. Die Regulation von zusammengehörigen Genen und Proteinen erschien allerdings zeitversetzt.

Neben den Wachstumsfaktoren wurden die extrazellulären Matrix Proteine Laminin A und Fibronektin sowie das zytoskelettale Protein Talin-1 untersucht. Nach 4 h waren ähnliche Mengen der extrazellulären Matrix Proteine nachweisbar, unabhängig davon, ob die Zellen auf der RPM oder bei 1*g* kultiviert wurden. Die Proteinkonzentration von Talin-1 war hingegen unter s-µ*g* deutlich verringert. Die Genexpression von *LAMA1*, *FN1* und *TLN1* sowie von *ITGB1* war nach 4 h deutlich erhöht. Interessant war die Genexpression nach 24 h in AD. In diesen Zellen war die Expression der genannten Komponenten signifikant erhöht. In den dazugehörigen MCS war sie auffallend erniedrigt. Bei den dazugehörigen Proteinmengen konnten dagegen nach 24 h nur marginale Veränderungen

festgestellt werden. Schwankungen waren bei der Genexpression dieser Proteine auch nach 3 d noch zu beobachten.

Zusammenfassend kann man sagen, dass sich die Genexpression von *FN1*, *LAMA1*, *ITGB1* und *TLN1* unter Einfluss von simulierter Mikrogravitation hauptsächlich in den adhärenten Zellen veränderte. Die Genexpression und die Veränderungen der Proteinkonzentration scheinen auch hier zeitversetzt zu erfolgen.

Um zu sehen, ob es sich bei den Veränderungen der untersuchten Zellkomponenten um isolierte Vorgänge handelte oder ob Zusammenhänge zwischen den beobachteten Vorgängen existieren, wurden Datenbankrecherchen mit Hilfe des Pathway Studio-Programms durchgeführt. Interaktionen der untersuchten Zellkomponenten auf Protein- oder auf Genebene konnten so ermittelt werden. Es zeigte sich, dass Laminin A, Fibronektin, β_1-Integrin und Talin-1 aneinander binden können. Die Stabilität der Bindung dieser extrazellulären und zytoskelettalen Proteine untereinander wird über den Tissue Inhibitor of Metalloproteinase-1 (TIMP-1) auf direkte (Jung *et al.* 2006) und über IL-8 auf indirekte Weise (Xie 2001) stabilisiert. Auch IL-7 und VEGF zeigen einen Einfluss (Shao *et al.* 2012, Ariel *et al.* 1997, Mitsi *et al.* 2006).

Auf Genebene interagieren, abgesehen von Laminin A, alle Komponenten miteinander. *VEGFA*, *IL6* und *CCL2* (MCP-1) fördern die Expression der Gene des β_1-Integrin (*ITGB1*) und Fibronektin (*FN1*) (Zhang *et al.* 2000, Suhr *et al.* 2003, Giunti *et al.* 2008, Ashida *et al.* 2001, Ancelin *et al.* 2004). *IL8* kann zu einer Hochregulierung von *FN1* beitragen (Mohamed 2012). Dagegen regulieren *IL6* und *IL8* die Expression von Talin-1 (*TLN1)* herab (Svejgaard *et al.* 2015). *IL7* hat Einfluss auf die Expression von MCP-1 (*CCL2*) und IL-8 (*CXCL8*) (Damas *et al.* 2003).
Zusammenfassend kann gesagt werden, dass auch normale Schilddrüsenzellen unter simulierter Mikrogravitation Sphäroidbildung zeigen. Die Sphäroidbildung geht mit einem komplexen Zusammenspiel löslicher Faktoren und zellgebundener extrazellulärer und zytoskelettaler Proteine einher. Die biophysikalische Interaktion der Proteine und die Induktion der Genexpression könnte durch die veränderten Gravitationsbedingungen ausgelöst werden und somit zur Sphäroidbildung beitragen.

6. Schlussfolgerungen

Sowohl für benigne als auch maligne Schilddrüsenzellen konnte die Bildung von 3D-Sphäroiden innerhalb von 24 h Kultivierung auf beiden GBF-Anlagen bestätigt werden. Dies zeigt eindeutig die Eignung des Klinostaten und der RPM zur Züchtung von Sphäroiden.

Für die Zelllinie FTC-133 ergaben sich abhängig von der genutzten GBF-Anlage Unterschiede im Sekretionsverhalten. Während eine Kultivierung unter 2D-Klinorotation auf dem CN eher eine reduzierte Sekretion der untersuchten Zytokine bewirkte, führte die 3D-Random Rotation auf der RPM zu einer erhöhten Sekretion. Lediglich VEGF und Eotaxin-1 wiesen vergleichbare Werte auf beiden Geräten auf. Auch bei der Expressionsanalyse der untersuchten Zielgene gab es diverse Differenzen, wobei hier Caveolin-1 (*CAV1*) und der Connective Tissue Growth Factor (*CTGF*) ein ähnliches Verhalten zeigten (Warnke *et al.* 2014). Aus diesem Grund wurde eine Beteiligung von VEGF, Eotaxin, *CAV1* und *CTGF* an der Sphäroidbildung vermutet. Obwohl sich auf beiden GBF-Anlagen die Ausbildung der zwei Phänotypen AD und MCS bestätigte, zeigen die Unterschiede in Bezug auf Zytokinsekretion, Gen- und Proteinexpression die Notwendigkeit von vergleichenden Untersuchungen. Um die Eignung der GBF-Anlagen zur Simulation von Mikrogravitation zu belegen, sind Studien unter r-µ*g* zwingend notwendig, damit µ*g*-Effekte von gerätespezifischen Effekten getrennt werden können. Auch der finale Nachweis eines Gravitationssensors in Schilddrüsenzellen und damit die Bestimmung von Grenzwerten für die Gravitationswahrnehmung in den Zelle steht noch aus (Albi *et al.* 2017).

Für die Untersuchung der Mechanismen der Sphäroidbildung und zur Validierung der Ergebnisse könnten auch Techniken wie Hanging Drop, Liquid-Overlay oder Spinner Flask zum Einsatz gebracht werden. Allerdings kann bei keiner dieser Methoden der Übergang von 2D- in 3D-Wachstum nachgeahmt werden. Ein weiterer Aspekt ist die Nekrosebildung im Zentrum der Sphäroide bei diesen drei 1*g*-Labormethoden. Dies stellt einen eindeutigen Nachteil dieser Methoden im Vergleich zum CN und der RPM bei der Sphäroidbildung dar.

Für die Zelllinien ML-1 und RO82-W-1 zeigten sich ähnliche Effekte der GBF-Anlagen hinsichtlich Zytokinausschüttung, Expression und Verteilung von Zytoskelettproteinen (Svejgaard *et al.* 2015). Mittels F-Aktinfärbungen konnte eine Ansammlung von Aktin an der äußeren Zellmembran nach CN- und RPM-Exposition gezeigt werden. Die Umverteilung des Aktins könnte einen weiteren, wichtigen Schritt auf dem Weg zur Sphäroidbildung darstellen. Für die Zelllinie Nthy-ori 3-1 konnten nach RPM Versuchen ein erhöhter β-Aktin- und β-Tubulin-Proteingehalt verzeichnet werden (Warnke *et al.* 2016).

Bisher wurden Färbungen der Zellen nach Beendigung der Versuche durchgeführt. Neue Methoden wie FLUMIAS, die ein online Life-cell imaging ermöglichen, das heißt die Beobachtung lebender Zellen unter Mikrogravitation, bieten vielversprechende Möglichkeiten für die Sphäroidforschung. Erste Ergebnisse des Mikroskops während der 24. DLR Parabelflugkampagne und der TEXUS 52 Mission wurden 2016 von Corydon *et al.* 2016 veröffentlicht. In diesen Studien konnte gezeigt werden, dass Änderungen im Zytoskelett sehr schnell nach Eintritt in die µ*g*-Phase stattfinden. Dies bestätigt unsere Vermutungen, dass das Zytoskelett eine Art Gravitationssensor für die Zellen darstellen könnte.

Bei normalen Nthy-ori 3-1 Thyreozyten konnte neben dem Sphäroidwachstum unter RPM-Exposition auch die veränderte Sekretion diverser Zytokine (IL-6 und IL-8) in Verbindung mit fokalen Adhäsionsproteinen beobachtet werden (Warnke *et al.* 2017). Pathway-Analysen zeigten ein Netzwerk aus positiven und negativen Interaktionen zwischen verschiedenen Proteinen, welche für die MCS Bildung eine Rolle spielen. Auf Grund der komplexen Interaktionen zwischen den Zellen sowohl *in vitro* als auch *in vivo* sollten Pathway-Analysen in zukünftigen Studien vermehrt eingesetzt werden. Neben der Einordnung bereits vorhandener Ergebnisse könnten sie einen wichtigen Beitrag zum Verständnis von Signalwegen leisten. In der Arbeit von Svejgaard *et al.* konnte 2015 auch ein verbessertes Sphäroidwachstum von ML-1 und RO82-W-1 Zellen durch IL-6- und IL-8- Applikation unter 1*g* mithilfe der Liquid-Overlay-Technik belegt werden.

Zusammenfassend wurde die Bildung von Sphäroiden diverser Zelllinien ohne Trägermaterialien oder künstliche Oberflächen bestätigt. Somit könnte den GBF-Anlagen, vor allem im Bereich Gewebezüchtung, zukünftig eine besondere Bedeutung zukommen. Da sich zum Teil sehr unterschiedliche Effekte in den verschiedenen betrachteten Zelllinien unter simulierter Mikrogravitation zeigten, sollte die Empfänglichkeit des ausgewählten Modellorganismus gegenüber den verschiedenen Simulationsansätzen, aber auch Störfaktoren wie Vibration und Hypergravitation in ergänzenden Studien getestet werden. Eine erste Empfehlung für die passende GBF-Anlage in Abhängigkeit von dem gewählten Modellorganismus ist in den Arbeiten von Herranz *et al*. 2013 zu finden.

Abschließend möchte ich noch einmal die Bedeutung von CN und RPM für die Bildung von Sphäroiden betonen. Da ein Übergang von 2D- in 3D-Wachstum der Zellen erfolgt, können sie einen wichtigen Ansatz für zukünftige Studien zur Metastasierung, aber auch für pharmazeutische Tests bieten. Als Grundlage und Vorbereitung für zukünftige Raumflüge zeigen die GBF-Anlagen ein hohes Potential. Vorab könnten Hardwaretests im Hinblick auf Biokompatibilität und raumflugbezogene Kultivierungsbedingungen (Temperatur, Startverschiebungen, etc.) durchgeführt werden. Simulationsanlagen bieten somit keinen Ersatz, aber eine wichtige Ergänzung für Studien unter r-µ*g*.

7. Zusammenfassung

Die vorliegende kumulative Dissertation beruht auf drei Publikationen, die ich als Erstautorin (Warnke *et al.* 2014, 2016 und 2017) veröffentlich habe sowie einer weiteren Publikation, an der ich als Mitautorin beteiligt war (Svejgaard *et al.* 2015).

In der ersten Veröffentlichung wurden humane Schilddrüsenkarzinomzellen FTC-133 für 4 h, 24 h und 3 d auf der Random Positioning Machine (RPM) und dem 2D-Klinostaten (CN) kultiviert. Die Zellen wuchsen auf beiden Geräten adhärent (AD) und bildeten Sphäroide (MCS). Zellen unter statischen 1*g*-Kontrollbedingungen zeigten hingegen ausschließlich Adhärenz. Die Kultivierung auf den beiden Bodenanlagen induzierte Unterschiede bezüglich der Zytokinsekretion und der Genexpression. Eine reduzierte *CAV1* und *CTGF* Genexpression in MCS im Vergleich zu AD wurde auf beiden Anlagen beobachtet. Dies deutet auf einen Zusammenhang mit der MCS Bildung hin.

Für die zweite Studie wurden ML-1 und RO82-W-1 Schilddrüsenkarzinomzellen nach jeweils 3 d und 7 d CN- bzw. RPM-Exposition untersucht. Nach 7 d fanden sich signifikant erhöhte Werte von IL-6 und IL-8 in den Kulturüberständen von RPM-exponierten RO82-W-1 Zellen. Darauf aufbauende Experimente mit IL-6 und IL-8 Supplementierung zeigten unter 1*g*, mit Hilfe des Liquid-Overlay-Verfahrens, eine deutliche Verbesserung im Sphäroidwachstum für beide Zelllinien. Die Supplementierung beeinflusste den Proteingehalt an $ß_1$-Integrin, Talin-1, Ki-67 sowie β-Aktin in Abhängigkeit von den IL-6 und IL-8 Konzentrationen. F-Aktinfärbungen zeigten eine Reorganisation von F-Aktin an der äußeren Zellmembran, was auf eine aktive Rolle des Zytoskeletts an der Gravitationswahrnehmung von Zellen hinweisen könnte. Dies konnte auch für gesunde Schilddrüsenzellen in meiner dritten Publikation gezeigt werden. Nthy-ori 3-1 Thyreozyten wiesen nach 7-tägiger RPM-Exposition erhöhte β-Aktin und β-Tubulinwerte auf. Die Nutzung von CN und RPM zur Simulation von Mikrogravitation wurde näher diskutiert, da diese Geräte in der Grundlagenforschung, zur Vorbereitung von Weltraumexperimenten, bei pharmakologischen Studien und zur Gewebezüchtung eingesetzt werden.

In der dritten Veröffentlichung wurden Nthy-ori 3-1 Schilddrüsenzellen nach 4 h, 24 h und 3 d auf der RPM näher beschrieben. *IL6*, *IL8* und *CCL2* zeigten bereits nach 4 h eine signifikant erhöhte Genexpression, obwohl zu diesem Zeitpunkt noch alle Zellen adhärent wuchsen. MCS wurden nach 24 h auf der RPM beobachtet. Dies ging mit einer signifikant reduzierten Genexpression in MCS für *IL6*, *IL8* und *CCL2* im Vergleich zu 1*g* einher. Nach 3 d RPM-Exposition war die Sekretion von IL-6 und IL-8 signifikant verringert. Pathway-Analysen zeigten, dass ein Zusammenspiel aus Zytokinen und fokalen Adhäsionsproteinen maßgeblich an der Ausbildung von MCS beteiligt sein könnte.

Auch wenn die Existenz eines Gravitationssensors in den untersuchten Zellen bisher nicht eindeutig belegt wurde, so stützen die Ergebnisse die Hypothese, dass das Zytoskelett maßgeblich an der Gravitationswahrnehmung von Zellen beteiligt ist. Darüber hinaus konnte die Eignung der GBF-Anlagen, CN und RPM, zur Bildung von MCS für diverse Schilddrüsenzelllinien nach 24 h nachgewiesen werden.

8. Summary

The present cumulative thesis is based on three publications published as first author (Warnke *et al.* 2014, 2016 and 2017) as well as one further publication with co-authorship (Svejgaard *et al.* 2015).

For the first study, human thyroid carcinoma cells, FTC-133 were cultivated for 4 h, 24 h and 3 d on either random positioning machine (RPM) or 2D-clinostat (CN). Cells showed adherent growth (AD) behaviour but also the induction of spheroids (MCS). In contrast, cells cultured under conditions of 1*g* just grew adherently. Concerning the secretion of cytokines and gene expression, differences were visible between CN- and RPM-exposed cells. Reduced *CAV1* and *CTGF* gene expressions were found in MCS compared to AD on both devices. This suggests the involvement in the formation of MCS.
The second study investigated ML-1 and RO82-W-1 thyroid carcinoma cells after a 3-day and 7-day CN- and RPM-exposure. After 7 d, significantly higher values of IL-6 and IL-8 were found in the supernatants of RPM-exposed RO82-W-1 cells. Constitutive experiments with IL-6 and IL-8 supplementation showed an improved growth of spheroids for both cell lines under conditions of 1*g* demonstrated by means of the liquid-overlay technique. The supplement influenced the protein content of $ß_1$-Integrin, talin-1, Ki-67 and β-actin. This was dependent on the IL-6 and IL-8 concentrations. F-actin staining showed a reorganization of f-actin towards the outer membrane, pointing towards an active role of the cytoskeleton in gravity perception of the cells.
This could also be shown for normal cells in my third publication. Nthy-ori 3-1 thyrocytes revealed increased values of β-actin and β-tubulin after a 7-day RPM-exposure. The use of CN and RPM for the simulation of microgravity was discussed in detail. Both devices can be used for basic science, to prepare for Space experiments, during pharmacological testing and for tissue engineering.
Within my last publication Nthy-ori 3-1 thyroid cells were investigated after 4 h, 24 h and 3 d on the RPM.
IL6, *IL8* and *CCL2* already showed a significantly increased expression after 4 h, although all cells were still growing adherently. MCS were visible after 24 h on the RPM, along with a significantly reduced gene expression in MCS for *IL6*, *IL8* and *CCL2* compared to 1*g*-controls. The secretion of IL-6 and IL-8 was significantly reduced after a 3-day RPM-exposure. Pathway analyses indicate an interaction of cytokines and focal adhesion proteins in MCS formation.
So far, a gravitation sensor has not been identified in cells, but our studies confirm the hypothesis that the cytoskeleton might be relevant for sensing of gravity by the cells. Furthermore, the capability of the Ground-Based Facilities CN and RPM for the induction of spheroid formation of various thyroid cell lines after 24 h was proven.

9. Literaturverzeichnis

Agate L, Lorusso L, Elisei R: New and old knowledge on differentiated thyroid cancer epidemiology and risk factors. J Endocrinol Invest. 35. 3-9 (2012)

Albi E, Krüger M, Hemmersbach R, Lazzarini A, Cataldi S, Codini M, Beccari T, Ambesi-Impiombato FS, Curcio F: Impact of Gravity on Thyroid Cells. Int J Mol Sci. 18. 972 (2017)

Albrecht-Buehler G: The simulation of microgravity conditions on the ground. ASGSB Bull. 5. 3–10 (1992)

Aleshcheva G, Sahana J, Ma X, Hauslage J, Hemmersbach R, Egli M, Infanger M, Bauer J, Grimm D: Changes in morphology, gene expression and protein content in chondrocytes cultured on a random positioning machine. PLoS One. 8. e79057 (2013)

Aleshcheva G, Wehland M, Sahana J, Bauer J, Corydon TJ, Hemmersbach R, Frett T, Egli M, Infanger M, Grosse J, Grimm D: Moderate alterations of the cytoskeleton in human chondrocytes after short-term microgravity produced by parabolic flight maneuvers could be prevented by up-regulation of BMP-2 and SOX-9. FASEB J. 29. 2303–2014 (2015)

Ancelin M, Chollet-Martin S, Herve MA, Legrand C, El Benna J, Perrot-Applanat M: Vascular endothelial growth factor VEGF189 induces human neutrophil chemotaxis in extravascular tissue via an autocrine amplification mechanism. Lab Invest 84. 502-512 (2004)

Ariel A, Hershkoviz R, Cahalon L, Williams DE, Akiyama SK, Yamada KM, Chen C, Alon R, Lapidot T, Lider O: Induction of T cell adhesion to extracellular matrix or endothelial cell ligands by soluble or matrix-bound interleukin-7. Eur J Immunol. 27. 2562-2570 (1997)

Ashida N, Arai H, Yamasaki M, Kita T: Distinct signaling pathways for MCP-1-dependent integrin activation and chemotaxis. J Biol Chem. 276. 16555-16560 (2001)

Baudin E, Schlumberger M: New therapeutic approaches for metastatic thyroid carcinoma. Lancet Oncol. 8. 148-156 (2007)

Becker JL, Souza GR: Using space-based investigations to inform cancer research on Earth. Nat Rev Cancer. 13. 315–327 (2013)

Boonstra J: Growth factor-induced signal transduction in adherent mammalian cells is sensitive to gravity. FASEB J. 13. 35–42 (1999)

Briegleb W: Some qualitative and quantitative aspects of the fast-rotating clinostat as a research tool. ASGSB Bull. 5. 23-30 (1992)

Brown AH: Centrifuges: evolution of their uses in plant gravitational biology and new directions for research on the ground and in spaceflight. ASGSB Bull. 5. 43-57 (1992)

Buravkova LB, Romanov YA: The role of cytoskeleton in cell changes under condition of simulated microgravity. Acta Astronaut. 48. 647–650 (2001)

Carlsson J, Yuhas JM: Liquid-overlay culture of cellular spheroids. Recent Results Cancer Res. 95. 1-23 (1984)

Corydon JT, Kopp, S, Wehland M, Braun M, Schütte A, Mayer T, Hülsing T, Oltmann H, Schmitz B, Hemmersbach R, Grimm D: Alterations of the cytoskeleton in human cells in space proved by life-cell imaging. Sci Rep. 6. 20043 (2016)

Cui L, Zhang Q, Mao Z, Chen J, Wang X, Qu J, Zhang J, Jin D: CTGF is overexpressed in papillary thyroid carcinoma and promotes the growth of papillary thyroid cancer cells. Tumour Biol. 32. 721–728 (2011)

Curcio F, Ambesi-Impiombato FS, Perrella G, Coon HG: Longterm culture and functional characterization of follicular cells from adult normal human thyroids. Proc. Natl. Acad. Sci. 91. 9004–9008 (1994)

Damas JK, Waehre T, Yndestad A, Otterdal K, Hognestad A, Solum NO, Gullestad L, Froland SS, Aukrust P: Interleukin-7-mediated inflammation in unstable angina: possible role of chemokines and platelets. Circulation. 107. 2670-2676 (2003)

Deleuran B, Lemche P, Kristensen M, Chu CQ, Field M, Jensen J, Matsushima K, Stengaard-Pedersen K: Localisation of interleukin 8 in the synovial membrane, cartilage- pannus junction and chondrocytes in rheumatoid arthritis. Scand J Rheumatol. 23. 2–7 (1994)

Demeure MJ, Damsky CH, Elfman F, Goretzki PE, Wong MG, Clark OH: Invasion by cultured human follicular thyroid cancer correlates with increased β1 integrins and production of proteases. World J Surg. 16. 770–776 (1992)

Durante C, Haddy N, Baudin E, Leboulleux S, Hartl D, Travagli JP, Caillou B, Ricard M, Lumbroso JD, De Vathaire F, Schlumberger M: Long-term outcome of 444 patients with distant metastases from papillary and follicular thyroid carcinoma: benefits and limits of radioiodine therapy. J Clin Endocrinol Metab. 91. 2892-2899 (2006)

Eiermann P, Kopp S, Hauslage J, Hemmersbach R, Gerzer R, Ivanova K: Adaptation of a 2D clinostat for simulated microgravity experiments with adherent cells. Microgravity Sci. Technol. 25. 153–159 (2013)

Ensinger C, Obrist P, Bacher-Stier C, Mikuz G, Moncayo R, Riccabona G: β1-Integrin expression in papillary thyroid carcinoma. Anticancer Res 18. 33–40 (1998)

Estour B, Van Herle AJ, Juillard GJ, Totanes TL, Sparkes RS, Giuliano AE, Klandorf H: Characterization of a human follicular thyroid carcinoma cell line (UCLA RO 82 W-1). Virchows Arch B Cell Pathol Incl Mol Pathol. 57. 167–174 (1989)

Foty R: A simple hanging drop cell culture protocol for generation of 3D spheroids. J Vis Exp. 51. 2720 (2011)

Freed LE, Langer R, Martin I, Pellis NR, Vunjak-Novakovic G: Tissue engineering of cartilage in space. Proc. Natl. Acad. Sci. USA 94. 13885–13890 (1997)

Giunti S, Tesch GH, Pinach S, Burt DJ, Cooper ME, Cavallo-Perin P, Camussi G, Gruden G: Monocyte chemoattractant protein-1 has prosclerotic effects both in a mouse model of experimental diabetes and in vitro in human mesangial cells. Diabetologia 51. 198-207 (2008)

Gopinathan G, Milagre C, Pearce OM, Reynolds LE, Hodivala-Dilke K, Leinster DA, Zhong H, Hollingsworth RE, Thompson R, Whiteford JR, Balkwill F: Interleukin-6 Stimulates Defective Angiogenesis. Cancer Res. 75. 3098-107 (2015)

Goretzki PE, Frilling A, Simon D, Roeher HD: Growth regulation of normal thyroids and thyroid tumors in man. Recent Results Cancer Res. 118. 48–63 (1990)

Grimm D, Bauer J, Kossmehl P, Shakibaei M, Schönberger J, Pickenhahn H, Schulze-Tanzil G, Vetter R, Eilles C, Paul M, Cogoli A: Simulated microgravity alters differentiation and increases apoptosis in human follicular thyroid carcinoma cells. FASEB J. 16. 604–606 (2002)

Grimm D, Bauer J, Hemmersbach R, Ulbrich C, Pietsch J, Wehland M, Infanger M: Biotechnologische Nutzung der Schwerelosigkeit für medizinische Forschung Analyse humaner Zellen nach Schwerelosigkeit. FTR. 20. 188–193 (2013)

Grimm D, Wehland M, Pietsch J, Aleshcheva G, Wise P, van Loon J, Ulbrich C, Magnusson NE, Infanger M, Bauer J: Growing tissues, in real and simulated microgravity: new methods for tissue engineering. Tissue Eng. Part B Rev. 20. 555–566 (2014)

Grosse J, Wehland M, Pietsch J, Schulz H, Saar K, Hübner N, Eilles C, Bauer J, Abou-El-Ardat K, Baatout S, Ma X, Infanger M, Hemmersbach R, Grimm D: Gravity-sensitive signaling drives 3-dimensional formation of multicellular thyroid cancer spheroids. FASEB J. 26. 5124–5140 (2012)

Grosse J, Warnke E, Pohl F, Magnusson NE, Wehland M, Infanger M, Eilles C, Grimm D: Impact of sunitinib on human thyroid cancer cells. Cell Physiol Biochem. 32. 154-170 (2013)

Häder DP, Braun M, Grimm D, Hemmersbach R: Gravireceptors in eukaryotes-a comparison of case studies on the cellular level. NPJ Microgravity. 3. 13 (2017)

Hauslage J, Cevik V, Hemmersbach R: Pyrocystis noctiluca represents an excellent bioassay for shear forces induced in ground-based microgravity simulators (clinostat and random positioning machine). NPJ Microgravity. 3. 12 (2017)

Hemmersbach R, Simon A, Waßer K, Hauslage J, Christianen PC, Albers PW, Lebert M, Richter P, Alt W, Anken R: Impact of a high magnetic field on the orientation of gravitactic unicellular organisms--a critical consideration about the application of magnetic fields to mimic functional weightlessness. Astrobiology. 14. 205-215 (2014)

Herranz R, Anken R, Boonstra J, Braun M, Christianen PC, de Geest M, Hauslage J, Hilbig R, Hill RJ, Lebert M, Medina FJ, Vagt N, Ullrich O, van Loon JJ, Hemmersbach R: Ground-based facilities for simulation of microgravity: organism-specific recommendations for their use, and recommended terminology. Astrobiology 13. 1–17 (2013)

Heinrich P, Müller M, Graeve L: Löffler/Petridas Biochemie und Pathobiochemie. 9. Auflage. p. 512 Springer-Verlag Berlin Heidelberg 2014

Horn A, Ullrich O, Huber K, Hemmersbach R: PMT (Photomultiplier) Clinostat. Microgravity Sci Technol. 23. 67–71 (2011)

Ivanova K, Das PK, van den Wijngaard RM, Lenz W, Klockenbring T, Malcharzyk V, Drummer C, Gerzer R: Differential expression of functional guanylyl cyclases in melanocytes: absence of nitric-oxide-sensitive isoform in metastatic cells. J. Invest. Dermatol. 116. 409–416 (2001)

Jung KK, Liu XW, Chirco R, Fridman R, Kim HR: Identification of CD63 as a tissue inhibitor of metalloproteinase-1 interacting cell surface protein. EMBO J. 25. 3934-3942 (2006)

Kong X, Wang X, Xu W, Behera S, Hellermann G, Kumar A, Lockey RF, Mohapatra S, Mohapatra SS: Natriuretic peptide receptor a as a novel anticancer target. Canc. Res. 68. 249–256 (2008)

Kopp S, Warnke E, Wehland M, Aleshcheva G, Magnusson NE, Hemmersbach R, Corydon TJ, Bauer J, Infanger M, Grimm D: Mechanisms of three-dimensional growth of thyroid cells during long-term simulated microgravity. Sci Rep 5. 16691 (2015)

Kossmehl P, Cogoli A, Shakibaei M, Pickenhahn H, Paul M, Grimm D: Simulated microgravity induces programmed cell death in human thyroid carcinoma cells. J. Gravit. Physiol. 9. 295–296 (2002)

Kossmehl P, Shakibaei M, Cogoli A, Infanger M, Curcio F, Schönberger J, Eilles C, Bauer J, Pickenhahn H, Schulze-Tanzil G, Paul M, Grimm D: Weightlessness induced apoptosis in normal thyroid cells and papillary thyroid carcinoma cells via extrinsic and intrinsic pathways. Endocrinology. 144. 4172–4179 (2003)

Lemoine NR, Mayall ES, Jones T, Sheer D, Mcdermid S, Kendalltaylor P, Wynfordthomas D: Characterisation of human thyroid epithelial-cells immortalised in vitro by simian-virus 40-DNA transfection. Br. J. Cancer. 60. 897–903 (1989)

Liao S, Shindo M: Management of well-differentiated thyroid cancer. Otolaryngol Clin North Am 45. 1163-1179 (2012)

Lu Z, Ghosh S, Wang Z, Hunter T: Downregulation of caveolin-1 function by EGF leads to the loss of E-cadherin, increased transcriptional activity of beta-catenin, and enhanced tumor cell invasion. Cancer Cell 4. 499–515 (2003)

Ma X, Wehland M, Aleshcheva G, Hauslage J, Waßer K, Hemmersbach R, Infanger M, Bauer J, Grimm D: Interleukin-6 expression under gravitational stress due to vibration and hypergravity in follicular thyroid cancer cells. PLoS One. 8. e68140 (2013)

Ma X, Pietsch J, Wehland M, Schulz H, Saar K, Hübner N, Bauer J, Braun M, Schwarzwälder A, Segerer J, Birlem M, Horn A, Hemmersbach R, Wasser K, Grosse J, Infanger M, Grimm D: Differential gene expression profile and altered cytokine secretion of thyroid cancer cells in space. FASEB J. 28. 813–835 (2014)

Maret G, Dransfeld K: Biomolecules and polymers in high steady magnetic fields. In: Topics in Applied Physics, Strong and ultrastrong magnetic fields and Their Applications. Vol. 57. pp 143–204. Springer New York 1985

Martin A, Zhou A, Gordon RE, Henderson SC, Schwartz AE, Schwartz AE, Friedman EW, Davies TF: Thyroid organoid formation in simulated microgravity: influence of keratinocyte growth factor. Thyroid 10. 481–487 (2000)

Masini MA, Albi E, Barmo C, Bonfiglio T, Bruni L, Canesi L, Cataldi S, Curcio F, D'Amora M, Ferri I, Goto K, Kawano F, Lazzarini R, Loreti E, Nakai N, Ohira T, Ohira Y, Palmero S, Prato P, Ricci F, Scarabelli L, Shibaguchi T, Spelat R, Strollo F, Ambesi-Impiombato FS: The impact of long-term exposure to space environment on adult mammalian organisms: a study on mouse thyroid and testis. PLoS One 7. e35418 (2012)

Meli A, Perrella G, Curcio F, Ambesi-Impiombato FS: Response to hypogravity of normal in vitro cultured follicular cells from thyroid. Acta Astronaut 42. 465–472 (1998)

Mitsi M, Hong Z, Costello CE, Nugent MA: Heparin-mediated conformational changes in fibronectin expose vascular endothelial growth factor binding sites. Biochemistry 45. 10319-10328 (2006)

Mo S, Yang S, Cui Z: New glimpses of caveolin-1 functions in embryonic development and human diseases. Front 6. 367–376 (2011)

Mohamed MM: Monocytes conditioned media stimulate fibronectin expression and spreading of inflammatory breast cancer cells in three-dimensional culture: A mechanism mediated by IL-8 signaling pathway. Cell Commun Signal. 10. 3 (2012)

O'Neill CJ, Oucharek J, Learoyd D, Sidhu SB: Standard and emerging therapies for metastatic differentiated thyroid cancer. Oncologist. 15. 146-156 (2010)

Pietsch J, Sickmann A, Weber G, Bauer J, Egli M, Wildgruber R, Infanger M, Grimm D: A proteomic approach to analysing spheroid formation of two human thyroid cell lines cultured on a random positioning machine. Proteomics. 11. 2095–2104 (2011a)

Pietsch J, Bauer J, Egli M, Infanger M, Wise P, Ulbrich C, Grimm D: The effects of weightlessness on the human organism and mammalian cells. Curr Mol Med. 11. 350–364 (2011b)

Pietsch J, Ma X, Wehland M, Aleshcheva G, Schwarzwälder A, Segerer J, Birlem M, Horn A, Bauer J, Infanger M, Grimm D: Spheroid formation of human thyroid cancer cells in an automated culturing system during the Shenzhou-8 Space mission. Biomaterials. 34. 7694–7705 (2013)

Santini MT, Rainaldi G: Three-dimensional spheroid model in tumor biology. Pathobiology. 67. 148–157 (1999)

Schmidbauer B, Menhart K, Hellwig D, Grosse J: Differentiated Thyroid Cancer-Treatment: State of the Art. Int J Mol Sci. 18. 1292 (2017)

Schönberger J, Bauer J, Spruß T, Weber G, Chahoud I, Eilles C, Grimm D: Establishment and characterization of the follicular thyroid carcinoma cell line ML-1. J. Mol. Med. 78. 102–110 (2000)

Schwarz RP, Goodwin TJ, Wolf DA: Cell culture for three-dimensional modeling in rotating-wall vessels: an application of simulated microgravity. J Tissue Cult Methods. 14. 51–57 (1992)

Shao B, Yago T, Coghill PA, Klopocki AG, Mehta-D'souza P, Schmidtke DW, Rodgers W, McEver RP: Signal-dependent slow leukocyte rolling does not require cytoskeletal anchorage of P-selectin glycoprotein ligand-1 (PSGL-1) or integrin alphaLbeta2. J Biol Chem 287. 19585-19598 (2012)

Sherman SI: Thyroid carcinoma. Lancet 361. 501–511 (2003)

Stamenkovi´c V, Keller G, Nesic D, Cogoli A, Grogan SP: Neocartilage formation in 1 g, simulated, and microgravity environments: implications for tissue engineering. Tissue Eng. Part A. 16. 1729–1736 (2010)

Suhr KB, Tsuboi R, Seo EY, Piao YJ, Lee JH, Park JK, Ogawa H: Sphingosylphosphorylcholine stimulates cellular fibronectin expression through upregulation of IL-6 in cultured human dermal fibroblasts. Arch Dermatol Res. 294. 433-437 (2003)

Sutherland RM, Durand RE: Growth and cellular characteristics of multicell spheroids. Recent Results Cancer Res. 95. 24-49 (1984)

Svejgaard B, Wehland M, Ma X, Kopp S, Sahana J, Warnke E, Aleshcheva G, Hemmersbach R, Hauslage J, Grosse J, Bauer J, Corydon TJ, Islam T, Infanger M, Grimm D: Common Effects on Cancer Cells Exerted by a Random Positioning Machine and a 2D Clinostat. PLoS One. 14. e0135157 (2015)

Tanaka K, Kurebayashi J, Sohda M, Nomura T, Prabhakar U, Yan L, Sonoo H: The expression of monocyte chemotactic protein-1 in papillary thyroid carcinoma is correlated with lymph node metastasis and tumor recurrence. Thyroid. 19. 21–25 (2009)

Terada H, Urano T, Konno H: Association of interleukin-8 and plasminogen activator system in the progression of colorectal cancer. Eur Surg Res. 37. 166–172 (2005)

Ulbrich C, Pietsch J, Grosse J, Wehland M, Schulz H, Saar K, Hübner N, Hauslage J, Hemmersbach R, Braun M, van Loon J, Vagt N, Egli M, Richter P, Einspanier R, Sharbati S, Baltz T, Infanger M, Ma X, Grimm D: Differential gene regulation under altered gravity conditions in follicular thyroid cancer cells: relationship between the extracellular matrix and the cytoskeleton. Cell Physiol Biochem. 28. 185–198 (2011)

Van Loon JJ: Some history and use of the random positioning machine, RPM, in gravity related research. Adv. Space Res. 39. 1161–1165 (2007)

Vorselen D, Roos WH, MacKintosh FC, Wuite GJ, van Loon JJ: The role of the cytoskeleton in sensing changes in gravity by non-specialised cells. FASEB J. 28. 536–547 (2014)

Warnke E, Pietsch J, Wehland M, Bauer J, Infanger M, Görög M, Hemmersbach R, Braun M, Ma X, Sahana J, Grimm D: Spheroid formation of human thyroid cancer cells under simulated microgravity: a possible role of CTGF and CAV1. Cell Commun Signal. 12. 32 (2014)

Warnke E, Kopp S, Wehland M, Hemmersbach R, Bauer J, Pietsch J, Infanger M, Grimm D: Thyroid Cells Exposed to Simulated Microgravity Conditions – Comparison of the Fast Rotating Clinostat and the Random Positioning Machine. Microgravity Sci. Technol. 28. 247–260 (2016)

Warnke E, Pietsch, J, Kopp S, Bauer J, Sahana J, Wehland M, Krüger M, Hemmersbach R, Infanger M, Lützenberg R, Grimm D: Cytokine release and focal adhesion proteins in normal thyroid cells cultured on the random positioning machine. Cell. Physiol. Biochem.43. 257-270 (2017)

Wehland M, Warnke E, Frett T, Hemmersbach R, Hauslage J, Ma X, Alehcheva G, Pietsch J, Bauer J, Grimm D: The impact of microgravity and vibration on gene and protein expression of thyroid cells. Microgravity Sci. Technol. 28. 261-274 (2016)

Xie K: Interleukin-8 and human cancer biology. Cytokine Growth Factor Rev. 12. 375-391 (2001)

Xu J, Zhang Z, Chen J, Liu F, Bai L: Overexpression of β-actin is closely associated with metastasis of gastric cancer. Hepatogastroenterology. 60. 620–623 (2013)

Zhang GJ, Crist SA, McKerrow AK, Xu Y, Ladehoff DC, See WA: Autocrine IL-6 production by human transitional carcinoma cells upregulates expression of the alpha5beta1 firbonectin receptor. J Urol. 163. 1553-1559 (2000)

10. Abbildungsverzeichnis

11. Danksagung

Als Erstes möchte ich Prof. Dr. Daniela Grimm für ihre fortwährende Unterstützung danken. Ihr Engagement und ihre Begeisterung für die Weltraumforschung, ihre Ausdauer und ihr Ehrgeiz große Ziele zu erreichen sind beeindruckend und motivierend.

Ein weiteres Dankeschön geht an meine Zweitbetreuerin PD Dr. Ruth Hemmersbach. Ihr offenes Ohr und ihre konstruktiven Hinweise waren sehr hilfreich. Auch ihrem Team am DLR in Köln danke ich für die herzliche Aufnahme sowie die tatkräftige Unterstützung bei allen Herausforderungen. Kai Wasser danke ich vor allem für die sehr unterhaltsamen Stunden am Klinostaten.

Prof. Dr. Infanger danke ich für die Unterstützung und freundliche Aufnahme an der Universitätsklinik für Plastische, Ästhetische und Handchirurgie.

Herrn Dr. Johann Bauer danke ich für die Hilfe bei der Erstellung von Publikationen, sowie die Einweisung in und Durchführung von Pathway-Analysen.

Dr. Jessica Pietsch gebührt ein riesiges Dankeschön für die grenzenlose Unterstützung bei der Planung von Projekten sowie der Bewältigung von auftretenden Problemen. Die stets geduldige Beantwortung meiner Fragen und ihr umfassendes Fachwissen sind bemerkenswert.

Für die Unterstützung in PCR- und Statistikfragen danke ich Dr. Markus Wehland-von Trebra. Dr. Ganna Aleshcheva, Sascha Kopp, David Echegoyen, Dr. Stefan Riwaldt, Dr. Xiao Ma und Jayashree Sahana danke ich für die motivierende Arbeitsatmosphäre und die tatkräftige Unterstützung im Labor.

PD Dr Christine Hellweg, Anna-Maria Trautmann und allen Organisatoren und Teilnehmern der Helmholtz Space Life Science Research School danke ich für die spannenden Workshops und die schönen gemeinsamen Stunden.

Weiterhin bedanke ich mich bei Prof. Dr. Mertens und den Mitarbeitern der Experimentellen Nephrologie für die Bereitstellung der Geräte für meine Messungen, sowie die Hilfestellung bei Problemen. Ein herzlicher Dank geht darüber hinaus an die Mitarbeiter des Instituts für Anatomie.

Meiner besten Freundin Julia Kazmierowski danke ich für das gewissenhafte Korrekturlesen meiner Arbeit und die Unterstützung, auch in schweren Phasen. Außerdem danke ich meinen Eltern, meinem Freund Matthias und unserem Sohn Gaius, der mir stets ein Lächeln ins Gesicht zaubert.

12. Erklärung

Ich erkläre, dass ich die der Medizinischen Fakultät der Otto-von-Guericke-Universität zur Promotion eingereichte Dissertation mit dem Titel

„**Untersuchungen zur Sphäroidbildung von Schilddrüsenkarzinomzellen in simulierter Mikrogravitation**„

in der Klinik für Plastische, Ästhetische und Handchirurgie ohne sonstige Hilfe durchgeführt und bei der Abfassung der Dissertation keine anderen als die dort aufgeführten Hilfsmittel benutzt habe.

Bei der Abfassung der Dissertation sind Rechte Dritter nicht verletzt worden.

Ich habe diese Dissertation bisher an keiner in- oder ausländischen Hochschule zur Promotion eingereicht. Ich übertrage der Medizinischen Fakultät das Recht, weitere Kopien meiner Dissertation herzustellen und zu vertreiben.

Magdeburg, den 30.08.2017

Elisabeth Warnke

13. Darstellung des Bildungsweges

Elisabeth Gerda Warnke
Westring 14
39110 Magdeburg

Mobil: 0176/72123058
E-Mail: elisabeth.warnke@med.ovgu.de

08.06.1988 geboren in Schönebeck (Elbe)
Verlobt, 1 Kind (2 Jahre)

Aktuelle Tätigkeit

Seit 08/2016 **Fachlehrerin an der Sekundarschule LebenLernen Magdeburg**

- Chemieunterricht in den Klassen 7 – 10
- Ab 08/2017 zusätzlich: Angewandte Naturwissenschaften und Hauswirtschaftsunterricht in den Klassen 5-10
- Sekundarschule LebenLernen in Magdeburg und Schönebeck
- Bildungsträger Oskar Kämmer

Ausbildung

02/2013 – 03/2017 **Doktorandin am Universitätsklinikum Magdeburg**

- Verfassen der Promotion zum Thema: „Untersuchung zur Sphäroidbildung von Schilddrüsenkarzinomzellen in simulierter Mikrogravitation“ in der Arbeitsgruppe Gravitationsbiologie und Translationale Regenerative Medizin
- Mitglied in der Graduiertenschule
- Elternzeit 04/2015 – 03/2016

10/2012 – 03/2017 Mitglied in der **Helmholtz Space Life Science Research School** des DLR, Institut für Luft- und Raumfahrtmedizin

- Interdisziplinäre Space Life Students-Workshops
- Diverse Softskill-Kurse (Research Skills Development, Scientific Writing, Communication and Presentation Skills)
- Diverse Kurse an der Graduiertenschule der Otto-von-Guericke-Universität in Magdeburg

10/2010 – 02/2013 **Studium der Toxikologie, Charité – Universitätsmedizin Berlin**

- Abschluss: Master of Science (1,5)
- Masterarbeit zum Thema „Untersuchung von humanen Schilddrüsenkarzinomzellen nach Bestrahlung: Effekte von Sunitinib“ (1,1) in der Arbeitsgruppe Weltraumbiologie von Prof. Dr. Grimm am Universitätsklinikum Magdeburg

10/2007 – 09/2010 **Studium der Ernährungswissenschaft, Universität Potsdam**

- Abschluss: Bachelor of Science (1,9)
- Bachelorarbeit zum Thema „Welche Rolle spielt p53 bei der Hemmung der Apoptose durch das Selenoprotein GPx2?“ (1,7) in der Arbeitsgruppe Biochemie der Mikronährstoffe von Prof. Dr. Brigelius-Flohé am Deutschen Institut für Ernährungsforschung

09/2000 – 07/2007 Werner-von-Siemens-Gymnasium Magdeburg

- Abschluss: Abitur (1,1)

01/2004 – 11/2004 Schuljahr in Neuseeland

Praktische Erfahrung

07/2008 – 03/2012 Studentische Hilfskraft am **Deutschen Institut für Ernährungsforschung**

- Datenbankarbeit, Literaturrecherche und –beschaffung

08/2011 – 10/2011 Praktikum am **„Aninwah Medical Center“, Ghana**

- Analytik von Blut-, Urin- und Stuhlproben
- Arzneimittelausgabe, Physiotherapie

09/2009 – 10/2009 Praktikum an der **BUAP Universität, Mexiko**

- Mikrobiologische Analyse von Lebensmittel- und Wasserproben

Ehrenamtliches Engagement

Seit 01/2011 Mitgründer der Initiative „Ernährungswissenschaft macht Karriere“

- Vorbereitung und Durchführung von Podiumsdiskussionen beim Kongress der Deutschen Gesellschaft für Ernährung (DGE)

04/2009 – 04/2012 Mitglied bei **IAESTE** – International Association for the Exchange of Students for Technical Experience

- Organisation der Betreuung von 50 ausländischen Praktikanten
- Projektmanagement

04/2008 – 09/2010 Mitglied im **Fachschaftsrat Biologie, Chemie und Ernährungswissenschaft**

- Studentischer Vertreter im Institutsrat und in Berufungskommissionen
- Erstsemesterbetreuung in den Jahren 2009 und 2010

Sprachkenntnisse

Deutsch	Muttersprache
Englisch	Verhandlungssicher
Spanisch	Grundkenntnisse

Magdeburg, 19.08.2017

Elisabeth Warnke

14. Wissenschaftliches Engagement

05/2016 "Lange Nacht der Wissenschaft", Magdeburg

- Organisation und Durchführung des Kongressauftrittes „Magdeburger Space Night"

10/2014 1-wöchiger Forschungsaufenthalt am DLR Institut für Luft- und Raumfahrtmedizin, Abteilung Gravitationsbiologie

- Experimente am 2D-Klinostaten

06/2014 "Science in the City Festival", Kopenhagen, Dänemark

- Organisation und Durchführung des 1-wöchigen Kongressauftrittes "Lift off! Cells in Space"
- Betreuung von Schülergruppen, Ausstellung, Space Quiz

02/2014 2-wöchiger Forschungsaufenthalt zur 24. DLR-Parabelflugkampagne, Bordeaux, Frankreich

- Unterstützung der Experimente am Boden und im Flieger
- Exp. 1: FLUMIAS – Testung eines Fluoreszensmikroskops
- Exp. 2: Einfluss von Kurzzeitschwerelosigkeit auf Zellen

12/2013 13th Gravimeeting, Erlangen

- Vortrag: „Untersuchung zur Sphäroidbildung von Schilddrüsenkarzinomzellen unter simulierter Mikrogravitation - Ein Vergleich von Klinostat und Random Positioning Machine"

11/2013 Seminar „Gravitationsbiologie", Köln

- IMBIO und Zoologisches Institut der RFWU Bonn
- Vortrag zu „Gravitationsbiologische Arbeitsmethoden 1: Zentrifuge und Klinostat"

11/2013 3-wöchiger Forschungsaufenthalt an der Aarhus Universität

- Arbeitsgruppe Space Medicine
- Zellkultur, Versuche auf der Desktop-Random Positioning Maschine, Durchflusszytometrie, Western Blot, Journal Clubs

07/2013 Humans in Space (HIS) 2013, Köln

- Posterpräsentation: „Spheroid formation of human thyroid cancer cells cultured on a 2D-clinostat and a Random Positioning Machine."

07/2013 „Young Fellows Award“ der Deutschen Gesellschaft für Luft- und Raumfahrtmedizin (DGLRM)

02/2013 Space Health Student Week, European Astronaut Center, Köln

- Besichtigung des EACs, Einblicke in das Astronautentraining
- Seminare zur Vorbereitung und Durchführung von Raumfahrtmissionen

09/2012 2-wöchiger Forschungsaufenthalt zur 20. DLR-Parabelflugkampagne, Bordeaux, Frankreich

- Unterstützung in der Zellkultur, Proben Vor- und Nachbereitung

15. Anhang

15.1 Publikation 1

Warnke E, Pietsch J, Wehland M, Bauer J, Infanger M, Görög M, Hemmersbach R, Braun M, Ma X, Sahana J, Grimm D: Spheroid formation of human thyroid cancer cells under simulated microgravity: a possible role of CTGF and CAV1. Cell Commun Signal. 12. 32 (2014).

CELL COMMUNICATION & SIGNALING

RESEARCH Open Access

Spheroid formation of human thyroid cancer cells under simulated microgravity: a possible role of CTGF and CAV1

Elisabeth Warnke[1], Jessica Pietsch[1], Markus Wehland[1], Johann Bauer[2], Manfred Infanger[1], Mark Görög[3], Ruth Hemmersbach[3], Markus Braun[4], Xiao Ma[5], Jayashree Sahana[5] and Daniela Grimm[1,5*]

Abstract

Background: Multicellular tumor spheroids (MCTS) formed scaffold-free under microgravity are of high interest for research and medicine. Their formation mechanism can be studied in space in real microgravity or on Earth using ground-based facilities (GBF), which simulate microgravity. On Earth, these experiments are more cost-efficient and easily performable. However, each GBF might exert device-specific and altered superimposingly gravity-dependent effects on the cells.

Results: FTC-133 human thyroid cancer cells were cultivated on a 2D clinostat (CN) and a random positioning machine (RPM) and compared with corresponding 1 *g* control cells. Harvested cell samples were investigated by microscopy, quantitative realtime-PCR and Multi-Analyte Profiling. Spheroid formation and growth occurred during 72 h of cultivation on both devices. Cytokine secretion and gene activation patterns frequently altered in different ways, when the cells were cultured either on the RPM or the CN. A decreased expression of *CAV1* and *CTGF* in MCTS compared to adherent cells was observed after cultivation on both machines.

Conclusion: The development of MCTS proceeds similarly on the RPM and the CN resembling the situation observed under real microgravity conditions, while no MCTS formation was observed at 1 *g* under identical experimental conditions. Simultaneously, changes in the regulation of *CTGF* and *CAV1* appeared in a comparable manner on both machines. A relationship between these molecules and MCTS formation is discussed.

Keywords: Adherent growth, Three-dimensional growth, Cytokine, Microgravity, MCTS, RPM, 2D clinostat

Background

During a recent flight on board the Shenzhou-8 spacecraft human follicular thyroid cancer cells (FTC-133) were exposed to real microgravity for 10 days [1,2]. The returned samples revealed that scaffold-free formation of multicellular tumor cell spheroids (MCTS) occurred while the cells had been exposed to real microgravity. The spheroids obtained after landing of the space ship return capsule showed a similar shape but larger diameters (5–10 mm) than those usually induced on Earth with the help of a random positioning machine (RPM) [1-4]. In contrast, 1 *g* controls kept under static conditions remained adherent and formed no spheroids. From these results we concluded that microgravity could be a major cause of transition from 2- to 3-dimensional cellular growth. However, involved molecules and signaling pathways responsible for this change of growth behavior remained unknown [5].

In order to understand and explain the effects of altered gravity on spheroid formation, we complemented our studies using two different ground-based facilities in order to simulate microgravity conditions – the 2D clinostat (CN) and the RPM. Both devices are cost-efficient and enable a sufficient number of experiments, which is rarely achieved under real microgravity conditions [6]. Each of these ground-based approaches prevents cell sedimenta-

* Correspondence: daniela.grimm@farm.au.dk
[1]Clinic for Plastic, Aesthetic and Hand Surgery, Otto-von-Guericke-University Magdeburg, Magdeburg, Germany
[5]Institute of Biomedicine, Pharmacology, Aarhus University, Wilhelm Meyers Allé 4, DK-8000 Aarhus C, Denmark
Full list of author information is available at the end of the article

tion, however, in a device-specific manner. On the clinostat, sedimentation is prevented by a fast and constant rotation of the samples around one horizontal axis, assuming that the sample does no longer perceive the gravity stimulus [7]. In contrast, the RPM consists of two independently rotating frames enabling a 3D rotation with random speed and random direction of the samples aiming to alter the influence of the gravity vector [8,9].

Considering the construction of both machines, we concluded that a permanent change of the direction of the gravity vector and thus prevention of sedimentation is a common capacity of both machines, while their particular modes of operations are rather different. Therefore, we aimed to analyze whether biological processes triggered by altered gravity may show identical or different results after exposure on these two kinds of devices.

In order to prove ground-based microgravity simulation approaches, we investigated human follicular thyroid cancer cells (FTC-133) cultivated either on the CN or the RPM in a parallel manner focusing on the formation of spheroids as well as on alterations of gene expression and protein secretion. We learned that spheroids are formed on both devices and concluded that caveolin-1 (CAV1) and connective tissue growth factor (CTGF) could be directly involved in the initiation of 3D cell growth.

Results

Spheroid formation on the RPM and the CN

Subconfluent monolayers of human follicular thyroid carcinoma cells (FTC-133) were cultivated either on the RPM or on the CN and in parallel to the 1 *g* controls located in the same incubator, respectively. On both devices spheroid formation progressed like shown in Figure 1 for cells harvested from the CN. While under static 1 *g* conditions (1 *g* controls), the cells remained adherent (Figure 1 A-C), two cell populations developed within the culture flasks mounted on each of the two machines, respectively (Figure 1 D-I). Of these populations, one continued to grow adherently (AD cells) (Figure 1 D-F), the other one detached from the bottom of the culture flask and assembled to MCTS (Figure 1 H-I). The separation of the two cell populations is delayed, as 4 h after exposure to the devices only adherent growth was observed in each sample (Figure 1 A, D, G). After approximately 24 h early spheroids became visible on each of both the devices in addition to the adherently growing cells (Figure 1 E, H). During the subsequent 48 h, spheroids became more numerous and larger, while adherently growing cells were still present (Figure 1 F, I). Spheroid size can be assumed to be around 100 μm on the clinostat, as shown in Figure 1, but also reaching up to 1 mm on the RPM as previously published by Pietsch *et al.* [4].

Differential gene expression in FTC-133 cells after exposure to CN and RPM

After spheroid formation was observed on the RPM and the CN, we were interested to see whether similar alterations of mRNA expression occurred on both machines. Therefore, qPCR on several types of mRNA was performed, which had been recognized in former experiments on FTC-133 cells exposed to the RPM for 24 h to be important for MCTS formation [10]. The selected genes belong to several biological categories including cytoskeletal proteins, and factors of growth, apoptosis, angiogenesis and signal transduction (Table 1).

As shown in Figure 1, after a 4 h-incubation on the RPM and on the CN the whole FTC-133 population grew adherently like in 1 *g*-control samples. Nevertheless, some mRNA changes were already found in cells harvested from either machine as compared to control cells. An up-regulation in the *CTGF* gene expression was observed in cell cultures on both devices. However, an up-regulation of *CAV2* and a down-regulation of *ERK1* gene expression were only evident after culturing on the CN (Figure 2).

After 72 h of exposure to the CN or the RPM, cells had parted into adherent cells (AD) and cells forming multicellular tumor spheroids (MCTS), which floated in the supernatant (Figure 1 I). At this time, two fractions were harvested from the CN and the RPM, respectively. Subsequently, it was investigated how the expression of the selected genes (Table 1) had been regulated within the 4 cell samples indicated in Figure 3 as compared to the corresponding static ground controls (1 *g*). Interestingly, the regulation of *CTGF* and *CAV1* split on both machines equally. In adherent cells, *CTGF* remained up-regulated and *CAV1* unchanged, while in MCTS the expression of these two genes was decreased (Figure 3 E-F). Other genes have also changed their expression behavior, but differently, when incubated on the two machines. Exposure of FTC-133 cells to the RPM led to an up-regulation of *ERK1* and *EGF* gene-expression in MCTS, but did not affect one of the selected genes in AD cells. In contrast, exposure of the same type of cells to CN triggered down-regulation of *ERK1*, *ITGB1,* and *PRKCA* gene-expression in MCTS only (Figure 3 I, M, O), but decreased expression of *CAV2* and *IL8* in both, AD and MCTS cells (Figure 3 C, K).

The translation from mRNA to protein is a complex process, and results obtained on mRNA level do not necessarily reflect the situation on the protein level. Therefore, investigations of CN- and RPM- related effects on cytokine release were performed additionally using Multi-Analyte Profiling Technology (MAP).

Cytokine release of FTC-133 cells after 72 h exposure to RPM and CN

Concentrations of selected cytokines within the various culture supernatants were determined by MAP in order to

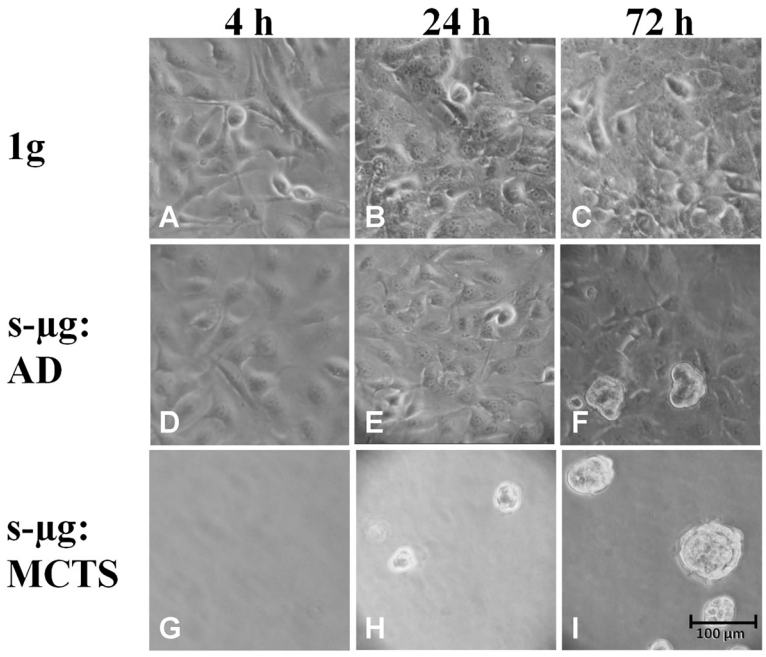

Figure 1 Phase-contrast microscopy of FTC-133 after culturing on the CN or as corresponding 1g control. The cells grew exclusively as adherent monolayers (AD) in 1 g controls **(A-C)**. On the CN, the FTC-133 cell population began to split in adherent cells **(E, F)** and MCTS cells **(H, I)** after 24 h clinorotation. 1 g control, adherent cells, and MCTS after 4 h **(A, D, G)**, 24 h **(B, E, H)**, and 72 h **(C, F, I)** of clinorotation.

estimate the secretion activities of the cells (Table 2). As compared to the relevant 1*g* ground controls, significantly higher amounts of GM-CSF, IL-6, IL-8, BDNF, Eotaxin-1, ICAM1, IL-1α, IL-1β, IL-1Ra, IL-12p40, IL-15, IL-17, IL-23, MMP-3 and SCF were detected in the supernatants of FTC-133 cells cultured on the RPM for 72 h. In contrast, significantly lower quantities of GM-CSF, IL-6, IL-8, MIP-1α, MIP-1β and BDNF were detected in cell supernatants of CN samples than in 1*g* control supernatants (Table 2) after 72 h cell culturing. After cultivation on both machines, however, a tendency of the cells to increase eotaxin-1 and to decrease VEGF secretion was observed in a comparable manner (Table 2).

Discussion

Spheroid formation occurs on both machines

The main result of this study is that FTC-133 cells form spheroids on the CN as well as on the RPM like they did during the Shenzhou-8 spaceflight in real microgravity [1,2]. During the MCTS formation process, the cells were separated into two populations. One continued adherent cell growth, while the other one detached and formed MCTS. Cultivation on the CN and the RPM resulted in spheroid formation like it was observed in real microgravity. Hence, both machines equally influence the cells in this respect. However, different device-specific alterations of gene-expression and cytokine secretion were found after 4 and 72 h cultivation, indicating device-specific characteristics. Common effects could be due to the prevention of sedimentation. Nevertheless, data from real microgravity are needed to clarify the situation and to control for any possibly confounding variables in the GBF and to choose the appropriate microgravity approach. A review on the suitability of diverse ground-based facilities was given by Herranz *et al.,* indicating that both, CN and RPM are generally suitable for adherent mammalian cells [6]. Nevertheless, it is also clearly stated, that although some similar results in s-µ*g* and real µ*g* were achieved, extensive studies have to be performed for each biological system and thus, individually for each type of the cell culture of interest [6]. For future studies, equal time frames, hardware and procedures should be used in space and ground-based studies in order to exclude an impact of external factors influencing the results.

Spheroids formed scaffold-free under the condition of microgravity are valuable models for tumor research [1,3,11], as they resemble the *in vivo* situation much better than 2D monolayer cultures or spheroids grown on Earth using liquid overlay or spinner flask techniques [12,13], which consist mainly of concentric layers surrounding central necrotic cells by a thin shell [14]. The importance of studies on tumor cells exposed to microgravity was recently reviewed by Becker and Souza [15]. However, MCTS generated under simulated microgravity conditions show viable cells throughout the whole body and lack necrotic centers, even if the thyroid cancer cells (ML-1) had formed spheroids with diameters of up to 300 µm [3]. The similarity between *in vivo* tumors and RPM- or CN-derived MCTS is explained by the following hypothesis:

Table 1 Primers used for quantitative real-time PCR

Gene	*Primer name*	*Sequence*
18S rRNA	18S-F	GGAGCCTGCGGCTTAATTT
	18S-R	CAACTAAGAACGGCCATGCA
CAV1	CAV1-F	GTACGACGCGCACACCAA
	CAV1-R	TCCCTTCTGGTTCTGCAATCA
CAV2	CAV2-F	GATCCCCACCGGCTCAAC
	CAV2-R	CACCGGCTCTGCGATCA
CD44	CD44-F	ACCCTCCCCTCATTCACCAT
	CD44-R	GTTGTACTACTAGGAGTTGCCTGGATT
CTGF	CTGF-F	ACAAGGGCCTCTTCTGTGACTT
	CTGF-R	GGTACACCGTACCACCGAAGAT
EGF	EGF-F	TGCCAGCTGCACAAATACAGA
	EGF-R	TCTTACGGAATAGTGGTGGTCATC
ERK1	ERK1-F	ACCTGCGACCTTAAGATTTGTGA
	ERK1-R	AGCCACATACTCCGTCAGGAA
IL8	IL8-F	TGGCAGCCTTCCTGATTTCT
	IL8-R	GGGTGGAAAGGTTTGGAGTATG
ITGB1	ITGB1-F	GAAAACAGCGCATATCTGGAAATT
	ITGB1-R	CAGCCAATCAGTGATCCACAA
NFKBP65	NFKBP65-F	CGCTTCTTCACACACTGGATTC
	NFKBP65-R	ACTGCCGGGATGGCTTCT
OPN	OPN-F	CGAGGTGATAGTGTGGTTTAT GGA
	OPN-R	CGTCTGTAGCATCAGGGTACTG
PRKCA	PKCC-F	CATTCAACAGCTGGGCAAGTT
	PKCC-R	GTAGATGATGCCCTGATTGTGAAG
TLN1	TLN1-F	GATGGCTATTACTCAGTACAGACAACTGA
	TLN1-F	CATAGTAGACTCCTCATCTCCTTCCA
VEGFA	VEGFA-F	GCGCTGATAGACATCCATGAAC
	VEGFA-R	CTACCTCCACCATGCCAAGTG
VEGFD	VEGFD-F	TGCAGGAGGAAAATCCACTTG
	VEGFD-R	CTCGCAACGATCTTCGTCAA
NGAL	NGAL-F	AGGGAGTACTTCAAGATCACCCTCTA
	NGAL-R	AGAGATTTGGAGAAGCGGATGA
MSN	MSN-F	GAAATTTGTCATCAAGCCCATTG
	MSN-R	CCATGCAAGGCCAAGAT

All sequences are given in 5′-3′ direction.

On the RPM or the CN, cells can undergo a transition from a 2- to a 3-dimensional growth, with the adherent layer serving as a starting point. Therefore, cell-cell contacts are established by forces of biochemical components expressed on the cell surfaces in a cell type specific manner under low shear forces [3]. Results of former RPM experiments with the two human follicular thyroid carcinoma cell lines FTC-133 and CGTH W-1 showed differences in the size of spheroids formed which were correlated to their capability to bind to fibronectin [4].

Genes and proteins playing a possible role in spheroid formation

As compared to the corresponding 1*g* controls, higher amounts of the selected cytokines were frequently detected in supernatants obtained from RPM cultures and lower quantities in those harvested from CN cultures, respectively (Table 2), clearly indicating device-specific differences. Interestingly, VEGF secretion indicated a tendency of down-regulation, while eotaxin-1 suggested up-regulation on the CN as well as on the RPM after 72 h (Table 2). Former investigations of culture supernatants of samples cultured on the RPM or returned from the Shenzhou-8 spaceflight experiment showed a different picture. No changes of EGF and VEGF secretion were observed after real microgravity exposure, while both cytokines were significantly down-regulated after a 10d-RPM-exposure [2]. The different cytokine concentrations could be due to a change of the secretion activity during prolonged incubation under microgravity when the transition from a 2- to a 3-dimensional growth is completed as it has been shown for human endothelial cells [16,17]. A comparison of cytokines in the supernatant appears only possible during incubation within a few days, as investigation of IL-6 after 1 and 3 days performed in this and a former study [10] suggested. VEGF prevents apoptosis in thyroid carcinomas in an autocrine manner [18]. Its reduction may contribute to an enhanced apoptotic rate in thyroid cells cultured on the RPM [3]. Eotaxin-1 induces changes in the cytoskeleton and cell morphology and thus could favor the transition from a 2- to a 3-dimensional kind of growth [19].

Although spheroids were not seen in the cultures on both machines after 4 h, a change in gene expression activity was already expected based on earlier parabolic flight experiments [20-22]. Indeed, three of the selected genes were found to be changed. Most interesting of them is *CTGF's* significantly enhanced expression as compared to the corresponding 1*g* controls. It remained up-regulated for another 68 h in AD cells on both machines, while the MCTS cells showed *CTGF* mRNA concentrations even lower than the control cells after 72 h of culturing. The split of *CTGF* gene expression between adherent and MCTS cells corresponds nicely to earlier data from 10 d RPM and spaceflight experiments, which indicated more mRNA in AD than in MCTS cells [2] and could therefore be a microgravity-dependent process involved in spheroid formation. *CTGF* was found to be over-expressed in papillary thyroid carcinoma correlating with metastasis, size and clinical stage [23]. It was also suggested to play an important role in angiogenesis and tumorigenesis of prostate cancer [24]. Its reduction in MCTS cells could hint to a diminished aggressiveness of cancer cells incorporated in MCTS (manuscript in preparation).

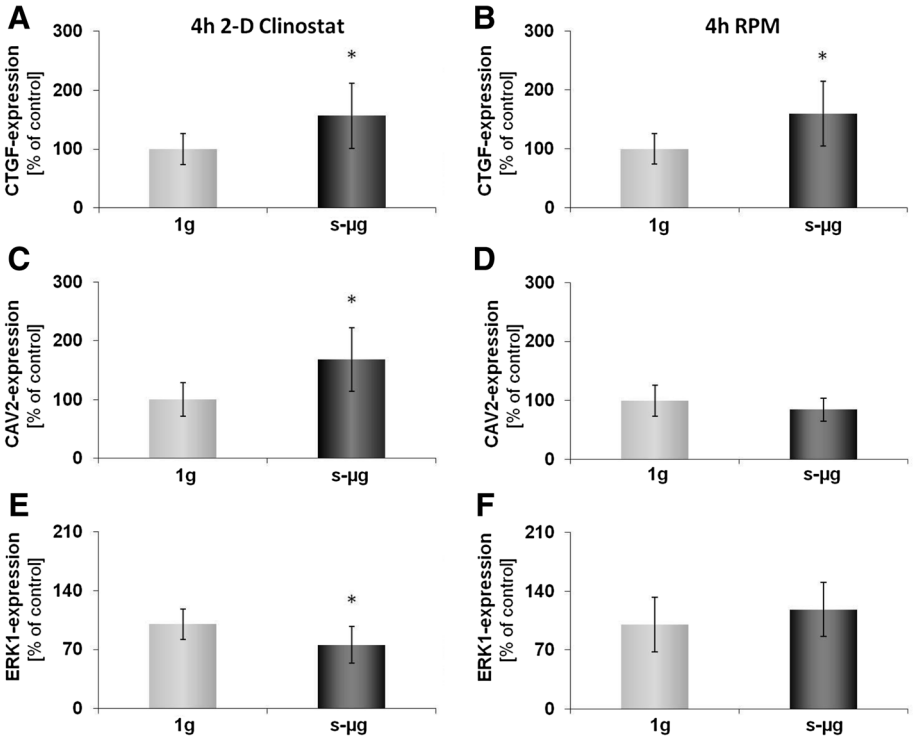

Figure 2 Quantitative real-time PCR for the determination of alterations in gene-expression of selected genes after 4 h. CTGF **(A, B)**, CAV2 **(C, D)** and ERK1 **(E, F)** gene expression was analyzed after 4 h exposure of the cells to 2-D Clinostat **(A, C, E)** or random positioning machine (RPM; **B**, **D**, **F**). CTGF **(A, B)** was upregulated on both machines while CAV2 **(C)** and ERK1 **(E)** were differentially expressed on the CN only. All results are shown as mean ± standard deviation (SD) of n = 10 independent samples, with significance indicated by *P < 0.05 vs. 1g.

Besides *CTGF*, genes of adherent cells remained unaffected until 72 h on the RPM, while expression of *CAV1, EGF* and *ERK1* had been altered in the MCTS. In contrast, after 72 h on the CN, *CAV2* and *IL8* expression were changed in AD cells and *CAV1*, *CAV2*, *CTGF*, *ERK1* and *IL8* in the MCTS. Most interesting of these observations was a down-regulation of *CAV1* and an up-regulation of *ERK1* in MCTS cells after three days following an at least one-day-lasting stability of these genes [10,25], which differ from the *CAV2* gene that is stable only for 4 h (Figure 2) but down-regulated after 24 h and 72 h [10]. Caveolin-1 is an integral membrane protein and plays crucial roles in the regulation of cellular proliferation, differentiation and apoptosis [26]. The down-regulation of caveolin-1 appears to enhance the capacity of the cell to incorporate in a tissue [27]. Furthermore, the expression of this protein seems to be gravisensitive, because an overexpression in healthy mice staying in space had been observed [28]. Since *CAV1* is an obviously gravisensitive gene and its product influences the incorporation of cells in tissue, we conclude from our observations that *CAV1* may play a role in microgravity-dependent MCTS formation.

Device-dependent cell modification

Unexpectedly, most of the selected genes and cytokines were differently expressed or secreted, respectively, depending on which kind of simulation device MCTS were formed. We conclude that during MCTS formation considerable alterations of various cellular molecules occur. Some of them might not be directly related to the process of 3D cell aggregation, but by products generated by device-dependent modifications [29]. A comparative study in space will help to discriminate microgravity-induced alterations from other physical stimuli due to vibration, shearing forces, etc. generated by the simulators. The 2D clinostat rotating constantly at 60 rpm generates residual accelerations below 0.012 *g* within the distance of ±3 mm around the center of the flask [30]. Cells located at further distance from the rotation axis are exposed to accelerations reaching up to 0.036 *g* at about ±9 mm. Significant differences in gene expression within these acceleration intervals have been shown by Eiermann *et al.* [30]. Based on these findings, only cells within the central 6 mm (≤0.012 *g*) of a slide were harvested and analyzed in the present study. An exception had to be made for supernatants which were collected in total, as a distinction

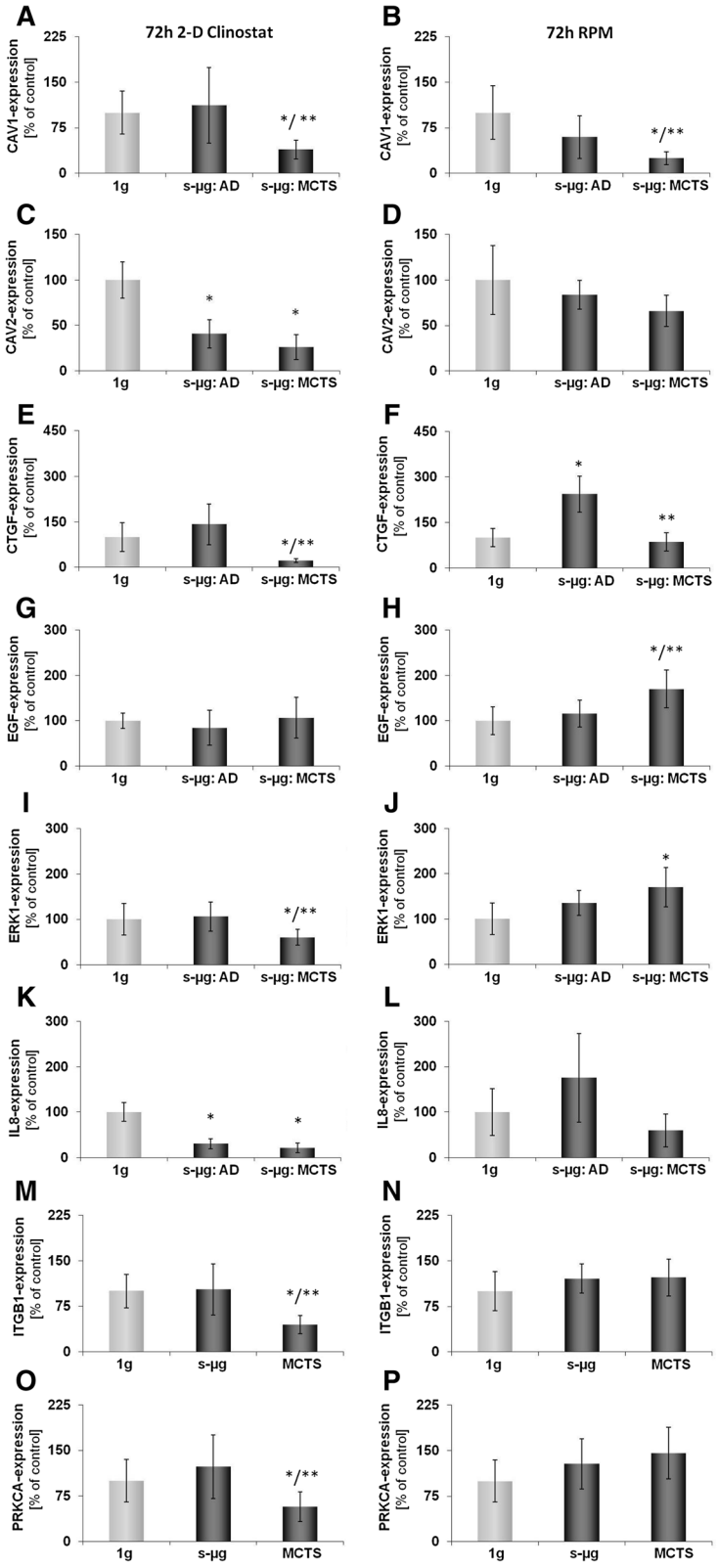

Figure 3 (See legend on next page.)

(See figure on previous page.)
Figure 3 Quantitative real-time PCR for the determination of alterations in gene-expression of selected genes after 72 h. CAV1 **(A, B)**, CAV2 **(C, D)**, CTGF **(E, F)**, EGF **(G, H)**, ERK1 **(I, J)**, IL-8 **(K, L)**, ITGB1 **(M, N)**, and PRKCA **(O, P)** gene expression was analyzed after 72 h exposure of the cells to 2-D Clinostat **(A, C, E, G, I, K, M, O)** or random positioning machine (RPM; **B**, **D**, **F**, **H**, **J**, **L**, **N**, **P**). After 72 h culturing, the FTC-133 cells grew adherently (AD) or within the MCTS. On both machines CAV1 **(C, D)** was down-regulated in the MCTS cells and CTGF **(E, F)** was differently expressed in AD and MCTS, respectively. All results are shown as mean ± standard deviation (SD) of n = 10 independent samples, with significance indicated by *P < 0.05 vs. 1g, **P < 0.05 vs. s-μg: AD.

between different acceleration levels was not possible. Therefore, supernatants were enriched by cytokines of all cells from the flasks. Whether gravity forces in a range of 0.012 *g* and 0.036 *g* have a separated influence on the cell behavior has not yet been clarified [30,31]. Either coating of the flasks in the parts outside the area of interest in order to prevent initial cell attachment or a different geometry of the flasks themselves, with an enlarged area along the rotation axis would be convenient to avoid a mixture in cytokine release.

Table 2 Cytokines detected in supernatants of FTC-133 cells after 72 h incubation

	2D Clinostat			Random positioning machine		
Factor	**LDD (pg/mL)**	**72 h 1g (pg/mL)**	**72 h s-μg (pg/mL)**	**LDD (pg/mL)**	**72 h 1g (pg/mL)**	**72 h s-μg (pg/mL)**
GM-CSF	3.2	1536 ± 166	1172 ± 31*	9.3	46.8 ± 6.9	110.8 ± 12.0*
IFN-γ	0.49	n.d.	n.d.	0.58	n.d.	n.d.
IL-2	1.0	1.9 ± 0.33	n.d.	2.6	n.d.	n.d.
IL-3	1.1	n.d.	n.d.	2.0	n.d.	n.d.
IL-4	4.4	n.d.	n.d.	3.2	n.d.	n.d.
IL-5	1.0	n.d.	n.d.	0.73	n.d.	n.d.
IL-6	0.84	282 ± 37	204 ± 17*	0.85	43.8 ± 8.4	70 ± 15.6*
IL-7	2.1	n.d.	2.1 ± 0.3	5.5	n.d.	n.d.
IL-8	0.63	7604 ± 410	5586 ± 267*	0.49	226 ± 31	350 ± 36*
IL-10	1.1	n.d.	n.d.	1.5	n.d.	n.d.
IL-18	3.7	n.d.	n.d.	3.2	n.d.	n.d.
MIP-1α	8.2	3086 ± 390	2198 ± 379*	6.0	113 ± 18	137 ± 24
MIP-1β	4.0	261 ± 46	166 ± 28*	4.6	n.d.	n.d.
MCP-1	4.6	47 ± 6	40 ± 3	4.9	n.d.	n.d.
TNF-α	2.9	8.9 ± 1.2	7.0 ± 1.3	3.1	n.d.	n.d.
TNF-β	2.3	2.3 ± 0.4	n.d.	4.4	n.d.	n.d.
BDNF	3.0	20 ± 1.7	16 ± 1.7*	6.2	41.2 ± 4.6	76.6 ± 4.7*
Eotaxin-1	3.7	11.8 ± 1.8	12.4 ± 2.3	13	75.4 ± 9.9	99.4 ± 9.8*
ICAM1	270	360 ± 74	350 ± 73	620	1328 ± 274	1840 ± 150*
IL-1α	0.24	n.d.	n.d.	0.19	0.85 ± 0.11	1.60 ± 0.29*
IL-1β	0.3	n.d.	n.d.	0.25	1.14 ± 0.22	2.02 ± 0.34*
IL-1ra	8.7	n.d.	n.d.	14	127 ± 38	226 ± 24*
IL-12p40	16	n.d.	n.d.	17	128 ± 21	206 ± 29*
IL-12p70	4.8	7.8 ± 0.6	7.3 ± 0.9	4.5	36.0 ± 4.2	46.2 ± 6.1
IL-15	39.0	n.d.	n.d.	41	142 ± 27	208 ± 28*
IL-17	0.51	1.14 ± 0.32	1.0 ± 0.16	0.6	2.5 ± 0.4	4.5 ± 0.6*
IL-23	51	n.d.	n.d.	69	590 ± 117	868 ± 78*
MMP-3	5.8	260 ± 22	256 ± 19	7.4	51.2 ± 11.3	90.8 ± 11.1*
SCF	13	24 ± 4	19 ± 2	9.0	59.0 ± 16.1	94.6 ± 11.5*
VEGF	1.4	3062 ± 539	2814 ± 309	4.2	6048 ± 791	5044 ± 677

Values are given with mean ± SD; 1*g*, corresponding ground control; n.d., not detectable; *P <0,05 for device sample vs. corresponding 1*g* ground control; LDD (Least Detectable Dose)-determined as the mean ± 3 standard deviations of 20 blank readings.

Concerning clinorotation, no relative fluid motion is assumed in a closed completely filled and air bubble-free container exposed to the CN due to its linear and constant acceleration mode [32]. In contrast, chaotic fluid motion is caused on a RPM operating in real random mode due to random changes of speed and direction of the platform movement [33-35]. Although the magnitude of forces of fluid motion, which does not exceed 0,44 dyn/cm^2 [35], is below that required to trigger cell detachment from surfaces [36,37], it is assumed to be high enough to induce an enhanced convective fluid mixing, which may support nutrient supply and removal of metabolic products and thus optimize the culture conditions for a cell.

Residual accelerations for RPM exposure have to be considered for all 3 *g*-vector components that means in x, y and z directions. Exemplary measurements of a RPM running at 60–120 °/s showed accelerations due to gravity of −1 to +1 *g* for each direction [38]. A slower rotation speed produces less residual acceleration but requires a longer time for averaging of the g-vector. The relation of rotation speed, resulting accelerations and the time a systems needs to detect the alterations of the influence of gravity has to be considered. Even though less residual accelerations can be achieved through a decreased rotation speed, a longer exposure stimulus will be inevitably connected which can possibly lead to a permanent stress stimulus, if sensed by the cells [39].

Shear stress has to be considered as a variable differing between the devices. As shown by Goodwin *et al.* BHK-21 cells exposed to 0.51 dyn/cm^2 consumed 60-70% less glucose, but achieved higher cell counts and aggregation than cells exposed to 0.92 dyn/cm^2, both on the integrated rotating wall vessel (RWV) [40]. Furthermore, experiments by Hammond *et al.* on primary cultures of human renal cortical cells exposed for 6 days to either real microgravity on a space shuttle or cultured on ground-based devices as controls demonstrated 1632 gene changes after the space flight, 5 gene changes after centrifugation and 914 gene changes after cell culturing on the RWV, if a threshold of more than ± three-fold change was set. In addition, as many gene changes in reciprocal as in the same direction were observed, when results from RWV and space cultures were compared [41]. The balancing forces, such as shear, used to offset gravity in RWV systems were suggested to be responsible for changing the character of the culture [41]. Further work by Kaysen *et al.* supports this hypothesis, showing a shear stress dependence of selected *de novo* gene and protein expression during renal epithelial cell culture in RWV [42]. Therefore, different shear stress situations on both devices used in our study seem to be a cause of differences in the results obtained. The problem of internal shear forces due to residual accelerations has been recognized not only in ground-based facilities, but was also predicted to be responsible for differences between 1 g ground controls and 1 *g*-in-flight controls using a 1 *g*-reference centrifuge in space, as described by van Loon *et al.* [43]. An adjustment of the culture flasks to the direction of the forces is suggested in order to obtain an optimal outcome and comparability of the data. Further experiments are required to clarify stress and gravity-related effects and to determine threshold levels for response time and optimal rotation speed in order to simulate optimal microgravity conditions on ground.

Also vibrations are often suggested as a critical parameter in microgravity simulation. As the corresponding 1 *g* controls were cultured next to the devices in the same incubator, the vibration effect should be neglected as both samples 1 *g* and s-μ*g* are exposed to the same external stimulus. The same matter has to be addressed in parabolic flights especially in combination with periods of hypergravity. Experiments with respect to vibration and hypergravity have been performed on two human follicular thyroid cancer cell lines (ML-1 and CGTH W-1) and endothelial cells (EA.hy 926), all suggesting that microgravity effects are stronger than the opposing vibration and hypergravity effects [20-22]. Nevertheless, additional vibration experiments for FTC-133 are of interest as final validation of ground- based and future space data.

A further aspect possibly influencing the results are the different culture containers used due to the geometry of the devices. As the same flasks were used for s-μ*g*-and corresponsing 1 *g*-samples and results were analyzed relatively to the in parallel obtained 1*g*-data, an influence should not be expected for the PCR data. Concerning the MAP data, a possible effect cannot be excluded due to different volume and area proportions.

For the CN, special slide flasks had to be used in order to utilize the harvesting area on the rotation axis to a maximum extent and to adjust a larger amount of samples on the machine. This leads to differences in the proportion of cells/cm^2 and cells/ml for both devices which might have an impact on the cytokine measurements in the supernatant and might influence interaction and signaling of the cells. For the clinostat, a maximum of 0.056×10^6 cells/cm^2 were used for 4 h-experiments. Longer experiments of 24–72 hours were seeded with less density in order to prevent overgrowing in the limited culture area of only 9 cm^2. A culture volume of 20 ml resembles 0.025×10^6 cells/ml. For the RPM equal amounts of cells were used for all time frames, as a bigger culture area of 75 cm^2 and a larger volume of 320 ml culture media was availabe. This leads to 0.053×10^6 cells/cm^2 and 0.0125×10^6 cells/ml. As a consequence, differences in autocrine and paracrine signaling between the cells, due to the differences in cell to area/volume proportion as well as different fluid behavior due to the geometry of the culture flask, clinorotation and random rotation have to be taken into consideration. The hypothesis, that *in vitro* responses of cells to modified inertial

environments might be a manifestation of modified extracellular convective flow has been suggested by Paul Todd already in 1992 [44]. For future experiments, equal culture conditions should be used in order to obtain an optimal comparability of the data. Still, the unique conditions of real microgravity with the loss of gravity-dependent convection and negligible hydrodynamic shear have to be considered when comparing real and s-μ*g* results [15,44,45].

Conclusion

On both, the CN and RPM, spheroid formation of human thyroid cancer cells was observed, whereas, besides a few exceptions, a considerable number of selected genes or cytokines were expressed or secreted differently, although equal kinds of cells formed MCTS on the two machines. The exceptions were *CAV1* and *CTGF* genes as well as VEGF and eotaxin-1 cytokines. We consider them involved in the process of spheroid formation, because their changes consistently accompanied the MCTS formation in similar manner, when cell sedimentation is prevented by RPM or CN or even in real microgravity in space. The study shows the advantage of searching for gravity-sensitive genes and proteins in comparative approach using different machines for microgravity simulation. Our study clearly shows the necessity to verify results from ground-based simulation approaches to the ones obtained in real microgravity conditions to avoid misinterpretations, to learn and to understand device-specific characteristics and finally choose the appropriate simulation approach.

Methods

Culturing of FTC-133 cells

The human follicular thyroid carcinoma cell line FTC-133 [46] was cultured in RPMI-1640 medium at 37°C and 5% CO_2. The medium was supplemented with 100 μg/mL streptomycin, 100 U/mL penicillin and 10% FCS (all Biochrom, Berlin, Germany). One day prior to the CN experiments, cells were seeded in 9 cm^2 slideflasks (Thermo Scientific, Roskilde, Denmark). A cell count of 5×10^5 cells was disseminated for 4 h experiments, 4×10^5 for 24 h and 2×10^5 for 72 h experiments. For the RPM experiments, cells were grown in T75 cell culture flasks (Sarstedt, Numbrecht, Germany). Cells were seeded at a density of 4×10^6 cells per flask. The cells were randomized to be cultivated as static ground controls (1 *g*) or under simulated microgravity conditions (s-μ*g*) on either a RPM or a CN. Ground controls were always placed next to the device in the same incubator. Cells and supernatants were harvested after 4 h or 72 h on ice. The supernatants were aspirated and centrifuged at 4°C. Afterwards, the fluid was transferred to another tube and frozen. The pellet was fixed with RNAlater. After removal of the culture supernatant, cells which remained adherent during incubation, were washed once with PBS and then fixed with RNAlater. For this, in case of the CN the slides were remove from their flask and were slowly dipped first in PBS (5 s) and then transfered to RNAlater until harvesting. T75 culture flasks from the RPM were slowly filled with 10 ml PBS while standing vertically, and were very carefully brought into horizontal position to avoid any disturbance of the cells. PBS was aspirated again before the addition of RNAlater. Afterwards, the cells cultured on the RPM were scraped off the whole bottom surface, while cells cultured on the CN samples were harvested from the inner 6 mm of the slide flask only, because cells of this part experience accelerations of ≤0.012 *g* [30].

Random Positioning Machine (RPM) and 2D clinostat (CN)

For a comparative methodical approach, cells were either cultivated on the Desktop RPM manufactured by Dutch Space (an EADS Astrium company, Leyden, Netherlands) [8] or the Fast Rotating 2D clinostat (DLR, Cologne, Germany) [30]. The Desktop RPM was operated in real random direction mode (60 °/s) and equipped with four T75 flasks per run, fixed to the ground plate, giving a maximum distance of 7.5 cm from the center of rotation.

The 2D clinostat constantly rotated with 60 rpm and was loaded with four slideflasks on each of the 6 parallel rotating axes, summing up to a total of 24 flasks per run. Both devices were placed inside an individual incubator with temperature of 37°C and 5% CO_2. Prior to the experiment, all flasks were completely filled with media avoiding air bubbles carefully, in order to reassure a minimization of turbulences. For harvesting of CN samples, cells of 16 flasks were pooled. Ten samples (n = 10) were collected for each condition: CN, CN corresponding 1*g* control, RPM and RPM corresponding 1*g* control.

Phase contrast microscopy

Phase contrast microscopy was performed for visual observation of the morphology of the cells, using the Axiovert 25 Microscope (Carl Zeiss Microscopy, LLC, United States).

Cytokine measurements by Multi-Analyte Profiling technology

The release of cytokines was investigated via Multi-Analyte Profiling (MAP) as previously described [16,47,48]. For each condition, five supernatants were collected after 72 h and stored at −80°C until testing. The MAP was carried out by Myriad RBM (Austin, Texas, USA) using the Human Cytokine MAP A and B. Briefly, Micro beads carrying specific antibodies, directed against the target analytes, are used to detect the cytokines. A second biotinylated reporter antibody is added, followed by an excess of streptavidin-phycoerythrin solution to develop the multiplexes and thereby enabling the quantification of the cytokines released, via fluorescence detection [49].

RNA isolation and quantitative real-time PCR

RNA isolation and quantitative real-time PCR were performed according to routine protocols [25,50,51]. For CN samples, only the inner 6 mm were harvested with a scratching device. RPM samples were harvested in total. RNA was isolated using RNeasy Mini Kit (Qiagen, Hilden, Germany) following manufacturer instructions. DNase (Qiagen, Hilden, Germany) was added in the process of RNA isolation, in order to diminish residual DNA contaminations. The RNA was quantified via Photometer Ultrospec2010 (Amersham Biosciences, Freiburg, Germany). Reverse transcription was performed using the first strand cDNA synthesis kit (ThermoFisher Scientific, Waltham, US), following manufacturer's instructions. Quantitative real-time PCR was utilized to determine the expression levels of target genes, shown in Table 1, using the 7500 Real-Time PCR System (Applied Biosystems, Darmstadt, Germany). cDNA-selective Primers were designed to span exon-exon boundaries and to have a T_m of ~ 60°C using Primer Express software (Applied Biosystems, Darmstadt, Germany), and were synthesized by TIB Molbiol (Berlin, Germany). All samples were measured in triplicate and normalized to the housekeeper 18S rRNA. Comparative C_T ($\Delta\Delta C_T$) methods were used for relative quantification of transcription levels, with 1 *g* set as 100%.

Statistical Evaluation

Statistical Evaluation was performed using SPSS 15.0 (SPSS, Inc., Chicago, IL, USA). The Mann–Whitney-U-Test was used to compare 1*g* and s-μ*g* conditions, as well as s-μ*g* adherent cells and s-μ*g* MCTS cells. All data is presented as mean ± standard deviation (SD) with a significance level of $p < 0.05$. * indicating the comparison of 1*g* vs. s-μ*g* and ** representing the comparison of s-μ*g* AD vs. s-μ*g* MCTS.

Abbreviations

BDNF: Brain-derived neutrophic factor; CAV: Caveolin; CN: Clinostat; CTGF: Connective tissue growth factor; EGF: Epidermal growth factor; ERK: Extracellular signal-regulated kinase; FCS: Fetal calf serum; FTC: Follicular thyroid cancer; GBF: Ground-based facilities; GM-CSF: Granulocyte-macrophage colony-stimulating factor; IFN: Interferon; IL: Interleukin; ITBG1: Integrin beta 1; LDD: Least detectable dose; MAP: Multi-Analyte Profiling; MCP: Monocyte chemotactic protein; MCTS: Multicellular tumor spheroids; MEK: Mitogen-activated protein kinases; MIP: Macrophage inflammatory protein; MMP: Matrix metalloproteinase; MRNA: Messenger ribonucleic acid; PCR: Polymerase chain reaction; PDGFR: Platelet-derived growth factor receptor; PRKCA: Protein kinase C alpha; RBM: Rules-based medicine; RPM: Random positioning machine; RWV: Rotating Wall Vessel; SCF: Stem cell factor; SD: Standard deviation.

Competing interests

The authors declare that they have no competing interests.

Authors' contributions

JB, DG and RH designed the study. EW and XM conducted the experiments. EW and JB drafted the manuscript. JP, MW and MI supervised and supported the ground-based experiments in Magdeburg. DG supervised the ground-based experiments in Aarhus and helped with the manuscript. RH and MB supervised and supported the ground-based experiments in Cologne. MG was responsible for the design of the 2D clinostat. All authors read and approved the final manuscript.

Acknowledgements

The study was supported by the European Space Agency (ESA; CORA-GBF-PROJECT-2011-005 with contract 4000104144; D.G.) and the German Space Administration (DLR; BMWi grant 50WB1124; D.G.). Elisabeth Warnke is a doctoral candidate of the Helmholtz Space Life Sciences Research School, German Aerospace Center Cologne, Germany and was further sponsored within the "Young Fellows" project of the Deutsche Gesellschaft für Luft- und Raumfahrtmedizin e.V (DGLRM).

Author details

[1]Clinic for Plastic, Aesthetic and Hand Surgery, Otto-von-Guericke-University Magdeburg, Magdeburg, Germany. [2]Max-Planck Institute of Biochemistry, Martinsried, Germany. [3]DLR, German Aerospace Center, Institute of Aerospace Medicine, Cologne, Germany. [4]Institute for Molecular Physiology and Biotechnology of Plants (IMBIO), University of Bonn, Gravitational Biology Group, Kirschallee 1, 53115, Bonn, Germany. [5]Institute of Biomedicine, Pharmacology, Aarhus University, Wilhelm Meyers Allé 4, DK-8000 Aarhus C, Denmark.

Received: 24 January 2014 Accepted: 28 April 2014
Published: 10 May 2014

References

1. Pietsch J, Ma X, Wehland M, Aleshcheva G, Schwarzwälder A, Segerer J, Birlem M, Horn A, Bauer J, Infanger M, Grimm D: **Spheroid formation of human thyroid cancer cells in an automated culturing system during the Shenzhou-8 Space mission.** *Biomaterials* 2013, **34:**7694–7705.
2. Ma X, Pietsch J, Wehland M, Schulz H, Saar K, Hübner N, Bauer J, Braun M, Schwarzwälder A, Segerer J, Birlem M, Horn A, Hemmersbach R, Waßer K, Grosse J, Infanger M, Grimm D: **Differential gene expression profile and altered cytokine secretion of thyroid cancer cells in space.** *FASEB J* 2014, **28:**813–835.
3. Grimm D, Bauer J, Kossmehl P, Shakibaei M, Schönberger J, Pickenhahn H, Schulze-Tanzil G, Vetter R, Eilles C, Paul M, Cogoli A: **Simulated microgravity alters differentiation and increases apoptosis in human follicular thyroid carcinoma cells.** *FASEB J* 2002, **16:**604–606.
4. Pietsch J, Sickmann A, Weber G, Bauer J, Egli M, Wildgruber R, Infanger M, Grimm D: **A proteomic approach to analysing spheroid formation of two human thyroid cell lines cultured on a random positioning machine.** *Proteomics* 2011, **11:**2095–2104.
5. Pietsch J, Bauer J, Egli M, Infanger M, Wise P, Ulbrich C, Grimm D: **The effects of weightlessness on the human organism and mammalian cells.** *Curr Mol Med* 2011, **11:**350–364.
6. Herranz R, Anken R, Boonstra J, Braun M, Christianen PC, de Geest M, Hauslage J, Hilbig R, Hill RJ, Lebert M, Medina FJ, Vagt N, Ullrich O, van Loon JJ, Hemmersbach R: **Ground-based facilities for simulation of microgravity: organism-specific recommend-dations for their use, and recommended terminology.** *Astrobiology* 2013, **13:**1–17.
7. Briegleb W: **Some qualitative and quantitative aspects of the fast-rotating clinostat as a research tool.** *ASGSB Bull* 1992, **5:**23–30.
8. van Loon JJWA: **Some history and use of the random positioning machine, RPM, in gravity related research.** *Adv Space Res* 2007, **39:**1161–1165.
9. van Loon JJWA, Veldhuijzen JP, Kiss J, Wood C, Vd Ende H, Guntemann A, Jones D, de Jong H, Wubbels R: **Microgravity Research Starts on the Ground! Apparatus for Longterm Ground-based Hypo- and Hypergravity Studies" Utilisation of the International Space station.** In *Proceedings of 2nd European Symposium, ESTEC, Noordwijk, The Netherland, 16-18 November 1998.* Edited by Wilson A. Paris: European Space Agency (ESA), ESA-SP Volume 433; 1999:415–419. ISBN 9290927321.
10. Grosse J, Wehland M, Pietsch J, Schulz H, Saar K, Hübner N, Eilles C, Bauer J, Abou-El-Ardat K, Baatout S, Ma X, Infanger M, Hemmersbach R, Grimm D: **Gravity-sensitive signaling drives 3-dimensional formation of multicellular thyroid cancer spheroids.** *FASEB J* 2012, **26:**5124–5140.
11. Santini MT, Rainaldi G: **Three-dimensional spheroid model in tumor biology.** *Pathobiology* 1999, **67:**148–157.
12. Sutherland RM, McCredie JA, Inch WR: **Growth of multicell spheroids in tissue culture as a model of nodular carcinomas.** *J Natl Cancer Inst* 1971, **46:**113–120.
13. Grimm D, Bauer J, Hofstädter F, Riegger GA, Kromer EP: **Characteristics of multicellular spheroids formed by primary cultures of human thyroid tumor cells.** *Thyroid* 1997, **7:**859–865.

14. Mueller-Klieser W: **Tumor Biology and experimental therapeutics.** *Crit Rev Oncol Hematol* 2000, **36:**123–139.
15. Becker JL, Souza GR: **Using space-based investigations to inform cancer research on Earth.** *Nat Rev Cancer* 2013, **13:**315–327.
16. Grimm D, Infanger M, Westphal K, Ulbrich C, Pietsch J, Kossmehl P, Vadrucci S, Baatout S, Flick B, Paul M, Bauer J: **A delayed type of three-dimensional growth of human endothelial cells under simulated weightlessness.** *Tissue Eng Part A* 2009, **15:**2267–2275.
17. Infanger M, Kossmehl P, Shakibaei M, Baatout S, Witzing A, Grosse J, Bauer J, Cogoli A, Faramarzi S, Derradji H, Neefs M, Paul M, Grimm D: **Induction of three-dimensional assembly and increase in apoptosis of human endothelial cells by simulated microgravity: Impact of vascular endothelial growth factor.** *Apoptosis* 2006, **11:**749–764.
18. Vieira JM, Santos SCR, Espadinha C, Correia I, Vag T, Casalou C, Cavaco BM, Catarino AL, Dias S, Leite V: **Expression of vascular endothelial growth factor (VEGF) and its receptors in thyroid carcinomas of follicular origin: a potential autocrine loop.** *Eur J Endocrinol* 2005, **153:**701–709.
19. Kang BN, Ha SG, Ge XN, Hosseinkhani MR, Bahaie NS, Greenberg Y, Blumenthal MN, Puri KD, Rao SP, Sriramarao P: **The p110 delta subunit of PI3K regulates bone marrow-derived eosinophil trafficking and airway eosinophilia in allergen-challenged mice.** *Am J Physiol Lung Cell Mol Physiol* 2012, **302:**L1179–L1191.
20. Ulbrich C, Pietsch J, Grosse J, Wehland M, Schulz H, Saar K, Hübner N, Hauslage J, Hemmersbach R, Braun M, van Loon J, Vagt N, Egli M, Richter P, Einspanier R, Sharbati S, Baltz T, Infanger M, Ma X, Grimm D: **Differential gene regulation under altered gravity conditions in follicular thyroid cancer cells: relationship between the extracellular matrix and the cytoskeleton.** *Cell Physiol Biochem* 2011, **28:**185–198.
21. Grosse J, Wehland M, Pietsch J, Ma X, Ulbrich C, Schulz H, Saar K, Hübner N, Hauslage J, Hemmersbach R, Braun M, van Loon J, Vagt N, Infanger M, Eilles C, Egli M, Richter P, Baltz T, Einspanier R, Sharbati S, Grimm D: **Short-term weightlessness produced by parabolic flight maneuvers altered gene expression patterns in human endothelial cells.** *FASEB J* 2012, **26:**639–655.
22. Wehland M, Ma X, Braun M, Hauslage J, Hemmersbach R, Bauer J, Grosse J, Infanger M, Grimm D: **The impact of altered gravity and vibration on endothelial cells during a parabolic flight.** *Cell Physiol Biochem* 2013, **31:**432–451.
23. Cui L, Zhang Q, Mao Z, Chen J, Wang X, Qu J, Zhang J, Jin D: **CTGF is overexpressed in papillary thyroid carcinoma and promotes the growth of papillary thyroid cancer cells.** *Tumour Biol* 2011, **32:**721–728.
24. Yang F, Tuxhorn JA, Ressler SJ, McAlhany SJ, Dang TD, Rowley DR: **Stromal expression of connective tissue growth factor promotes angiogenesis and prostate cancer tumorigenesis.** *Cancer Res* 2005, **65:**8887–8895.
25. Infanger M, Faramarzi S, Grosse J, Kurth E, Ulbrich C, Bauer J, Wehland M, Kreutz R, Kossmehl P, Paul M, Grimm D: **Expression of vascular endothelial growth factor and receptor tyrosine kinases in cardiac ischemia/reperfusion injury.** *Cardiovasc Pathol* 2007, **16:**291–299.
26. Mo S, Yang S, Cui Z: **New glimpses of caveolin-1 functions in embryonic development and human diseases.** *Front* 2011, **6:**367–376.
27. Lu Z, Ghosh S, Wang Z, Hunter T: **Downregulation of caveolin-1 function by EGF leads to the loss of E-cadherin, increased transcriptional activity of beta-catenin, and enhanced tumor cell invasion.** *Cancer Cell* 2003, **4:**499–515.
28. Masini MA, Albi E, Barmo C, Bonfiglio T, Bruni L, Canesi L, Cataldi S, Curcio F, D'Amora M, Ferri I, Goto K, Kawano F, Lazzarini R, Loreti E, Nakai N, Ohira T, Ohira Y, Palmero S, Prato P, Ricci F, Scarabelli L, Shibaguchi T, Spelat R, Strollo F, Ambesi-Impiombato FS: **The impact of long-term exposure to space environment on adult mammalian organisms: a study on mouse thyroid and testis.** *PLoS One* 2012, **7:**e35418.
29. Pietsch J, Riwaldt S, Bauer J, Sickmann A, Weber G, Grosse J, Infanger M, Eilles C, Grimm D: **Interaction of proteins identified in human thyroid cells.** *Int J Mol Sci* 2013, **14:**1164–1178.
30. Eiermann P, Kopp S, Hauslage J, Hemmersbach R, Gerzer R, Ivanova K: **Adaptation of a 2D clinostat for simulated microgravity experiments with adherent cells.** *Micrograv Sci Technol* 2013, **25:**153–159.
31. de Groot RP, Rijken PJ, den Hertog J, Boonstra J, Verkleij AJ, de Laat SW, Kruijer W: **Microgravity decreases c-fos induction and serum response element activity.** *J Cell Sci* 1990, **97:**33–38.
32. Klaus DM: **Clinostats and Bioreactors.** *Gravit Space Biol Bul* 2001, **14:**55–64.
33. Leguy CAD, Delfos R, Pourquie MJBM, Poelma C, Krooneman J, Westerweel J, van Loon JJWA: **Fluid motion for microgravity simulations in a random positioning machine.** *Gravitat Space Biol* 2011, **25:**36–39.
34. Hemmersbach R, von der Wiesche M, Seibt D: **Ground-based experimental platforms in gravitational biology and human physiology.** *Signal Transduction Special Issue: Signaling in gravity perception: From microorganisms to mammals* 2006, **6:**381–387.
35. Pardo SJ, Patel MJ, Sykes MC, Platt MO, Boyd NL, Sorescu GP, Xu M, van Loon JJ, Wang MD, Jo H: **Simulated microgravity using the Random Positioning Machine inhibits differentiation and alters gene expression profiles of 2T3 preosteoblasts.** *Am J Physiol Cell Physiol* 2005, **288:**C1211–C1221.
36. Zhang X, Jones P, Haswell SJ: **Attachment and detachment of living cells on modified microchannel surfaces in a microfluidic-based lab-on-a-chip system.** *Chem Eng J* 2008, **135:**82–88.
37. Haier J, Nicolson GL: **Role of the cytoskeleton in adhesion stabilization of human colorectal carcinoma cells to extracellular matrix components under dynamic conditions of laminar flow.** *Clin Exp Metastasis* 1999, **17:**713–721.
38. Borst AG, van Loon JJWA: **Technology and Developments for the Random Positioning Machine, RPM.** *Microgravity Sci Technol* 2009, **21:**287–292.
39. Horn A, Ullrich O, Huber K, Hemmersbach R: **PMT (Photomultiplier) Clinostat.** *Microgravity Sci Technol* 2011, **23:**67–71.
40. Goodwin TJ, Prewett TL, Wolf DA, Spaulding GF: **Reduced Shear Stress: A Major Component in the Ability of Mammalian Tissues to Form Three-Dimensional Assemblies in Simulated Microgravi ty.** *J Cell Biochem* 1993, **51:**301–311.
41. Hammond TG, Benes E, O'Reilly KC, Wolf DA, Linnehan RM, Taher A, Kaysen JH, Allen PL, Goodwin TJ: **Mechanical culture conditions effect gene expression: gravity-induced changes on the space shuttle.** *Physiol Genomics* 2000, **3:**163–173.
42. Kaysen JH, Campbell WC, Majewski RR, Goda FO, Navar GL, Lewis FC, Goodwin TJ, Hammond TG: **Select de novo gene and protein expression during renal epithelial cell culture in rotating wall vessels is shear stress dependent.** *J Membr Biol* 1999, **168:**77–89.
43. van Loon JJ, Folgering EH, Bouten CV, Veldhuijzen JP, Smit TH: **Inertial shear forces and the use of centrifuges in gravity research. What is the proper control?** *J Biomech Eng* 2003, **125:**342–346.
44. Todd P: **Physical effects at the cellular level under altered gravity conditions.** *Adv Space Res* 1992, **12:**43–49.
45. Todd P: **Gravity-dependent phenomena at the scale of the single cell.** *ASGSB Bull* 1989, **2:**95–113.
46. Goretzki PE, Frilling A, Simon D, Roeher HD: **Growth regulation of normal thyroids and thyroid tumors in man.** *Recent Results Cancer Res* 1990, **118:**48–63.
47. Grimm D, Bauer J, Ulbrich C, Westphal K, Wehland M, Infanger M, Aleshcheva G, Pietsch J, Ghardi M, Beck M, El-Saghire H, de Saint-Georges L, Baatout S: **Different responsiveness of endothelial cells to vascular endothelial growth factor and basic fibroblast growth factor added to culture media under gravity and simulated microgravity.** *Tissue Eng Part A* 2010, **16:**1559–1573.
48. Grosse J, Warnke E, Pohl F, Magnusson NE, Wehland M, Infanger M, Eilles C, Grimm D: **Impact of sunitinib on human thyroid cancer cells.** *Cell Physiol Biochem* 2013, **32:**154–170.
49. Infanger M, Ulbrich C, Baatout S, Wehland M, Kreutz R, Bauer J, Grosse J, Vadrucci S, Cogoli A, Derradji H, Neefs M, Küsters S, Spain M, Grimm D: **Modeled gravitational unloading induced downregulation of endothelin-1 in human endothelial cells.** *J Cell Biochem* 2007, **101:**1439–1455.
50. Kossmehl P, Kurth E, Faramarzi S, Habighorst B, Shakibaei M, Wehland M, Kreutz R, Infanger M, Danser AH, Grosse J, Paul M, Grimm D: **Mechanisms of apoptosis after ischemia and reperfusion: role of the renin-angiotensin system.** *Apoptosis* 2006, **11:**347–358.
51. Rothermund L, Kreutz R, Kossmehl P, Fredersdorf S, Shakibaei M, Schulze-Tanzil G, Paul M, Grimm D: **Early onset of chondroitin sulfate and osteopontin expression in angiotensin II-dependent left ventricular hypertrophy.** *Am J Hypertens* 2002, **15:**644–652.

doi:10.1186/1478-811X-12-32
Cite this article as: Warnke *et al.*: Spheroid formation of human thyroid cancer cells under simulated microgravity: a possible role of CTGF and CAV1. *Cell Communication and Signaling* 2014 **12**:32.

15.2 Publikation 2

Svejgaard B, Wehland M, Ma X, Kopp S, Sahana J, **Warnke E,** Aleshcheva G, Hemmersbach R, Hauslage J, Grosse J, Bauer J, Corydon TJ, Islam T, Infanger M, Grimm D: Common Effects on Cancer Cells Exerted by a Random Positioning Machine and a 2D Clinostat. PLoS One. 10. e0135157. (2015)

PLOS | ONE

RESEARCH ARTICLE

Common Effects on Cancer Cells Exerted by a Random Positioning Machine and a 2D Clinostat

Benjamin Svejgaard[1], Markus Wehland[2], Xiao Ma[1], Sascha Kopp[1], Jayashree Sahana[1], Elisabeth Warnke[2], Ganna Aleshcheva[2], Ruth Hemmersbach[3], Jens Hauslage[3], Jirka Grosse[4], Johann Bauer[5], Thomas Juhl Corydon[1], Tawhidul Islam[1], Manfred Infanger[2], Daniela Grimm[1]*

1 Department of Biomedicine, Aarhus University, Aarhus, Denmark, **2** Clinic for Plastic, Aesthetic and Hand Surgery, Otto-von-Guericke-University Magdeburg, Magdeburg, Germany, **3** DLR, German Aerospace Center, Institute of Aerospace Medicine, Cologne, Germany, **4** Department of Nuclear Medicine, University of Regensburg, Regensburg, Germany, **5** Max-Planck Institute for Biochemistry, Martinsried, Germany

* daniela.grimm@farm.au.dk

Citation: Svejgaard B, Wehland M, Ma X, Kopp S, Sahana J, Warnke E, et al. (2015) Common Effects on Cancer Cells Exerted by a Random Positioning Machine and a 2D Clinostat. PLoS ONE 10(8): e0135157. doi:10.1371/journal.pone.0135157

Editor: Yoshiaki Taniyama, Osaka University Graduate School of Medicine, JAPAN

Received: January 31, 2015

Accepted: July 19, 2015

Published: August 14, 2015

Data Availability Statement: All relevant data are within the paper.

Funding: The authors would like to thank the German Space Agency (DLR; (DG) BMWi projects 50WB1124 and 50WB1524), the European Space Agency (ESA; ESA-CORA-GBF-2011-005 project Device Comparison; ESA-CORA-GBF- 2013-001 project THYROID 3) (DG), Aarhus University, Denmark (DG), the University of Regensburg (JG), and DGLRM (Young Fellow Program for EW and GA). The funders had no role in study design, data collection and analysis, decision to publish, or preparation of the manuscript.

Abstract

In this study we focused on gravity-sensitive proteins of two human thyroid cancer cell lines (ML-1; RO82-W-1), which were exposed to a 2D clinostat (CLINO), a random positioning machine (RPM) and to normal 1*g*-conditions. After a three (3d)- or seven-day-culture (7d) on the two devices, we found both cell types growing three-dimensionally within multicellular spheroids (MCS) and also cells remaining adherent (AD) to the culture flask, while 1*g*-control cultures only formed adherent monolayers, unless the bottom of the culture dish was covered by agarose. In this case, the cytokines IL-6 and IL-8 facilitated the formation of MCS in both cell lines using the liquid-overlay technique at 1*g*. ML-1 cells grown on the RPM or the CLINO released amounts of IL-6 and MCP-1 into the supernatant, which were significantly elevated as compared to 1*g*-controls. Release of IL-4, IL-7, IL-8, IL-17, eotaxin-1 and VEGF increased time-dependently, but was not significantly influenced by the gravity conditions. After 3d on the RPM or the CLINO, an accumulation of F-actin around the cellular membrane was detectable in AD cells of both cell lines. IL-6 and IL-8 stimulation of ML-1 cells for 3d and 7d influenced the protein contents of $ß_1$-integrin, talin-1, Ki-67, and beta-actin dose-dependently in adherent cells. The $ß_1$-integrin content was significantly decreased in AD and MCS samples compared with 1*g*, while talin-1 was higher expressed in MCS than AD populations. The proliferation marker Ki-67 was elevated in AD samples compared with 1*g* and MCS samples. The ß-actin content of R082-W-1 cells remained unchanged. ML-1 cells exhibited no change in ß-actin in RPM cultures, but a reduction in CLINO samples. Thus, we concluded that simulated microgravity influences the release of cytokines in follicular thyroid cancer cells, and the production of $ß_1$-integrin and talin-1 and predicts an identical effect under real microgravity conditions.

Competing Interests: The authors have declared that no competing interests exist.

Introduction

Prolonged spaceflights often cause deleterious health problems in humans. A number of spaceflight effects have been extensively studied in the past and reviewed [1–4]. Some effects may be explained by well-known physiology; e.g. the lack of gravitational stress on the leg musculature results in a rapid loss of bone and muscle, and the lack of the gravitational vector causes problems related to balance and eye movements [1]. It had been shown that annulling of gravity influences the molecular mechanisms of the cells directly [3]. Cells exposed to real or simulated microgravity change their gene and protein expression behavior [5–7], increase apoptosis [8, 9], retard cell growth [10] and alter the cytoskeleton [11–13]. Moreover, multicellular aggregates were detected, which resembled the organs from which their cells had been derived [14].

In recent years it became apparent that studies on the behavior of cancer cells in space might support cancer research on Earth [15]. Now it is of interest to compare the roles of distinct proteins in cellular adaption to changed environmental conditions (microgravity). We characterized various lines of human thyroid cancer cells grown under conditions of real and simulated microgravity with the aim to find possibilities of reducing the cancer cell aggressiveness [16–18]. Since experiments under real microgravity i.e. spaceflight possibilities are rare and expensive [16], a great part of the studies was performed using devices aiming to simulate microgravity on Earth [3, 19]. However, each device affects the cells not only by preventing sedimentation, but also by characteristics of its operation mode, which include transient hypergravity or vibration [20]. Therefore, it was considered that some observations made on cells cultured on a microgravity simulating device may not solely be due to preventing cell sedimentation but also due to device-specific effects [18]. Furthermore, we also observed that effects are specific for defined types of the thyroid cell lines [21]. In order to investigate the influence of altered gravity on the cellular level, we studied different cancer cells on different devices simulating microgravity according to comparable protocols. Prior to characterization, human thyroid cells FTC-133, ML-1, and HTU-5 were cultured on the Random Positioning Machine (RPM, Fig 1A) [17], but only FTC-133 cells on the RPM and the fast rotating 2D-Clinostat (CLINO, Fig 1B) [18] and in Space [16, 22, 23]. The experiments revealed several aspects and pointed to cytoskeletal proteins and cytokines as prime targets of microgravity effects [3, 19, 22, 23].

In this study we investigated the impact of simulated microgravity using the RPM and the CLINO devices on two human follicular thyroid cancer cell lines (ML-1, RO82-W-1) in a parallel manner either for three (3d) or seven (7d) days, respectively, before selected cytokines and cytoskeletal proteins were quantified. To evaluate the possible role of the cytokines IL-6 and IL-8 for the expression of selected proteins in thyroid cancer cells, we studied the impact of IL-6 and IL-8 application on Ki-67, $ß_1$-integrin, talin-1, and beta-actin proteins in adherent ML-1 cells. Moreover, we focused on the role of the cytokines IL-6 and IL-8 in ML-1 and RO82-W-1 spheroid formation using the liquid-overlay technique under 1*g*-conditions [24]. Cytokines and cytoskeletal proteins, whose release or expression was altered, respectively, are discussed with respect to their specific roles in thyroid cancer.

Methods

Cell lines

ML-1 cell line. Monolayers of ML-1 follicular thyroid cancer cells [25] were cultured on either the RPM or the clinostat. The ML-1 cell line derived from a recurring tumor of a poorly differentiated follicular thyroid carcinoma (stage pT4) of a 50-year-old woman [25]. The cell line has a doubling time of 4 days. The cells take up glucose, secrete thyroglobulin, thyroxine, and triiodothyronine and are tumorigenic in nude mice.

Fig 1. A: Random Positioning Machine (RPM) and **B**: 2D-Clinostat.

doi:10.1371/journal.pone.0135157.g001

UCLA RO82-W-1 cell line. The RO82-W-1 cell line was established by Estour *et al.* in 1989 [26]. The cell line was purchased from Sigma-Aldrich Chemie (Munich, Germany). This cell line derived from the metastases of a follicular carcinoma in a female patient. Although the primary tumor of RO82-W-1 released thyroglobulin (Tg) into the circulation, the uptake of I131 was less than 2% [26]. RO82-W-1 cells are Tg-positive and are also tumorigenic in nude mice [26].

Both cell lines were cultivated in RPMI-1640 medium at 37°C and 5% CO_2. The medium was supplemented with 100 μg/mL streptomycin, 100 U/mL penicillin and 10% FCS (all Biochrom, Berlin, Germany).

Because both malignant human thyroid follicular cell lines had retained the ability to synthesize Tg, they represent valuable models for the study of human follicular carcinomas.

Cell Culture Procedure

24 hours before the experiments, cells of both types were seeded into either slide flasks (Thermo Scientific, Roskilde, Denmark) with a growing area of 9 cm^2 for the CLINO or into T25 flasks (Sarstedt, Nümbrecht, Germany) with a growing area of 25 cm^2 for the RPM. The cells for each type of culture flasks were randomized to be cultivated as static ground controls (1*g*-condition) or on one of the devices. Phase contrast images were captured. The morphological pictures for RO82-W-1 cells are given in Fig 2. CLINO and RPM experiments were performed in individual incubators at 37°C, and ground controls were always kept next to the experiments in the same respective incubator, resting under static 1*g*-conditions. Cells of both types were harvested after 3d days and 7d.

Effects of IL-6 and IL-8 on adherent ML-1 cells grown under 1*g*-conditions

ML-1 cells from frozen stocks were cultivated in T75 flasks in RPMI 1640 medium until they reached subconfluence (3–5 days). Afterwards the cells were subcultured in 5 T175 and as soon

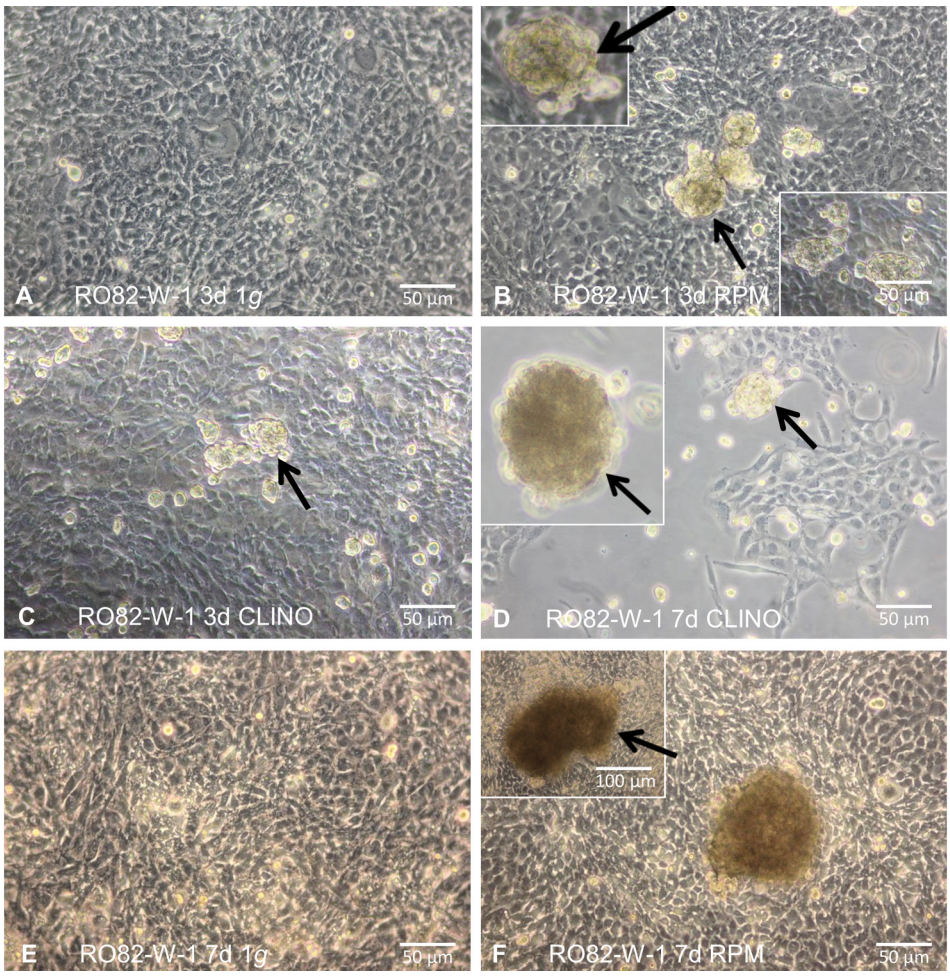

Fig 2. Phase contrast microscopy of RO82-W-1 cells. A: Follicular thyroid cancer cells cultured for 3d at static 1*g*. The cells proliferated as 2D monolayer. **B:** RO82-W-1 cells incubated for 3d on the RPM. The arrows show 3D aggregates (multicellular spheroids; MCS). The inserts show swimming 3D spheroids in the supernatant. **C:** MCS formed on the CLINO after 3 days. **D:** RO82-W-1 cells cultured for 7 days on the CLINO. The arrows show 3D spheroids. The insert demonstrates a floating spheroid in the supernatant. **E:** RO82-W-1 cells cultured for 7 days at static 1*g*-conditions grow as well as a confluent monolayer. **F:** 7-day-old MCS formed on the RPM (arrows) could be detected and adherent RO82-W-1 cells.

doi:10.1371/journal.pone.0135157.g002

as they reached subconfluence they were subcultured again in 20 T175 flasks. After getting subconfluent, the cells were treated with vehicle RPMI 1640 medium or with 0.03 ng/mL, 1 ng/mL, 10 ng/mL, 100 ng/mL of IL-6 or 1 ng/mL, 10 ng/mL, 45 ng/mL or 100 ng/mL of IL-8 concentrations, respectively [27–29]. We also applied for the IL-6 group 0.03 ng/mL and for IL-8 45 ng/mL, because these concentrations were released in the supernatant by ML-1 cells after 7 days.

10 T175 flasks (2 T175 without IL-6 or IL-8 and 8 T175 with different concentrations of IL-6 or IL-8) were cultivated in the incubator (1*g*) for 3d, and another set of 10 T175 for 7d.

After 3d or 7d the medium in the culture flasks has been discarded, the cells were scraped in 10 ml of DPBS and centrifuged by 6000 rpm for 15 minutes. The supernatant was removed, the pellet was dissolved in 1 ml of DPBS and centrifuged again by 6000 rpm for 15 minutes. The pellets were immediately used for protein extraction, Western blot analysis of beta-actin, $ß_1$-integrin, talin-1 and Ki-67 and following densitometry [17,19]. The results are given in Fig 3.

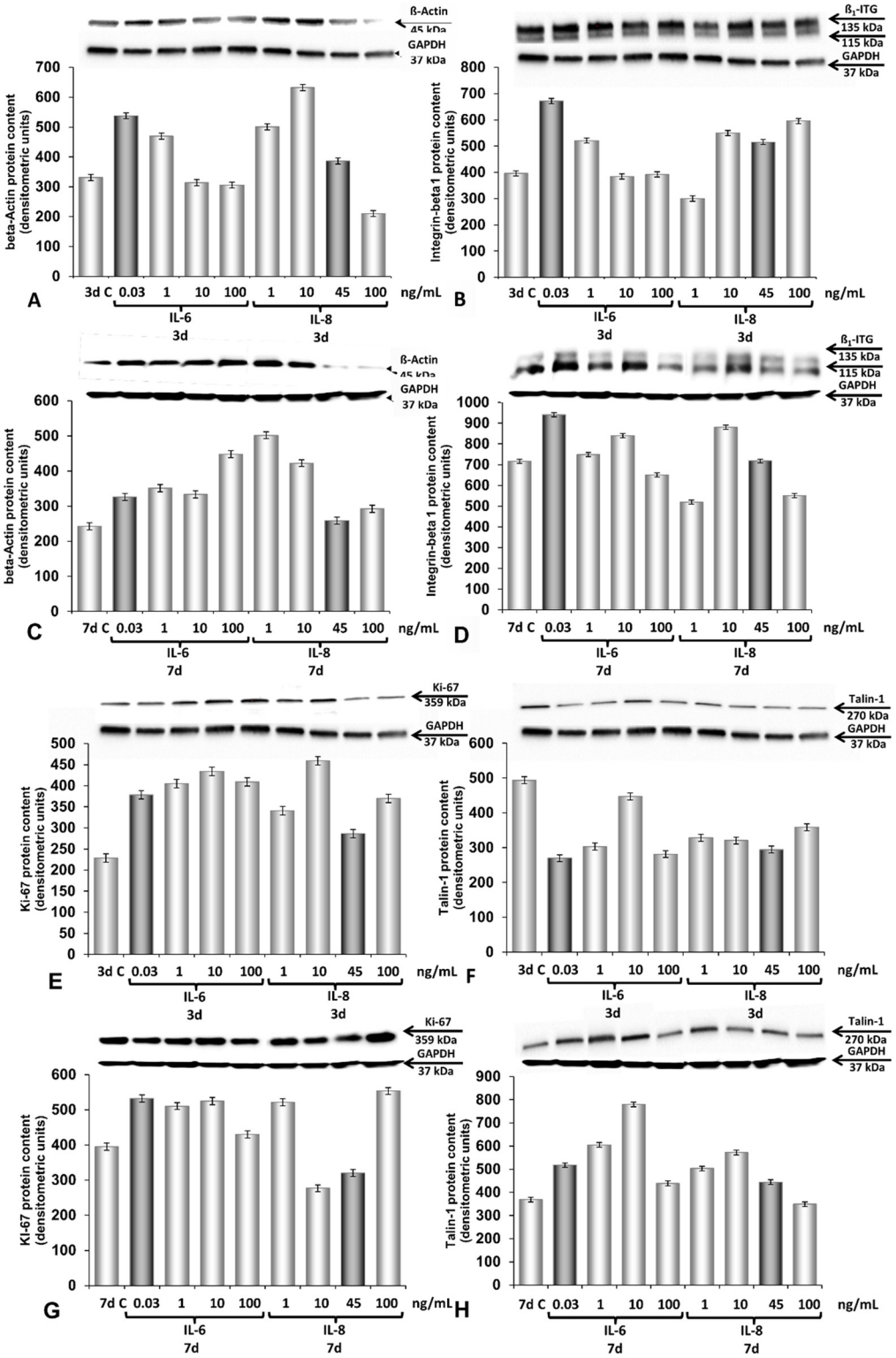

Fig 3. Effects of IL-6 and IL-8 on the amount of selected proteins in adherent ML-1 cells grown under normal 1*g*-conditions. Western blot analyses and densitometric data are given. **A, C:** beta-actin, 3d and 7d; **B, D:** ß$_1$-integrin, 3d and 7d; **E, G:** Ki-67, 3 and 7 days; **F, H**: Talin-1, 3 and 7 days. IL-6 doses: 0.03 ng/mL; 1 ng/mL; 10 ng/mL and 100 ng/mL. The dose 0.03 ng/mL is the maximal amount of IL-6 released by ML-1 cells in the supernatant and measured by MAP (dark-grey columns). IL-8 doses: 1 ng/mL; 10 ng/mL; 45 ng/mL and 100 ng/mL. The dose 45 ng/mL is the maximal amount of IL-8 released by ML-1 cells in the supernatant and measured by MAP (dark-grey columns).

doi:10.1371/journal.pone.0135157.g003

Liquid-overlay technique

Multicellular tumor spheroids were produced with the help of the liquid-overlay technique [24]. Thyroid cancer cells of the ML-1 cell line and the UCLA RO82-W-1 cell line harvested from adherently growing confluent monolayers were plated on agarose-coated 96-multiwell test plates (Nunc GmbH, Wiesbaden, Germany) at a concentration of 4000 cells/200 μL RPMI 1640 medium and were incubated at 37°C and 5% CO_2. The cells were stimulated with vehicle, IL-6 (1 ng/mL, 10 ng/mL and 100 ng/mL) and IL-8 (1 ng/mL, 10 ng/mL and 45 ng/mL). After 3d and 7d pictures were taken and the results presented in Fig 4.

Random Positioning Machine

The RPM was purchased from ADS, former Dutch Space, Leyden, the Netherlands (Fig 1A). Its construction and function was described earlier by van Loon [30]. It consists of two independent rotating frames within each other. In our experiments, the RPM was operated in "random mode" (60°/s), in which direction is changed continuously and randomly. Over time, the gravity vector of the Earth is nullified. During experiments, the RPM was loaded with up to 15 T25 cm^2 flasks that were fixed to the ground plate of the machine. In effect, all flasks resided within a distance of 7.5 cm from the center of rotation. In the relatively low speed (60°/s) of the RPM, the centrifugal force experienced by cells even at the furthest points from the center of rotation is assumed to be negligible [30].

2D Clinostat

The 2D CLINO device (manufactured by DLR, Cologne, Germany, Fig 1B) consists of six arms enabling the rotation of the samples around an axis perpendicular to the force of gravity [31]. Each rotating arm was loaded with 4 slide flasks, for a total of 24 flasks per run. On the CLINO, the gravity vector is randomized by fast and constant rotation. Great care was taken to ensure that all flasks selected for clinorotation were free of air bubbles that would otherwise induce chaotic fluid movement. The 2D CLINO rotating constantly at 60 rpm generates residual accelerations within the distance of 3 mm around the center of rotation in the order of 0.012*g*, while cells located at further distance experience up to 0.036*g* [18, 31]. Although the gravity-related threshold of thyroid cancer cells is unknown, only the cells located within the distance of 3 mm around the rotational axis were harvested for the analyses, meaning that these cells had experienced a very low residual acceleration.

pH measurements

The pH was measured with a Metrohm 827 pH-meter no more than 1 hour after experiment termination. All measurements were performed twice, and the samples were kept in closed Eppendorf tubes until measurement to avoid reactions with atmospheric gases.

Phase contrast microscopy

The Axiovert 25 Microscope (Carl Zeiss Microscopy, LLC, USA) was used for visual observation of the morphology of the cells.

Western blot analyses

Western blot analyses, immunoblotting, and densitometry were performed according to routine protocols [32–37]. The following antibodies were used to quantify the antigens: Anti-beta-actin, and anti-talin-1 were used at a dilution of 1:1000 (Cell Signaling Technology, Inc., Danvers, MA, USA); as well as anti-integrin-$beta_1$ antibody (Epitomics, Burlingame, USA); Ki-67

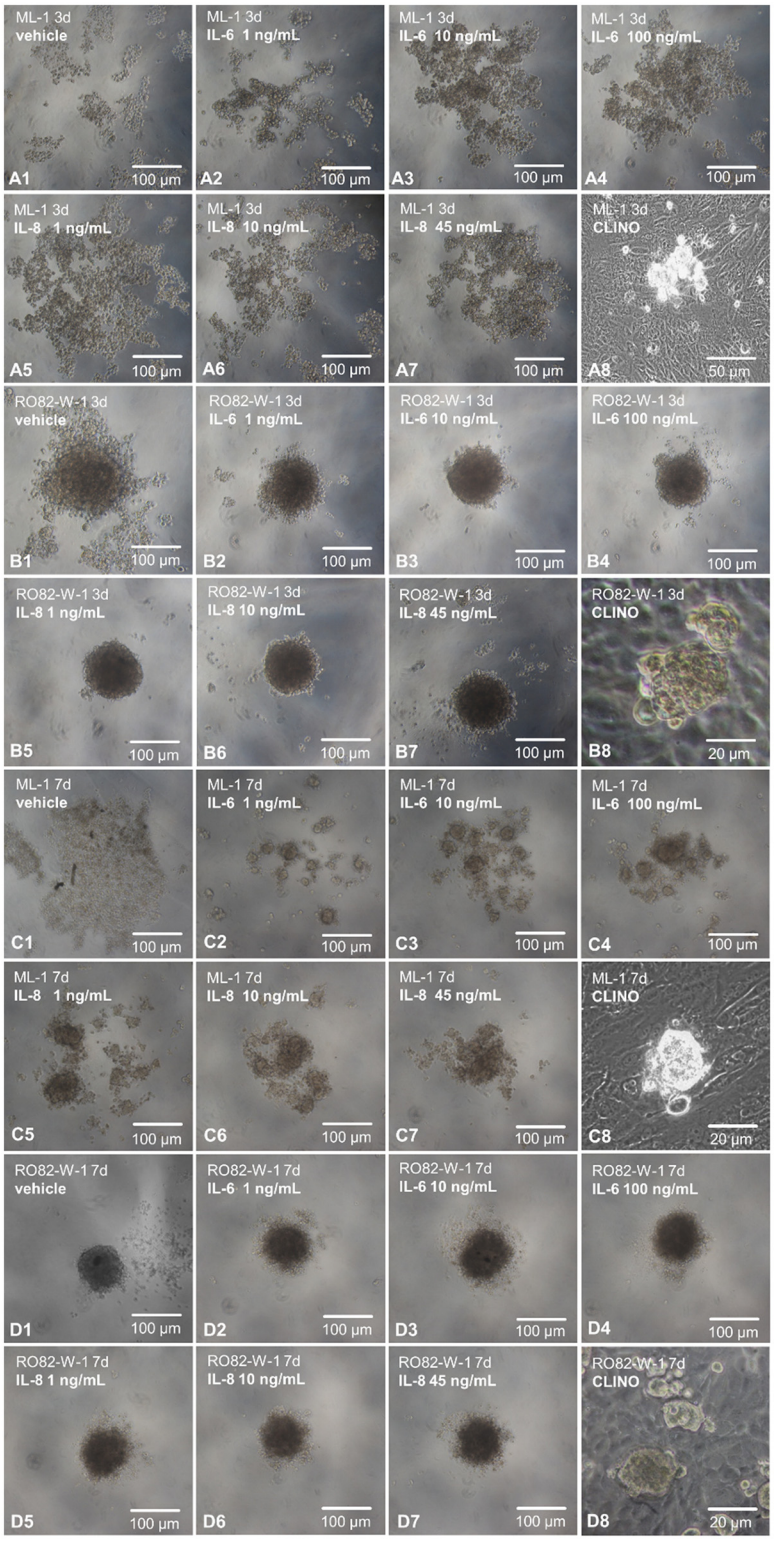

Fig 4. Liquid-overlay technique. A1-A7: Phase contrast microscopic pictures taken after 3d. ML-1 cells grown in agarose-coated wells, treated with vehicle or different doses of IL-6 or IL-8, respectively. **A8:** 3-day-old spheroid and adherent ML-1 cells on the CLINO. **B1-B7:** Photos taken after 3d. RO82-W-1 thyroid cancer cells grown in agarose-coated wells, treated with vehicle or different doses of IL-6 or IL-8, respectively. **B8:** 3-day-old spheroid and adherent RO82-W-1 cells on the CLINO. **C1-C7:** Pictures taken after 7d. ML-1 cells

grown in agarose-coated wells, treated with vehicle or different doses of IL-6 or IL-8, respectively. B8: 7-day-old spheroid and adherent ML-1 cell population after incubation in the 2D CLINO. **D1-D7:** Phase contrast images taken after 7d. RO82-W-1 thyroid cancer cells grown in agarose-coated wells, treated with vehicle or different doses of IL-6 or IL-8, respectively. **D8:** 7-day-old MCS and adherent RO82-W-1 cells after culture in the CLINO.

doi:10.1371/journal.pone.0135157.g004

was purchased from Santa Cruz Biotechnology, Santa Cruz, TX, USA (dilution 1:500); the secondary, HRP-linked antibody was utilized at a dilution of 1:4000 (Cell Signaling Technology, Inc., Danvers, MA, USA). As a loading control glyceraldehyde 3-phosphate dehydrogenase (ABR-Affinity BioReagents, Golden, USA; dilution: 1:10 000) was used.

The membranes were analyzed using ImageJ software (U.S. National Institutes of Health, Bethesda, MD, USA; http://rsb.info.nih.gov/ij/), for densitrometric quantification of the bands.

F-actin staining

F-actin was visualized by rhodamine-phalloidin staining (Molecular Probes, Eugene, OR, USA) and the nuclei were stained with Hoechst 33342 (Molecular Probes, Eugene, OR, USA), as published earlier [36, 37]. The samples were mounted with Vectashield (Vector, Burlingame, CA, USA) and analyzed microscopically. The F-actin stained samples were examined using a Zeiss 510 META inverted confocal laser scanning microscope (Zeiss, Germany), equipped with a Plan-Apochromat 63×1.4 objective. Excitation and emission wavelengths were: λexc = 488 nm and λem = ≥505 nm for FITC. Afterwards, the samples were analyzed with the help of the image analysis program Scion Image (Version 1.63 MacOs, Scion Corporation, USA).

Cytokine measurements by Multi-Analyte Profiling technology

The release of cytokines was investigated via Multi-Analyte Profiling (MAP) as previously described [18, 22]. For each condition, five supernatants were collected after 72 h and stored at -80°C until testing. The MAP was carried out by the company Myriad RBM (Austin, Texas, USA), they determined the Human Cytokines of the selections MAP A and B.

Cytokine measurement by Enzyme Linked Immunosorbent Assay

IL-6, IL-8, and MCP-1 proteins released from RO82-W-1 cells in the cell culture supernatants during RPM and CLINO experiments were detected by ELISAs purchased from R&D systems [38]. The ELISAs have been performed according to the protocols supplied by the manufacturer.

Statistical Evaluation

SPSS 15.0 (SPSS, Inc., Chicago, IL, USA) was used for statistical evaluation. The Mann-Whitney-U-Test was performed to compare 1 g and s-μg conditions, as well as s-μg adherent cells and s-μg MCTS cells. All data is presented as mean ± standard deviation (SD). Values of $p < 0.05$ were considered significant.

Results

The cells of the follicular thyroid cancer cell lines ML-1 and RO82-W-1 were cultivated for 3d and 7d on the RPM, on the 2D CLINO, and under normal static laboratory 1*g*-conditions. Up to the seventh day, the pH remained in the normal range, irrespective of whether the cells were cultured on the RPM, under 1*g* or on the CLINO. However, the cells remained growing in a monolayer only if culturing was performed under 1*g*, while, when cultured under altered

gravity conditions, the cells split into two populations of which one comprised cells remaining adherently, while the other contained cells forming 3D aggregates similar to those described for the FTC-133 cells [18].

We received similar results with the RO82-W-1 and ML-1 cells. Both types of cells proliferated like the RO82-W-1 cells shown in Fig 2 as an adherent monolayer (Fig 2A and 2E) and as multicellular spheroids on the RPM (Fig 2B and 2F) and the CLINO (Fig 2C and 2D). There were no differences in terms of number of spheroids of each cell line that arose on either the RPM or the CLINO. Both devices delivered spheroids of different sizes (max. diameter 0.4 mm) at both time points as shown in Fig 2B, 2C, 2D and 2F. Detachment of AD cells started early and cell detachment and spheroid formation occurred also after 7d.

Impact of IL-6 and IL-8 on ML-1 cells grown under 1*g*-conditions

IL-6 (0.03 ng/mL and 1 ng/mL) stimulation increased the amount of beta-actin and ß$_1$-integrin protein in adherent ML-1 cells. Moreover, IL-8 (1, 10 and 45 ng/mL) increased the beta-actin protein content in these cells, whereas only higher doses (10–100 ng/mL) elevated the protein content of ß$_1$-integrin within 3 days (Fig 3A and 3B).

After 7d, an increase was found for beta-actin protein in all IL-6-treated samples as well as in samples treated with 1 and 10 ng/mL IL-8 (Fig 3C). The ß$_1$-integrin protein was induced by 0.03 ng/mL as well as by 10 ng/mL IL-6, whereas only 10 ng/mL IL-8 induced the amount of the protein after a 7-day-stimulation (Fig 3D).

In addition, both cytokines (IL-6 and IL-8, all doses) induced an elevation of the Ki-67 protein content after 3d (Fig 3E). After 7d, all IL-6 doses as well as 1 ng/mL and 100 ng/mL IL-8 increased the amount of Ki-67 protein in ML-1 cells (Fig 3G). In contrast, the talin-1 protein content was clearly reduced by IL-6 and IL-8 application to the medium. Low doses of IL-6 and all doses of IL-8 were effective (Fig 3F) during the 3-day-1*g*-experiment. Another result was found after 7d. IL-6 stimulation resulted in an increase of talin-1 (Fig 3H). A similar finding was seen in IL-8-treated samples (1, 10 and 45 ng/mL) of the ML-1 cell line.

These experiments defined firstly, the optimal IL-6 and IL-8 doses for the expression of distinct proteins under 1*g*-conditions and secondly, the doses to test their impact on MCS formation using the liquid-overlay method (see below and Fig 4).

Impact of IL-6 and IL-8 on spheroid formation under 1*g*-conditions

After 3d, ML-1 cells only showed loose cell aggregates, when cultured under 1*g*-conditions on agarose. 10 and 100 ng/mL IL-6 and 1, 10 and 45 ng/mL IL-8 treatment resulted in a better aggregation of the ML-1 cells to spheroids, when they are cultured in the agarose-coated wells (Liquid-overlay technique) (Fig 4A1–4A7). RO82-W-1 cells formed large irregular aggregates after a 3-day-incubation in agarose-coated wells. Both cytokines improved the formation of RO82-W-1 multicellular spheroids using the liquid-overlay method (Fig 4B1–4B7).

After 7d, ML-1 cells showed irregular formed cellular aggregates on agarose. The cytokine-treated groups contained several dense spheroids after one week of stimulation (Fig 4C). The ML-1 spheroids formed on the CLINO were similar to the liquid-overlay spheroids treated with 45 ng/mL IL-8 (Fig 4C7 and 4C8).

After 7d, the RO82-W-1 cells grew in form of dense multicellular spheroids as well as single cells swimming in the supernatant in agarose-coated wells. Cytokine application to the medium enhanced slightly the size of the spheroids (Fig 4D1–4D7).

The spheroids of both cell types formed after IL-6 and IL-8 treatment exhibited a similar morphology than the MCS produced after incubation on the CLINO (Fig 4A8, 4B8, 4C8 and 4D8).

Cytokine release by ML-1 cells

Measuring the cytokines of the Human Cytokine selections MAP A and B we detected IL-4, IL-6, IL-7, IL-8, IL-17, MCP-1, VEGF-A and eotaxin-1 in the supernatants of the various cell cultures. We measured about 32 pg/mL IL-4 and IL-7 in the supernatants of 3-day-old cell cultures, irrespective of whether the cells had been incubated on the RPM, on the CLINO or in the stationary 1*g*-control. After a 7-day-exposure, the cell culture supernatants contained around 47 pg/mL IL-4 and about 43 pg/mL Il-7, independently of the culture conditions (Fig 5A and 5C). A similar phenomenon was observed with respect to IL-8 and VEGF-A. About 710 pg/mL VEGF-A and 11,000 pg/mL IL-8 were found in the supernatants of 3-day-old cultures, irrespective of whether the cells had been incubated on the RPM, on the CLINO or under stationary 1*g*-conditions. After a 7-day-exposure, VEGF-A and IL-8 concentrations were enhanced to around 3000 pg/mL VEGF-A and about 35,000 pg/mL Il-8 were detected, again without significant difference with respect to culturing conditions (Fig 5D and 5F). Taken together, Fig 5A, 5C, 5D and 5F show that the content of IL-4, IL-7, VEGF-A and IL-8 in the culture supernatants were enhanced in the 7-day-samples as compared to the 3-day-samples, while a significant influence of exposing cells to the RPM or the CLINO could not be seen for these 4 types of cytokines.

In contrast, the accumulation of IL-6 and MCP-1 in the different culture supernatants clearly depended on the culture conditions. A release of 27 and 33 pg/mL IL-6 was found in the supernatants of RPM samples after 3d and 7d of culturing, respectively, while an amount of 22.5 pg/mL IL-6 was measured in relevant 1*g*-controls (Fig 5B). Similarly, a concentration of 24 and 36 pg/mL IL-6 was found in the supernatants of CLINO samples after a 3- and 7-day-experiment, respectively, while about an amount of 25 pg/mL IL-6 was measured in relevant 1*g*-controls (Fig 5B). In addition, the monocyte chemoattractant protein-1 (MCP-1) levels changed, when cell culturing was performed on devices simulating microgravity. Under normal gravity conditions, about 600 pg/mL MCP-1 were found after 3 days and between 700 and 750 pg/mL after 7 days, while MCP-1 concentrations increased from 750 to 950 pg/mL on the RPM and from 700 to 1000 pg/mL on the CLINO (Fig 5E).

In addition to the six cytokines shown in Fig 5 we searched for further cytokines as shown in Table 1. However, we did not detect further cytokines released into the supernatant during 3 days of cell culturing under any condition. Release of IL-17 and eotaxin was detectable in samples cultured for 7 days on the CLINO, on the RPM as well as on the ground with no significant differences at concentrations of around 1 pg/mL (IL-17) and 15 pg/mL (eotaxin) (Table 1).

Cytokine release by RO82-W-1 cells

We investigated the release of selected cytokines in the supernatant of RO82-W-1 cells after a 3-day-exposure to the RPM or the CLINO devices. The amount of IL-6 was significantly elevated from 56.9 pg/mL to 75.2 pg/mL on the RPM (Fig 6A). A similar result was obtained for IL-8 (Fig 6B). Non-significant increases for both cytokines were measured for the CLINO-samples.

The secretion of MCP-1 of RO82-W-1 cells was much lower than the release of ML-1 cells (Figs 5E and 6C). Culture of RO82-W-1 cells on the RPM or the CLINO completely blunted the release of MCP-1 (Fig 6C).

Effects of simulated microgravity on the cytoskeleton

Since earlier studies have shown that cytoskeletal proteins of different types of cells are severely affected by microgravity [11–13, 37, 39–41], we performed F-actin staining on cells cultured on the RPM and on the 2D CLINO for 3d and 7d. After 3 days, an accumulation of F-actin along

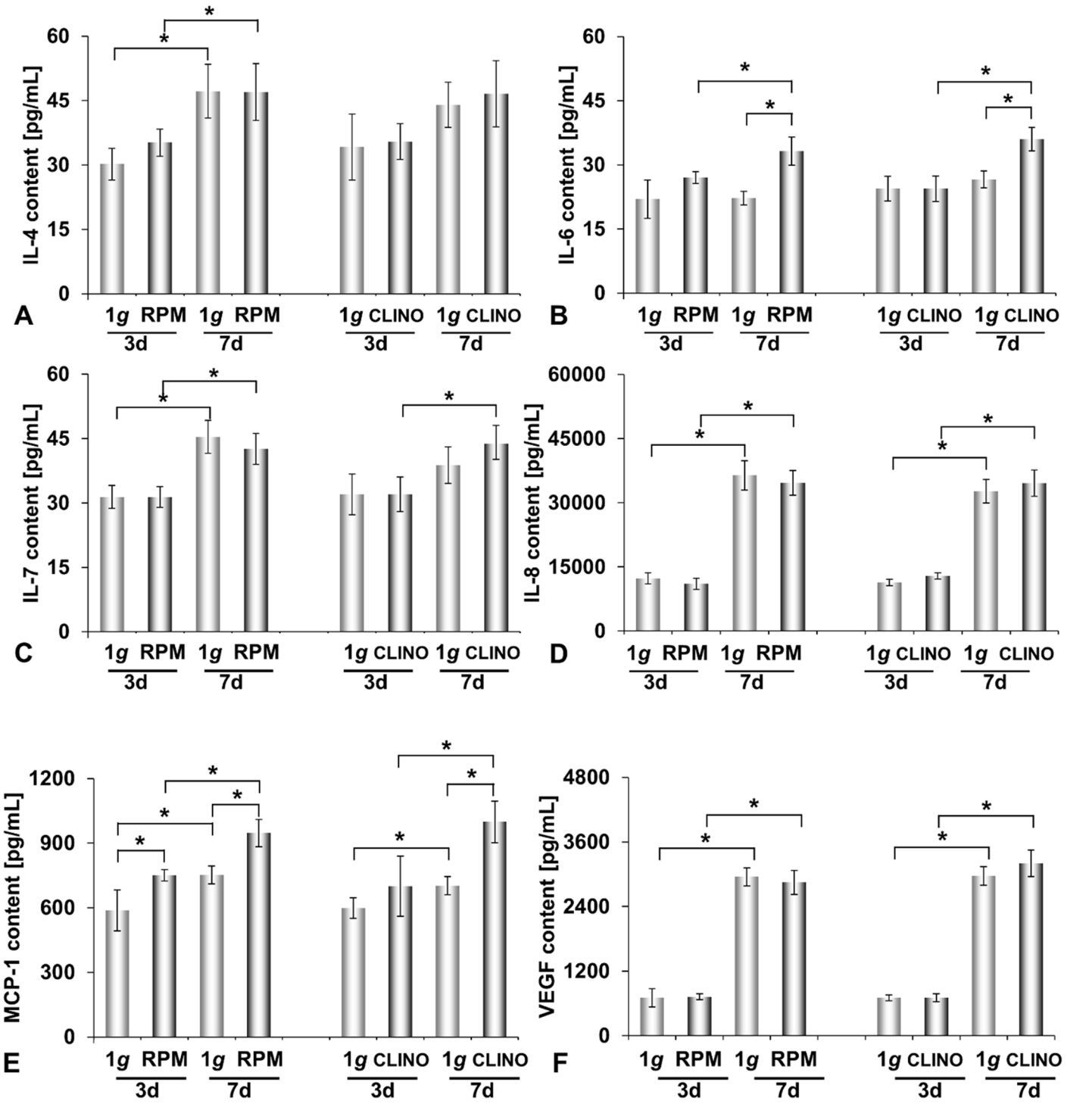

Fig 5. **A**: IL-4, **B**: IL-6, **C**: IL-7, **D**: IL-8, **E**: MCP-1, **F**: VEGF-A proteins released by ML-1 cells into the supernatant after a 3- and 7-day-exposure to the RPM or the 2D Clinostat, determined by Multi-Analyte Profiling of the supernatant. RPM: Random Positioning Machine; CLINO: 2D Clinostat; *p<0.05

doi:10.1371/journal.pone.0135157.g005

Table 1. Soluble factors secreted by ML-1 cells.

	Factor	LDD		Random Positioning Machine				Clinorotation			
				3d	3d control	7d	7d control	3d	3d control	7d	7d control
Human CytokineMAP A 1.0	**GM-CSF**	2,9	[pg/ml]	n.d.	n.d.	n.d.	n.d.	n.d.	n.d.	n.d.	n.d.
	IFN-γ	0,32	[pg/ml]	n.d.	n.d.	n.d.	n.d.	n.d.	n.d.	n.d.	n.d.
	IL-2	1,2	[pg/ml]	n.d.	n.d.	n.d.	n.d.	n.d.	n.d.	n.d.	n.d.
	IL-3	0,00032	[pg/ml]	n.d.	n.d.	n.d.	n.d.	n.d.	n.d.	n.d.	n.d.
	IL-5	0,55	[pg/ml]	n.d.	n.d.	n.d.	n.d.	n.d.	n.d.	n.d.	n.d.
	IL-10	0,66	[pg/ml]	n.d.	n.d.	n.d.	n.d.	n.d.	n.d.	n.d.	n.d.
	IL-18	1,3	[pg/ml]	n.d.	n.d.	n.d.	n.d.	n.d.	n.d.	n.d.	n.d.
	MIP-1α	3,6	[pg/ml]	n.d.	n.d.	n.d.	n.d.	n.d.	n.d.	n.d.	n.d.
	MIP-1β	3,2	[pg/ml]	n.d.	n.d.	n.d.	n.d.	n.d.	n.d.	n.d.	n.d.
	TNF-α	2,6	[pg/ml]	n.d.	n.d.	n.d.	n.d.	n.d.	n.d.	n.d.	n.d.
	TNF-β	0,6	[pg/ml]	n.d.	n.d.	n.d.	n.d.	n.d.	n.d.	n.d.	n.d.
Human CytokineMAP B 1.0	**BDNF**	0,0054	[ng/ml]	n.d.	n.d.	n.d.	n.d.	n.d.	n.d.	n.d.	n.d.
	Eotaxin-1	13	[pg/ml]	n.d.	n.d.	13.4 ± 7.9	17.6 ± 2.3	n.d.	n.d.	16.4 ± 1.8	13.6 ± 7.8
	ICAM-1	0,65	[pg/ml]	n.d.	n.d.	n.d.	n.d.	n.d.	n.d.	n.d.	n.d.
	IL-1α	0,0003	[pg/ml]	n.d.	n.d.	n.d.	n.d.	n.d.	n.d.	n.d.	n.d.
	IL-1β	0,44	[pg/ml]	n.d.	n.d.	n.d.	n.d.	n.d.	n.d.	n.d.	n.d.
	IL-1ra	31	[pg/ml]	n.d.	n.d.	n.d.	n.d.	n.d.	n.d.	n.d.	n.d.
	IL-12p40	0,019	[ng/ml]	n.d.	n.d.	n.d.	n.d.	n.d.	n.d.	n.d.	n.d.
	IL-12p70	6,8	[pg/ml]	n.d.	n.d.	n.d.	n.d.	n.d.	n.d.	n.d.	n.d.
	IL-15	0,039	[ng/ml]	n.d.	n.d.	n.d.	n.d.	n.d.	n.d.	n.d.	n.d.
	IL-17	0,31	[pg/ml]	n.d.	n.d.	1.078 ± 0.229	1.2 ± 0,071	n.d.	n.d.	1.12 ± 0.16	1.02 ± 0.602
	IL-23	0,13	[ng/ml]	n.d.	n.d.	n.d.	n.d.	n.d.	n.d.	n.d.	n.d.
	MMP-3	0,0052	[ng/ml]	n.d.	n.d.	n.d.	n.d.	n.d.	n.d.	n.d.	n.d.
	SCF	13	[pg/ml]	n.d.	n.d.	n.d.	n.d.	n.d.	n.d.	n.d.	n.d.

Values are given with mean ± SD; 1*g*, corresponding ground control; n.d., not detectable; LDD (Least Detectable Dose)-determined as the mean ± 3 standard deviations of 20 blank readings.

doi:10.1371/journal.pone.0135157.t001

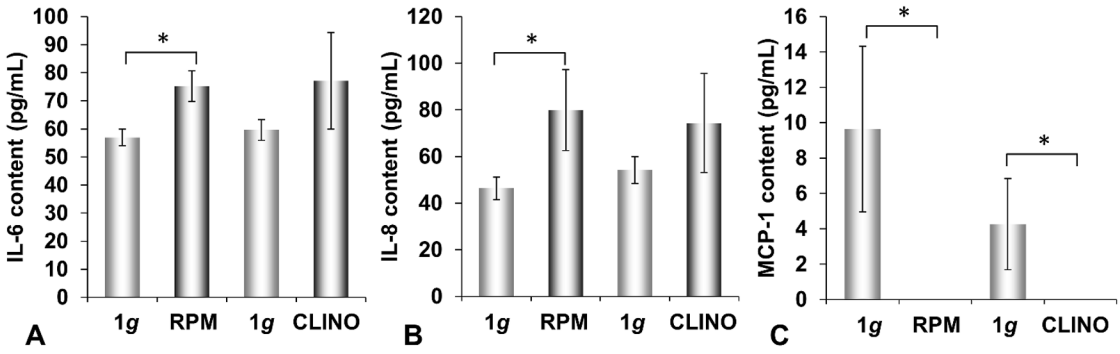

Fig 6. A: IL-6, **B:** IL-8, and **C:** MCP-1 proteins released by RO82-W-1 thyroid cancer cells into the supernatant after a 3-day-exposure to the RPM or the 2D CLINO, determined by ELISA technique. RPM: Random Positioning Machine; CLINO: 2D Clinostat; *p<0.05.

doi:10.1371/journal.pone.0135157.g006

the outer cellular membrane was visible in ML-1 cells as well as in RO82-W-1 cells cultured on the CLINO and the RPM (Fig 7). After 7 days, the cells were completely confluent and overgrew each other. A thickening of the outer membrane was found under both conditions (1*g* and simulated microgravity), but was more pronounced on the RPM and the CLINO.

Western blot analyses of β-actin in ML-1 cells revealed a decrease after 7d of clinorotation (Fig 8A), but the protein remained unchanged after 7d of RPM-exposure. Exposure of the ML-1 cells to the RPM and clinostat induced significant decreases of β_1-integrin in AD and MCS cells after 7d (Fig 8B). Talin-1 protein was significantly reduced in AD cells only, when the ML-1 cells were incubated on the CLINO (Fig 8C). Ki-67 protein, a nuclear protein, associated with the cellular proliferation process, was significantly elevated in AD cells compared with MCS and 1*g*-control cells on both devices (Fig 8D).

No change in beta-actin was found in RO82-W-1 cells after a 7-day-culture on the RPM or the CLINO (Fig 8E). The protein content of beta-actin remained constant. The protein contents of $beta_1$-integrin, talin-1 and Ki-67 of RO82-W-1 cells were comparable to those of the ML-1 cell line, irrespective of culture conditions (Fig 8F–8H).

Discussion

Ground-based facilities such as the RPM and the CLINO, used to simulate conditions of microgravity on Earth, have various benefits. They are important tools to prepare a future space mission [3, 4, 7, 30, 39–42]. They allow us also to explore altered gravity (microgravity)–related effects on Earth. However, most often they show superimposing effects, which may be due to the characteristics of a device. Common effects exerted by the RPM and the CLINO on target cells of interest may be induced due to prevention of sedimentations. We have recently demonstrated that the CLINO and the RPM are suitable to trigger FTC-133 cells to develop MCS and to decrease expression of CAV1 and CTGF genes in MCS [18]. In this study we focused on the regulation of cytokines and cytoskeletal proteins of two follicular thyroid cancer cell lines ML-1 and RO82-W-1 under the influence of the devices. In Ml-1 cells, we observed an enhanced release of IL-6 and MCP-1, an elevated Ki-67 protein content in AD cells, but a reduced production of ß$_1$-integrin and talin-1 in AD cells. RO82-W-1 cells exhibited a similar production of these proteins, when the cells were exposed to simulated microgravity conditions. The release of IL-6 and IL-8 was enhanced in RO82-W-1 cells, but MCP-1 secretion was blunted under conditions of microgravity. Different reactions of the two cell lines under CLINO- or RPM-exposure might be due to their different origin and characteristics.

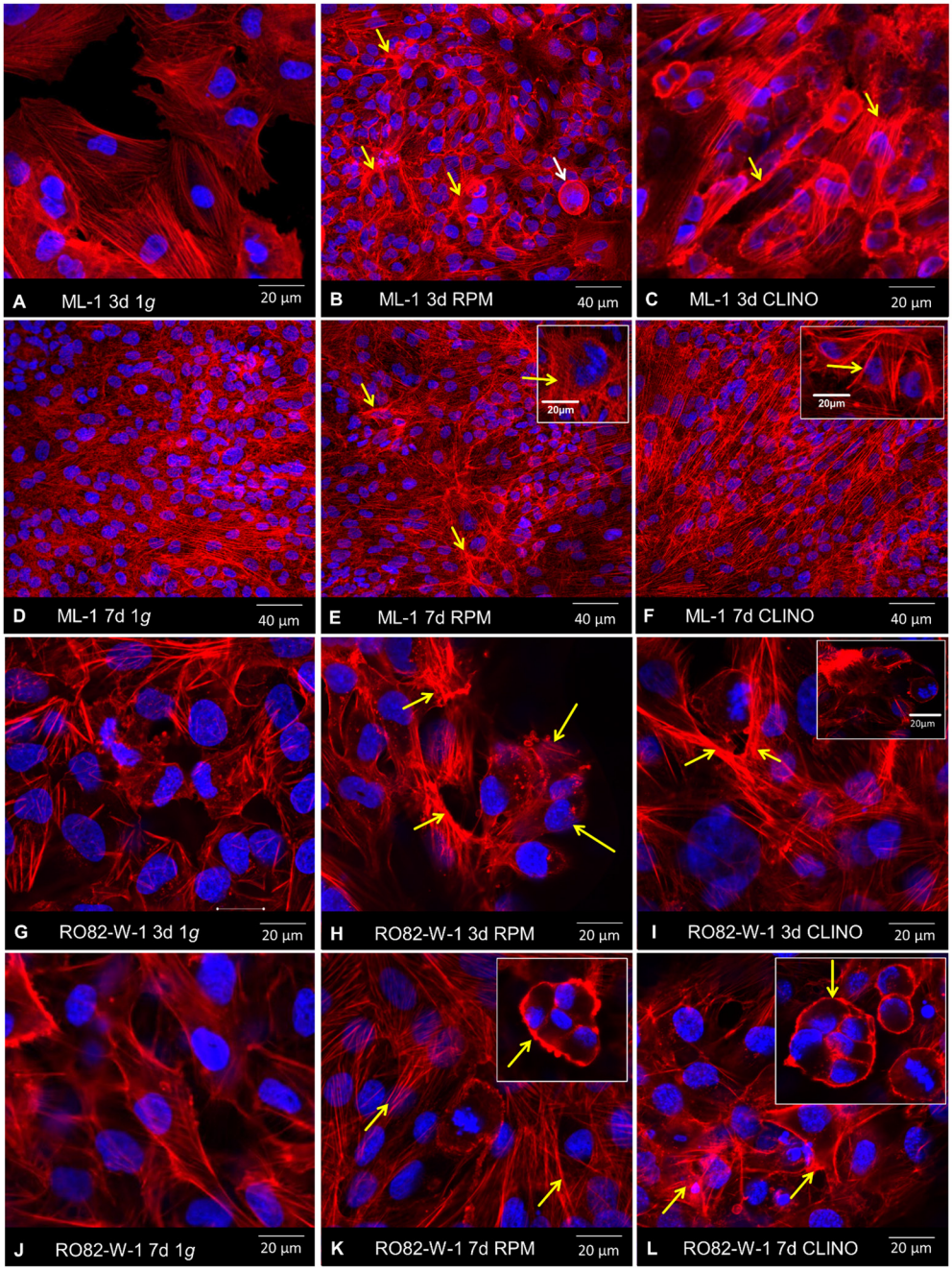

Fig 7. F-Actin staining of ML-1 and RO82-W-1 cells after 3d and 7d on the RPM and on the CLINO. A-C: ML-1 3-day-experiment. **A:** ML-1 cells, 3d, 1*g*-condition: normal cells with normal F-actin cytoskeleton **B:** ML-1 cells, 3d, accumulation of F-actin at the outer cellular membrane (yellow arrows) after RPM-exposure. The white arrow marks the detaching of cell aggregates from the adherent cell layer. **C:** ML-1 cells, 3d, thicker layers of F-actin at the outer cellular membrane (yellow arrows). **D-F:** ML-1 7-day-experiment. **D:** ML-1 cells, 7d, 1*g*-condition: confluent normal cells with normal F-actin cytoskeleton. **E:** ML-1 cells cultured on the RPM for 7d revealed thicker layers of F-actin at the outer membrane (insert). **F:** A 7-day-exposure of ML-1 cells to the CLINO induced similar changes of the F-actin cytoskeleton. The insert shows ticker F-actin fibers at the cellular membranes. **G-I:** RO82-W-1 3-day-experiment. **G:** normal F-actin cytoskeleton of RO82-W-1 cells. **H:** MCS formation (yellow arrows) after a 3-day-incubation on the RPM. An accumulation of F-actin at the outer cellular membrane is visible (yellow arrows). **I:** RO82-W-1 cultured for 3d on the clinostat revealed a clear thickening of the F-actin fibers (arrows). Insert: 3D MCS. **J-L**: RO82-W-1 7-day-experiment. **J:** F-actin cytoskeleton of confluent RO82-W-1 cells grown at 1*g*. **K, L:** MCS formation of RO82-W-1 cells after RPM-

(**K**) and CLINO-exposure (**L**). The arrows indicate the 3D MCS and a thickening of F-actin fibers at the outer membranes.

doi:10.1371/journal.pone.0135157.g007

Since both machines trigger similar cytoskeletal changes in both cell lines, we concluded that these alterations might be important in adaptation to microgravity [4, 11–13, 36, 37]. Furthermore, the proteins investigated play also a role in cancer development and progression.

A number of cytokines are known to play a role in tumor cell proliferation, apoptosis, and angiogenesis [43]. IL-4 has been described as a growth factor of thyroid cancer cells. It promotes resistance to chemotherapy by upregulating secondary messengers [44]. The role of IL-7 in relation to thyroid cancer remains largely unknown. Increased serum levels of IL-7 in conjunction with IL-6, IL-10 and IL-14 had been shown to indicate both benign and malignant thyroid disease [45]. IL-8 plays a role in arthroid disease [46]. In addition, IL-8 is responsible to tumor progression and liver metastasis of colorectal tumors [47]. IL-17 plays a role in tumor development, but the mechanisms of IL17 involvement are still uncharacterized [48]. Also VEGF promotes neoangiogenesis. It is produced by many thyroid cancer cells and supports infiltration of thyroid tumors by vasculature and thus promotes tumor growth [49, 50]. Its neutralization by antibodies or drugs is currently of great interest in tumor therapy [51, 52]. All these cytokines were accumulated in supernatants of ML-1 cultures progressively during time, while a number of other cancer cell-related cytokines could not be detected in the various supernatants (Table 1). There was no gravity-dependent influence on the secretion of the various cytokines by ML-1 cells mentioned in Table 1 and of those described above besides slight differences found for IL-7 and IL-8 (Fig 5). Hence, we concluded that a number of cytokines, playing a role in tumor development are not affected by culturing the cells on the devices applied. It is of interest that also the amounts of VEGF-A and eotaxin in the supernatants of the FTC-133 cells cultured during the Shenzhou-8 flight in real microgravity and on 1*g*-reference centrifuge were equal, respectively [22].

The up-regulation of IL-6 and MCP-1 occurred in RPM and CLINO samples of the ML-1 cell line (Fig 5B and 5E). IL-6, along with IL-8, had already been suggested to play a role in gravity-sensitive signaling required for spheroid formation [19]. To investigate the role of IL-6 and IL-8 on spheroid formation under 1*g*-conditions, we used the liquid-overlay technique [24]. We could show for the first time that both cytokines improve 3D aggregation of both ML-1 and RO-82-W-1 cells, which were cultured on agarose-coated wells for 3d and 7d (Fig 4). The 3- and 7-day-old MCS were comparable to the spheroids grown under conditions of simulated microgravity. In addition, we demonstrated that both cytokines induced the protein expression of beta-actin, $beta_1$-integrin, talin-1 and Ki-67 within 3 and 7 days (Fig 3). These results support recent research suggesting that IL-6 might be an important factor in tumor cell growth, metastasis and angiogenesis [53]. Immunohistochemical staining of papillary thyroid tumor samples indicated that MCP-1 expression correlated with an aggressive behavior of this tumor [54]. MCP-1 was highly secreted and elevated in ML-1 cells cultured under simulated microgravity. This cell line derived from a poorly differentiated follicular thyroid carcinoma. In contrast, RO82-W-1 cells exhibited a low secretion rate of this cytokine. A 3-day-incubation on the RPM and CLINO blunted the secretion of MCP-1 (Fig 6C). In space during the Shenzhou-8 mission, we also had measured after 10 days in FTC-133 supernatants 8pg/mL MCP-1 in spaceflight 1g-samples and 6.15 pg/mL MCP-1 in real μg-samples [22]. This reduction is in accordance with the results obtained from RO82-W1 samples, which also exhibited a reduction for this cytokine.

In addition, we investigated the F-actin cytoskeleton of the thyroid cancer cells. F-actin accumulated at the outer cellular membranes in both types of follicular thyroid cancer cells

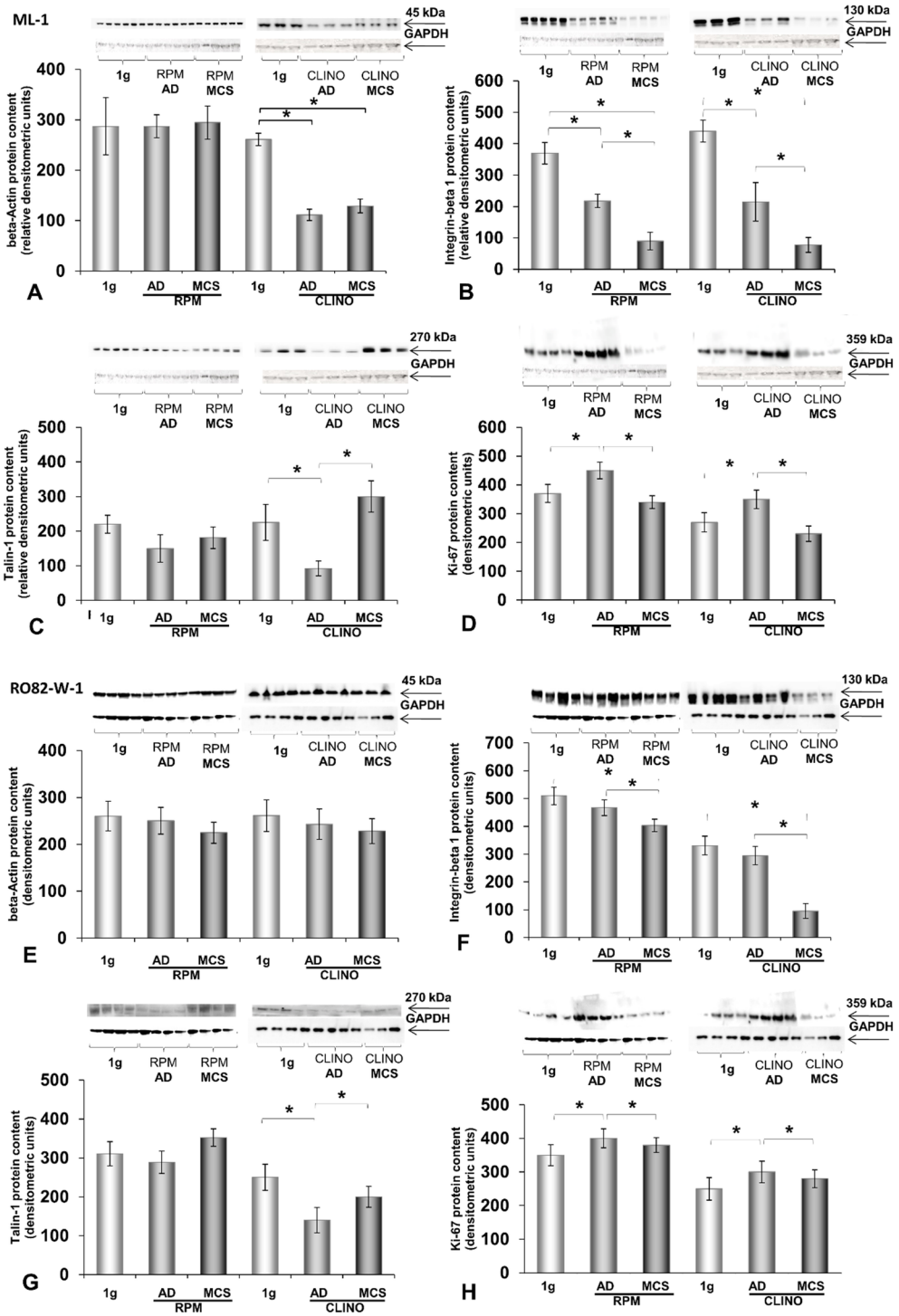

Fig 8. Western blot analyses of **A-D:** ML-1 cells after a 7-day-exposure on the RPM and CLINO. **A**: ß-actin, **B**: $ß_1$-integrin, **C**: talin-1 and **D:** Ki-67 proteins. Clear differences between the two devices are found for ß-actin. Western blot analyses of **E-H:** RO82-W-1 cells after a 7-day-exposure on the RPM and CLINO. **E:** ß-actin, **F:** $ß_1$-integrin, **G:** talin-1 and **H:** Ki-67 proteins. There was no change in the beta-actin content of RO82-W-1 cells cultured on the RPM or the CLINO for 7d. The amount of $ß_1$-integrin and Ki-67 was comparable to the ML-1 cultures grown under s-*μg*. *P<0.05.

doi:10.1371/journal.pone.0135157.g008

cultured on both devices for 3d and 7d (Fig 7), corresponding to our earlier studies on endothelial cells and human chondrocytes [4, 36, 37, 40] and further proves cytoskeletal alterations in cells cultured under microgravity conditions as reported by several authors [11–13, 55–57]. It is well known that microgravity induces changes in the actin cytoskeleton, which is connected to several membrane proteins with impact on cellular polarity, adhesion, migration, and may respond to extracellular signals [55]. These alterations occur very early. After the first microgravity phase of a DLR Parabolic Flight a clear rearrangement of the F-actin network with perinuclear clustering was demonstrated in ML-1 cells [55]. In addition, MCS formation occurred after 3d and 7d, a thick F-actin layer is visible at the outer membrane of the developing spheroids (Fig 7K and 7L).

Furthermore, we found a significant reduction of β-actin in CLINO-samples of the ML-1 cell line, whereas, a 7-day-RPM-exposure did not alter the expression of the protein (Fig 8A). Interestingly, RO82-W-1 cells exhibited no change in β-actin after a 7-day-culture on the RPM and the CLINO (Fig 8E). This protein is one of two non-muscular cytoskeletal actin types and is important for the stability of cells as well as for motility and structure. β-actin is expressed by tumor cells as well as by healthy cells, and overexpression of β-actin had been found to be associated to metastasis of gastric cancer [58], however, its role in thyroid cancer cells is currently unknown. The finding that β-actin is not changed in RO82-W-1 cells and the differences found for CLINO- and RPM-ML1 samples may be explained as follows: The notable differences between the amounts of β-actin on the RPM vs. the clinostat could be firstly, due to patient-specific properties of the two cell lines. Secondly, they may occur because of device characteristic reasons. The RPM consists of two independently rotating frames enabling a 3D rotation with random speed and random direction of the samples aiming to alter the influence of the gravity vector [30]. This might induce stress experienced by cells on the RPM when the direction is changed, where cells will experience numerous brakes for changing the vector and for inducing gravitational unloading may be also one possible reason for the difference. ML-1 cells may be more sensitive and can stabilize their cytoskeleton by producing more β-actin on the RPM [7, 30]. This does not occur in the CLINO due to constant rotating with respect to speed and direction. Moreover, on the CLINO, sedimentation is prevented by a fast and constant rotation of the samples around one horizontal axis, assuming that the sample does no longer perceive the gravity stimulus.

Both cell lines exhibit MCS formation on both devices. During MCS formation considerable alterations of various cellular molecules can occur. Some of them might not be directly related to the process of 3D cell aggregation, but by products generated by device-dependent modifications [59]. Examples are physical stimuli due to vibration, shearing forces, etc. generated by the simulators [18]. The CLINO device rotates constantly at 60 rpm and generates residual accelerations below 0.012*g* within the distance of ±3 mm around the culture flask center [31]. Cells located at further distance from the rotation axis are exposed to accelerations reaching up to 0.036 g at about ±9 mm [18]. Eiermann *et al.* had demonstrated significant differences in several genes in a human 1F6 melanoma cell line within these acceleration intervals [31]. To be sure to keep residual acceleration low, we only collected cells within the central 6 mm ($\leq$ 0.012 g) of a slide flask were collected and analyzed by Western blot analysis in the present study. Such a procedure is not possible for supernatants, and therefore IL-6 and IL-8 as well as all other soluble factors produced by cells from the periphery have a significant influence on cells growing in the center of the slide flasks. This may be one reason for the differences in beta-actin and also talin-1 protein expression. Most importantly, research in simulated microgravity has to be confirmed by a real space experiment.

β_1-integrin belongs to a family of adhesion molecules and is known to be important in binding the basal membrane and release proteases, thus facilitating the invasion of cancer cells into

the surrounding tissue. Follicular as well as papillary thyroid carcinoma cells express increased levels of β_1-integrin [60, 61]. Talin is a high-molecular weight cytoskeletal protein, which links integrins to the actin cytoskeleton [62]. Its overexpression enhanced prostate cancer cell adhesion, migration, and invasion [63]. β_1-integrin and talin-1 are reduced in adherent ML-1 cells. MCS cells of both cell lines contain a lower amount of β_1-integrin, whereas talin-1 is not significantly changed in MCS as compared with 1*g*-samples, irrespective of the used microgravity simulator (Fig 8). The protein content of talin-1 in RO82-W-1 MCS is higher than in AD cells on both devices. The differences between the RPM and CLINO devices as already discussed may be the reason for this finding. In an earlier study we had already investigated ML-1 cells for 72 h on a 3D clinostat and detected an increase in ß$_1$-integrin in AD cells [64]. After 72 h the protein content of AD cells was comparable to the content of MCS samples, but remained elevated as compared to 1*g*-samples [64]. Cellular adhesion and adhesion to the extracellular matrix is very important for the organism and is mediated by integrins. This process occurs early, which might explain why after a 7-day-exposure to s-µg, ß$_1$-integrin was reduced in MCS and AD cells. Talin is also required for a normal integrin function and is necessary for the activation of ß$_1$-integrins in many cell types. When ML-1 cells were cultured under s-µg, talin was early elevated and MCS exhibited a higher amount of talin compared with 1*g* and AD cells [64]. Talin is a cytoskeletal actin-binding protein that binds to integrin and also colocalized with activated integrins. Therefore, an early increase of this protein in parallel to ß$_1$-integrin can be expected in microgravity. Afterwards, the cells produce a constant level of this protein on the RPM.

Moreover, we evaluated the proliferation of the cells and measured the amount of Ki-67 protein. Ki-67 is an excellent proliferation marker, which is detectable during the cell cycle phases G1, S, G2, and mitosis, but is absent from resting cells (G0). It indicated a high proliferation in 7-day-old ML-1 and RO82-W-1-cultures, which was higher in AD than in MCS (Fig 8D and 8H). MCS exhibited an unaltered Ki-67 content compared with corresponding controls (Fig 8D and 8H). The Ki-67 content was also measured in human endothelial cells [41]. In human EAhy926 cells cultured on an RPM, equal amounts of Ki-67 were detectable in adherent cells under both 1*g*- and s-µg-conditions. Ki-67 was reduced by about 50% in MCS floating in the culture medium after 7 days under simulated microgravity [41].

In summary, these results support the hypothesis that simulated microgravity using the RPM or the CLINO favors 3D growth of thyroid cancer cells and that IL-6 plays an important role in this process. Il-6 favoring MCS formation and cell aggregation at 1*g* (liquid overlay technique) and simulated microgravity was elevated in simulated microgravity produced on the RPM or CLINO, which is in contrast to experiments in space using the FTC-133 cell line [22]. In addition, also IL-8 exerted beneficial effects on spheroid formation under 1g-conditions. This finding has to be investigated in more detail in future s-µg experiments. Cell line-specific differences between ML-1 and RO82-W-1 were found for the release of MCP-1. Therefore, further studies are required to elaborate possible relationships between the differentiation of cancer cells and gravity-dependent changes of cells.

Conclusions

Taken together, the results obtained in this study reveal that experiments with the RPM and the CLINO show similar effects on ML-1 and RO82-W-1 cells with regard to cytokine release and expression of cytoskeletal proteins. Only in 2 out of 14 cytokines released by ML-1 cells and measured by Multianalyte Profiling technology, we found significantly different effects exerted by the CLINO in comparison to the RPM. Hence, the presented results demonstrate a number of common effects of the two devices on the cells. This makes simulation of

microgravity on Earth to a valuable method, if one takes in mind that the simulations have to be verified under real microgravity conditions. Experiments in microgravity provide an interesting tool for exploring new targets for cancer therapy. Staying critical and taking side effects into account, ground-based facilities could provide cheaper alternatives of spaceflight research at least for studies on dedicated aspects. The signaling pathways resulting in microgravity-related alterations have to be determined [59] in order to identify and separate distinct proteins playing a role in adaption to microgravity and to cancer progression.

Acknowledgments

The authors would like to thank the German Space Agency (DLR; (DG) BMWi projects 50WB1124 and 50WB1524), the European Space Agency (ESA; ESA-CORA-GBF-2011-005 project Device Comparison; ESA-CORA-GBF- 2013–001 project THYROID 3) (DG), Aarhus University, Denmark (DG), the University of Regensburg (JG), and DGLRM (Young Fellow Program for EW and GA). The funders had no role in study design, data collection and analysis, decision to publish, or preparation of the manuscript.

Author Contributions

Conceived and designed the experiments: DG RH JB. Performed the experiments: BS SK JS XM MW GA TI. Analyzed the data: EW MW DG JG GA. Contributed reagents/materials/analysis tools: JH MI JG RH DG TJC. Wrote the paper: BS DG JB EW TJC.

References

1. White RJ, Averner M. Humans in Space. Nature. 2001; 409: 1115–1118. PMID: 11234026
2. Hughes-Fulford M. To infinity. . .and beyond! Human spaceflight and life science. FASEB J. 2011; 25: 2858–2864. doi: 10.1096/fj.11-0902ufm PMID: 21880668
3. Pietsch J, Bauer J, Egli M, Infanger M, Wise P, Ulbrich C, et al. The effects of weightlessness on the human organism and mammalian cells. Curr Mol Med. 2011; 11: 350–364. PMID: 21568935
4. Grimm D, Wise P, Lebert M, Richter P, Baatout S. How and why does the proteome respond to microgravity? Expert Rev Proteomics. 2011; 8: 13–27. doi: 10.1586/epr.10.105 PMID: 21329425
5. Hammond TG, Benes E, O'Reilly KC, Wolf DA, Linnehan RM, Taher A, et al. Mechanical culture conditions effect gene expression: gravity-induced changes on the space shuttle. Physiol Genomics. 2000; 3: 16–173.
6. Griffoni C, Di Molfetta S, Fantozzi L, Zanetti C, Pippia P, Tomasi V, et al. Modification of proteins secreted by endothelial cells during modeled low gravity exposure. J Cell Biochem. 2011; 112: 265–272. doi: 10.1002/jcb.22921 PMID: 21069737
7. Grimm D, Pietsch J, Wehland M, Richter P, Strauch SM, Lebert M, et al. The impact of microgravity-based proteomics research. Expert Rev. Proteomics. 2014; 11: 465–476. doi: 10.1586/14789450.2014.926221 PMID: 24957700
8. Maccarrone M, Battista N, Meloni M, Bari M, Galleri G, Pippia P, et al. Creating conditions similar to those that occur during exposure of cells to microgravity induces apoptosis in human lymphocytes by 5-lipoxygenase-mediated mitochondrial uncoupling and cyto- chrome c release. J Leukoc Biol. 2003; 73, 472–481. PMID: 12660222
9. Uva BM, Masini MA, Sturla M, Bruzzone F, Giuliani M, Tagliafierro G, et al. Microgravity-induced apoptosis in cultured glial cells. Eur J Histochem. 2002; 46, 209–214. PMID: 12472115
10. Boonyaratanakornkit JB, Cogoli A, Li CF, Schopper T, Pippia P, Galleri G, et al. Key gravity-sensitive signaling pathways drive T cell activation. FASEB J. 2005; 19, 2020–2022. PMID: 16210397
11. Buravkova LB, Romanov YA. The role of cytoskeleton in cell changes under condition of simulated microgravity. Acta Astronaut. 2001; 48: 647–650. PMID: 11858272
12. Kumei Y, Morita S, Katano H, Akiyama H, Hirano M, Oyha K, et al. Microgravity signal ensnarls cell adhesion, cytoskeleton, and matrix proteins of rat osteoblasts Ann. N.Y. Acad. Sci. 2006; 1090: 311–317.

13. Grimm D, Bauer J, Kossmehl P, Shakibaei M, Schönberger J, Pickenhahn H, et al. Simulated microgravity alters differentiation and increases apoptosis in human follicular thyroid carcinoma cells. FASEB J. 2002; 16: 604–606. PMID: 11919168

14. Grimm D, Wehland M, Pietsch J, Aleshcheva G, Wise P, Van Loon J, et al. Growing tissues in real and simulated microgravity: New methods for tissue engineering. Tissue Engineering—Part B: Reviews. 2014; 20: 555–566.

15. Becker JL, Souza GR. Using space-based investigations to inform cancer research on Earth. Nat Rev Cancer. 2013; 13: 315–327. doi: 10.1038/nrc3507 PMID: 23584334

16. Pietsch J, Ma X, Wehland M, Aleshcheva G, Schwarzwälder A, Segerer J, et al. Spheroid formation of human thyroid cancer cells in an automated culturing system during the Shenzhou-8 space mission. Biomaterials. 2013; 34: 7694–7705. doi: 10.1016/j.biomaterials.2013.06.054 PMID: 23866977

17. Pietsch J, Kussian R, Sickmann A, Bauer J, Weber G, Nissum M, et al. Application of free-flow IEF to identify protein candidates changing under microgravity conditions. Proteomics. 2010; 10: 904–913. doi: 10.1002/pmic.200900226 PMID: 20049858

18. Warnke E, Pietsch J, Wehland M, Bauer J, Infanger M, Görög M, et al. Spheroid formation of human thyroid cancer cells under simulated microgravity: a possible role of CTGF and CAV1. Cell Commun Signal. 2014; 12: 32. doi: 10.1186/1478-811X-12-32 PMID: 24885050

19. Grosse J, Wehland M, Pietsch J, Schulz H, Saar K, Hübner N, et al. Gravity-sensitive signaling drives 3-dimensional formation of multicellular thyroid cancer spheroids. FASEB J. 2012; 26: 5124–5140. doi: 10.1096/fj.12-215749 PMID: 22964303

20. Ma X, Wehland M, Aleshcheva G, Hauslage J, Waßer K, Hemmersbach R, et al. Interleukin-6 expression under gravitational stress due to vibration and hypergravity in follicular thyroid cancer cells. PLoS ONE. 2013; 8: e68140. doi: 10.1371/journal.pone.0068140 PMID: 23844163

21. Pietsch J, Sickmann A, Weber G, Bauer J, Egli M, Wildgruber R, et al. A proteomic approach to analysing spheroid formation of two human thyroid cell lines cultured on a random positioning machine. Proteomics. 2011; 11: 2095–2104. doi: 10.1002/pmic.201000817 PMID: 21520503

22. Ma X, Pietsch J, Wehland M, Schulz H, Saar K, Hübner N, et al. Differential gene expression profile and altered cytokine secretion of thyroid cancer cells in space. FASEB J. 2014; 28: 813–835. doi: 10.1096/fj.13-243287 PMID: 24196587

23. Riwaldt S, Pietsch J, Sickmann A, Bauer J, Braun M, Segerer J, et al. Identification of proteins involved in inhibition of spheroid formation under microgravity. Proteomics. 2015 Apr 29. [Epub ahead of print]

24. Grimm D, Bauer J, Kromer E, Steinbach P, Riegger G, Hofstädter F. Human follicular and papillary thyroid carcinoma cells interact differently with human venous endothelial cells. Thyroid. 1995; 5: 155–164. PMID: 7580262

25. Schönberger J, Bauer J, Spruß T, Weber G, Chahoud I, Eilles C, et al. Establishment and characterization of the follicular thyroid carcinoma cell line ML-1. J Mol Med. 2000; 78: 102–110. PMID: 10794546

26. Estour B, Van Herle AJ, Juillard GJ, Totanes TL, Sparkes RS, Giuliano AE, Klandorf H. Characterization of a human follicular thyroid carcinoma cell line (UCLA RO 82 W-1). Virchows Arch B Cell Pathol Incl Mol Pathol. 1989; 57: 167–174. PMID: 2570483

27. Rochfort KD, Cummins PM. Cytokine-mediated dysregulation of zonula occludens-1 properties in human brain microvascular endothelium. Microvasc Res. 2015; 100: 48–53. doi: 10.1016/j.mvr.2015.04.010 PMID: 25953589

28. Sun Q, Sun F, Wang B, Liu S, Niu W, Liu E, Peng C, Wang J, Gao H, Liang B, Niu Z, Zou X, Niu J. Interleukin-8 promotes cell migration through integrin αvβ6 upregulation in colorectal cancer. Cancer Lett. 2014; 354: 245–53. doi: 10.1016/j.canlet.2014.08.021 PMID: 25150782

29. Li X, Xu M, Liu M, Ji Y, Li Z. TNF-alpha and IL-6 inhibit apolipoprotein A-IV production induced by linoleic acid in human intestinal Caco2 cells. J Inflamm (Lond). 2015; 12: 22.

30. van Loon JJWA. Some history and use of the random positioning machine, RPM, in gravity related research. Advances in Space Research. 2007; 39: 1161–1165.

31. Eiermann P, Kopp S, Hauslage J, Hemmersbach R, Gerzer R, Ivanova K: Adaptation of a 2D clinostat for simulated microgravity experiments with adherent cells. Micrograv Sci Technol. 2013; 25: 153–159.

32. Ulbrich C, Westphal K, Pietsch J, Winkler HD, Leder A, Bauer J, et al. Characterization of human chondrocytes exposed to simulated microgravity. Cell Physiol Biochem. 2010; 25: 551–560. doi: 10.1159/000303059 PMID: 20332636

33. Riecke K, Grimm D, Shakibaei M, Kossmehl P, Schulze-Tanzil G, Paul M, et al. (2002) Low doses of 2,3,7,8-tetrachlorodibenzo- p-dioxin increase transforming growth factor beta and cause myocardial fibrosis in marmosets (Callithrix jacchus). Arch Tox. 2002; 76: 360–366.

34. Rothermund L, Kreutz R, Kossmehl P, Fredersdorf S, Shakibaei M, Paul M, et al. Early onset of chondroitin sulfate and osteopontin expression in angiotensin II dependent left ventricular hypertrophy. Am J of Hypertens. 2002; 15: 644–652.

35. Ma X, Wildgruber R, Bauer J, Weber G, Infanger M, Grosse J, et al. The use of sigmoid pH gradients in free-flow isoelectric focusing of human endothelial cell proteins. Electrophoresis. 2012; 33: 1349–1355. doi: 10.1002/elps.201100598 PMID: 22648801

36. Aleshcheva G, Sahana J, Ma X, Hauslage J, Hemmersbach R, Egli M, et al. Changes in morphology, gene expression and protein content in chondrocytes cultured on a random positioning machine. PLoS One. 2013; 8: e79057. doi: 10.1371/journal.pone.0079057 PMID: 24244418

37. Aleshcheva G, Wehland M, Sahana J, Bauer J, Corydon TJ, Hemmersbach R, et al. Moderate alterations of the cytoskeleton in human chondrocytes after short-term microgravity produced by parabolic flight maneuvers could be prevented by up-regulation of BMP-2 and SOX-9. FASEB J. 2015; 29: 2303–2014. doi: 10.1096/fj.14-268151 PMID: 25681461

38. Wehland M, Aleshcheva G, Schulz H, Saar H, Hübner N, Hemmersbach R, et al. Differential gene expression of human chondrocytes cultured under short-term altered gravity conditions during parabolic flight maneuvers. Cell Commun Signal. 2015; 13:18 doi: 10.1186/s12964-015-0095-9 PMID: 25889719

39. Versari S, Villa A, Bradamante S, Maier JA. Alterations of the actin cytoskeleton and increased nitric oxide synthesis are common features in human primary endothelial cell response to changes in gravity. Biochim Biophys Acta. 2007; 1773: 1645–1652. PMID: 17609119

40. Infanger M, Ulbrich C, Baatout S, Wehland M, Kreutz R, Bauer J, et al. Modeled gravitational unloading induced downregulation of endothelin-1 in human endothelial cells. J Cell Biochem. 2007; 101: 1439–1455. PMID: 17340622

41. Grimm D, Bauer J, Ulbrich C, Westphal K, Wehland M, Infanger M, et al. Different responsiveness of endothelial cells to vascular endothelial growth factor and basic fibroblast growth factor added to culture media under gravity and simulated microgravity. Tissue Eng Part A. 2010; 16: 1559–1573. doi: 10.1089/ten.TEA.2009.0524 PMID: 20001221

42. Herranz R, Anken R, Boonstra J, Braun M, Christianen PC, de Geest M, et al. Ground-based facilities for simulation of microgravity: organism-specific recommend-dations for their use, and recommended terminology. Astrobiology. 2013; 13: 1–17. doi: 10.1089/ast.2012.0876 PMID: 23252378

43. Zeng J, Xie K, Wu H, Zhang B, Huang C. Identification and functional study of cytokines and chemokines involved in tumorigenesis. Comb. Chem. High Throughput Screen. 2012; 15: 276–285. PMID: 22221060

44. Todaro M, Zerilli M, Ricci-Vitiani L, Bini M, Perez Alea M, Maria Florena A, et al. Autocrine production of interleukin-4 and interleukin-10 Is required for survival and growth of thyroid cancer cells. Cancer Res. 2006; 66: 1491–1499. PMID: 16452205

45. Provatopoulou X, Georgiadou D, Sergentanis TN, Kalogera E, Spyridakis J, Gounaris A, et al. Interleukins as markers of inflammation in malignant and benign thyroid disease—Inflamm Res. 2014; 63: 667–674.

46. Deleuran B, Lemche P, Kristensen M, Chu CQ, Field M, Jensen J, et al. Localisation of interleukin 8 in the synovial membrane, cartilage- pannus junction and chondrocytes in rheumatoid arthritis. Scand J Rheumatol. 1994; 23: 2–7. PMID: 8108662

47. Terada H, Urano T, Konno H. Association of interleukin-8 and plasminogen activator system in the progression of colorectal cancer. Eur Surg Res. 2005; 37: 166–172. PMID: 16088182

48. Lee YC, Chung JH, Kim SK, Rhee SY, Chon S, Oh SJ, et al. Association between interleukin 17/interleukin 17 receptor gene polymorphisms and papillary thyroid cancer in Korean population. Cytokine. 2015; 71: 283–288. doi: 10.1016/j.cyto.2014.11.011 PMID: 25484349

49. Tuttle RM, Fleisher M, Francis GL, Robbins RJ. Serum vascular endothelial growth factor levels are elevated in metastatic differentiated thyroid cancer but not increased by short-term TSH stimulation. J Clin Endocrinol Metab. 2002; 87: 1737–1742. PMID: 11932308

50. Grimm D, Bauer J, Schoenberger J. Blockade of neoangiogenesis, a new and promising technique to control the growth of malignant tumors and their metastases. Curr Vasc Pharmacol. 2009; 7: 347–357. PMID: 19601859

51. Kristensen TB, Knutsson ML, Wehland M, Laursen BE, Grimm D, Warnke E, et al. Anti-vascular endothelial growth factor therapy in breast cancer. Int J Mol Sci. 2014; 15: 23024–23041. doi: 10.3390/ijms151223024 PMID: 25514409

52. Wehland M, Bauer J, Infanger M, Grimm D. Target-based anti-angiogenic therapy in breast cancer. Curr Pharm Des. 2012; 18: 4244–4257. PMID: 22632607

53. Balkwill F, Gopinathan G, Milagre C, Pearce OM, Reynolds LE, Hodivala-Dilke K, et al. Interleukin-6 stimulates defective angiogenesis. Cancer Res. 2015 Jun 16. [Epub ahead of print]

54. Tanaka K, Kurebayashi J, Sohda M, Nomura T, Prabhakar U, Yan L, et al. The expression of monocyte chemotactic protein-1 in papillary thyroid carcinoma is correlated with lymph node metastasis and tumor recurrence. Thyroid. 2009; 19: 21–25. doi: 10.1089/thy.2008.0237 PMID: 19072670

55. Ulbrich C, Pietsch J, Grosse J, Wehland M, Schulz H, Saar K, et al. Differential gene regulation under altered gravity conditions in follicular thyroid cancer cells: relationship between the extracellular matrix and the cytoskeleton. Cell Physiol Biochem. 2011; 28: 185–198. doi: 10.1159/000331730 PMID: 21865726

56. Grosse J, Wehland M, Pietsch J, Ma X, Ulbrich C, Schulz H, et al. Short-term weightlessness produced by parabolic flight maneuvers altered gene expression patterns in human endothelial cells. FASEB J. 2012; 26: 639–655. doi: 10.1096/fj.11-194886 PMID: 22024737

57. Lewis ML, Reynolds JL, Cubano LA, Hatton JP, Lawless BD, Piepmeier EH. Spaceflight alters microtubules and increases apoptosis in human lymphocytes (Jurkat). FASEB J. 1998; 12: 1007–1018. PMID: 9707173

58. Xu J, Zhang Z, Chen J, Liu F, Bai L. Overexpression of β-actin is closely associated with metastasis of gastric cancer. Hepatogastroenterology. 2013; 60: 620–623. PMID: 23635433

59. Pietsch J, Riwaldt S, Bauer J, Sickmann A, Weber G, Grosse J, et al. Interaction of proteins identified in human thyroid cells. Int J Mol Sci. 2013; 14: 1164–1178. doi: 10.3390/ijms14011164 PMID: 23303277

60. Ensinger C, Obrist P, Bacher-Stier C, Mikuz G, Moncayo R, Riccabona G. β1-Integrin expression in papillary thyroid carcinoma. Anticancer Res 1998; 18: 33–40. PMID: 9568052

61. Demeure MJ, Damsky CH, Elfman F, Goretzki PE, Wong MG, Clark OH. Invasion by cultured human follicular thyroid cancer correlates with increased β1 integrins and production of proteases. World J Surg. 1992; 16: 770–776. PMID: 1384245

62. Vignoud L, Albigès-Rizo C, Frachet P, Block MR. NPXY motifs control the recruitment of the α5β1 integrin in focal adhesions independently of the association of talin with the β1 chain. J Cell Sci. 1997; 110: 1421–1430. PMID: 9217328

63. Sakamoto S, McCann RO, Dhir R, Kyprianou N. Talin1 promotes tumor invasion and metastasis via focal adhesion signaling and anoikis resistance. Cancer Res. 2010; 70: 1885–1895. doi: 10.1158/0008-5472.CAN-09-2833 PMID: 20160039

64. Infanger M, Kossmehl P, Shakibaei M, Schulze-Tanzil G, Cogoli A, Faramarzi S, et al. Longterm conditions of mimicked weightlessness influences the cytoskeleton in thyroid cells. J Gravit Physiol. 2004; 11: P169–P172. PMID: 16237826

15.3 Publikation 3

Warnke E, Kopp S, Wehland M, Hemmersbach R, Bauer J, Pietsch J, Infanger M, Grimm D: Thyroid Cells Exposed to Simulated Microgravity Conditions – Comparison of the Fast Rotating Clinostat and the Random Positioning Machine. Microgravity Sci. Technol. 28. 247-260 (2016)

Microgravity Sci. Technol. (2016) 28:247–260
DOI 10.1007/s12217-015-9456-7

ORIGINAL PAPER

Thyroid Cells Exposed to Simulated Microgravity Conditions – Comparison of the Fast Rotating Clinostat and the Random Positioning Machine

Elisabeth Warnke[1] · Sascha Kopp[1] · Markus Wehland[1] · Ruth Hemmersbach[2] · Johann Bauer[3] · Jessica Pietsch[1] · Manfred Infanger[1] · Daniela Grimm[4]

Received: 26 March 2015 / Accepted: 3 September 2015 / Published online: 3 October 2015

Abstract The ground-based facilities 2D clinostat (CN) and Random Positioning Machine (RPM) were designed to simulate microgravity conditions on Earth. With support of the CORA-ESA-GBF program we could use both facilities to investigate the impact of simulated microgravity on normal and malignant thyroid cells. In this review we report about the current knowledge of thyroid cancer cells and normal thyrocytes grown under altered gravity conditions with a special focus on growth behaviour, changes in the gene expression pattern and protein content, as well as on altered secretion behaviour of the cells. We reviewed data obtained from normal thyrocytes and cell lines (two poorly differentiated follicular thyroid cancer cell lines FTC-133 and ML-1, as well as the normal thyroid cell lines Nthy-ori 3-1 and HTU-5). Thyroid cells cultured under conditions of simulated microgravity (RPM and CN) and in Space showed similar changes with respect to spheroid formation. In static 1*g* control cultures no spheroids were detectable. Changes in the regulation of cytokines are discussed to be involved in MCS (multicellular spheroids) formation. The ESA-GBF program helps the scientists to prepare future spaceflight experiments and furthermore, it might help to identify targets for drug therapy against thyroid cancer.

Keywords Thyroid cells · Simulated microgravity · Random Positioning Machine · Clinostat · Cytokines · Spheroids

✉ Daniela Grimm
dgg@biomed.au.dk

[1] Clinic for Plastic, Aesthetic and Hand Surgery, Otto-von-Guericke-University Magdeburg, Magdeburg, Germany

[2] German Aerospace Center, DLR, Institute of Aerospace Medicine, Cologne, Germany

[3] Max-Planck-Institute for Biochemistry, Martinsried, Germany

[4] Department of Biomedicine, Aarhus University, Wilhelm Meyers Allé 4, 8000, Aarhus, Denmark

Introduction

Previous studies have shown, that thyroid cells *in vitro* and *in vivo* respond to altered gravity conditions (Grimm et al. 2002; Kossmehl et al. 2002, 2003; Meli et al. 1998, 1999; Martin et al. 2000; Masini et al. 2012; Albi et al. 2011, 2012, 2014). This response might play an important role for physiological changes at the organism level during spaceflight but could also give important hints for cancer research on Earth (Becker et al. 2013; Grimm et al. 2002, 2014).

An impressive example for the response to altered gravity conditions is the spheroid formation, which was observed after exposure of thyroid cancer cells to real microgravity in Space for 10 days (Pietsch et al. 2013). This experiment was part of the Sino-German Shenzhou-8/SIMBOX-mission in 2011 (Ma et al. 2014; Pietsch et al. 2013). 3D growth and spheroid formation in Space were also observed for other cell types like chondrocytes (Freed et al. 1997; Stamenkovic et al. 2010). These multicellular spheroids mirror the alteration in cell-cell adhesion, a transition from 2- to 3-dimensional growth and might be beneficial for studies on biological processes such as metastasis or tumor-neovascularization and for pharmacological testing (Grimm et al. 2014).

In order to get a deeper insight into the molecular mechanisms behind this phenomenon, ground-based facilities (GBF) are valuable tools, as they enable a cost efficient preparation of spaceflights but also continuous research in stand-alone studies. In this context, the fast rotating clinostat (CN) and the Random Positioning Machine (RPM) have been suggested for studies with adherent mammalian cells, as they often showed similar results compared to real microgravity in earlier studies (Herranz et al. 2013). The most important findings concerning thyroid cells cultured *in vitro* under conditions of simulated and real microgravity (μ*g*), published by our group and others, as well as data obtained from Space missions from mouse thyroid glands *in vivo*, published by Professor Ambesi-Impiombato and coworkers, are listed in Table 1. In addition, we listed published data concerning changes in the gene expression pattern and protein content of different cell types obtained after culture under simulated and real microgravity conditions in Table 2.

This review summarizes the results from the ESA-CORA-GBF-PROJECT-2011-005 (ACRONYM DEVICE COMPARISON) and ESA-CORA-GBF-PROJECT-2013-001 (ACRONYM THYROID III). It gives an overview on the behaviour of thyroid cells under real and simulated microgravity.

Experimental Approach

The thyroid cells were cultured in a comparative methodological approach as published in detail before (Warnke et al. 2014; Grosse et al. 2012). Static 1*g*-control cells were always stored together with the microgravity simulation device in the same standard cell culture incubator. We used either a fast-rotating 2D clinostat (German Aerospace Center, Cologne, Germany; Fig. 1a), operated constantly at 60 rpm, or a Random Positioning Machine (ADS, former Dutch space, the Netherlands; Fig. 1b), operated in real random speed and direction mode (60-75°/s) (Fig. 1a, b). The spheroid formation was documented microscopically. Molecular biological analyses (quantitative real-time PCR, gene array, bioinformatics), Western blot technique and Multi-Analyte Profiling (MAP) as well as cytoskeletal staining were performed according to established methods (Warnke et al. 2014; Kossmehl et al. 2006; Grosse et al. 2012; Rothermund et al. 2002; Infanger et al. 2007; Pietsch et al. 2013).

The Ground-Based Facilities Random Positioning Machine and 2D Clinostat

The magnitude of the gravity vector on Earth cannot be altered, but its direction and thus its influence can be changed (Briegleb 1992; Herranz et al. 2013). This is the underlying principle for the simulation devices of interest in this review. Therefore, the term 'simulated microgravity' is used, as the cell might experience a condition comparable to that of real microgravity, due to a randomization of the direction of the gravity vector over time. However, device-specific side effects like centrifugal accelerations, shearing forces and vibrations remain and possibly mask the desired microgravity effects. Therefore, a careful and conscious handling and discussion of the results are suggested (Herranz et al. 2013).

Nevertheless, ground-based facilities (RPM, CN) used for the experiments have been previously described as promising candidates for microgravity simulations in adherent mammalian cells (Herranz et al. 2013; Eiermann et al. 2013; van Loon 2007; Grimm et al. 2006; Grimm et al. 2014).

The 2D clinostat (Fig. 1a) contains a horizontal rotation axis, where the sample is constantly rotated perpendicular to the gravity vector. In contrast, the RPM (Fig. 1b) contains two independently rotating frames, enabling a rotation around two axes (van Loon 2007). The RPM is operated in a random direction and random speed mode. Therefore, the influence of the gravity vector with respect to the samples is constantly changed, which assures a maximum of randomization.

The 2D clinostat is operated with a constant speed of 60 rpm, which enables highest μ*g*-simulation quality. In addition, the radius around the rotation axis should not exceed 1-1.5 mm because of increasing centrifugal forces (Häder et al. 2005; Klaus et al. 1998). Given a speed of 60 rpm and a radius around the centre of 1.5 mm, the residual acceleration is $10^{-3}g$.

In case of the RPM, operated in real random mode with a highest speed of 60-75°/s (which is equivalent to 12.5 rpm) and a maximum distance of 7 cm to the rotation centre, the residual acceleration over time is between 10^{-4} and $10^{-2}g$ (van Loon 2007).

Thyroid Cell Lines Cultured Under Conditions of Simulated and Real Microgravity

Nthy-ori 3-1

The cell line Nthy-ori 3-1 was derived from normal human primary thyroid follicular epithelial cells of a 35-year-old female patient. The cells were transfected with a plasmid containing an origin-defective SV40 genome for immortalization (Lemoine et al. 1989). They show thyroid epithelial functions like iodide trapping and thyroglobulin production, but are non-tumorigenic in nude mice (Lemoine et al. 1989).

Table 1 Summary of articles addressing research on thyroid cells *in vitro* and *in vivo* cultured under real or simulated microgravity, ordered by cell line

Cell line	Device and duration of exposure	Findings in microgravity (μ*g*)	Reference
ML-1	RPM, 7 and 11 d	- proteome analysis - equal proteins from cells cultured under 1*g* and on the RPM, were detected in comparable gel pieces - many of these proteins showed different Mascot scores - glutathione S-transferase P, nucleoside diphosphate kinase A and heat shock cognate 71 kDa protein concentrations were enhanced on the RPM	Pietsch et al. Microgravity Sci. Technol. 2011; 23: 381–390.
ML-1	PFC, Vibraplex, SAHC	- gene array analysis: 2430 significantly changed transcripts (PFC, 22 seconds) - F-actin and cytokeratin cytoskeleton, *ACTB* significantly up-regulated - hypergravity and vibrations did not change *ACTB* - data indicate that the graviresponse of ML-1 cells is occurring very early	Ulbrich et al. Cell Physiol Biochem. 2011; 28: 185-198.
ML-1	RPM	- spheroid formation - signs of apoptosis - elevated amounts of apoptosis-associated Fas protein, p53 and Bax - caspase-3 was clearly upregulated	Kossmehl et al. J Gravit Physiol. 2002; 9: P295-296.
ML-1	RPM 24 and 48 h	- spheroid formation - elevated intermediate filaments, cell adhesion molecules, and extracellular matrix proteins - induced apoptosis - decreased fT3 and fT4 secretion	Grimm et al. FASEB J. 2002; 16: 604-606.
ML-1 RO82-W-1	CN and RPM 72 h, 7 d	- Spheroid formation on both devices - elevated release of IL-6 and MCP-1 by ML-1 cells compared with 1*g* - reduced integrin-b_1 in MCS compared with 1*g*	Svejgaard et al. PLoS One. 2015; 10:e0135157
FTC-133	CN and RPM 4 h, 24 h, 72 h	- Spheroid formation - CN: decreased cytokine release - RPM: increased cytokine release - decreased expression of *CAV1* and *CTGF* in MCS compared to AD	Warnke et al. Cell Commun Signal. 2014; 10; 12: 32.
FTC-133	PFC, 10 d Space (SIMBOX/Shenzhou-8), 10 d RPM	- microarray analysis: 63 sig. regulated transcripts after 22 s of microgravity (PFC) - 2881 sig. regulated transcripts after 10 d on the RPM or in Space	Ma et al. FASEB J. 2014; 28: 813-835.

Table 1 (continued)

Cell line	Device and duration of exposure	Findings in microgravity (μg)	Reference
		- genes involved in several biological processes: apoptosis, cytoskeleton, adhesion/extracellular matrix, proliferation, stress response, migration, angiogenesis, signal transduction, regulation of cancer cell proliferation and metastasis	
FTC-133	Space and RPM 10 d	- Spheroid formation - enhanced *EGF* and *CTGF* in both real and s-µ*g*	Pietsch et al. Biomaterials. 2013; 34: 7694-7705.
FTC-133, CGTH W-1, HTU-5	RPM 1 and 3 d	- protein pathways influenced by s-µ*g*: - Carbohydrate and protein metabolism, regulation of cell growth and cell membrane structuring.	Pietsch et al. Int J Mol Sci. 2013; 14: 1164-1178.
FTC-133	RPM 24 h	- spheroid formation - 487 sign. regulated transcripts (Gene Array) - IL-6, IL-8, OPN, TLN-1, CTGF, NF-kB suggested as relevant for RPM-dependent spheroid formation	Grosse et al. FASEB J. 2012; 26: 5124-5140.
FTC-133, CGTH W-1	RPM 3 d	- Proteomic analysis of differences - collagen only detected in CGTH W-1 - integrin a-5 chains, myosin-10 and filamin B only found in FTC-133 - FTC-133 cells express surface proteins that bind fibronectin, this strengthens the 3D cell cohesion	Pietsch et al. Proteomics. 2011; 11: 2095-2104.
Human thyrocytes	RCCS 14 d	- 3D aggregates - human thyroglobulin level increased - keratinocyte growth factor facilitated 3D aggregation	Martin et al. Thyroid. 2000; 10: 481-487.
FRTL-5 rat	Texus-44 mission 6 min 19 s r-µ*g*	- no response to TSH - irregular shape - shedding of TSH-R in the supernatant - increase in Bax - increase in sphingomyelin-synthase - rearrangement of the cell membrane	Albi et al. Astrobiology. 2011; 11: 57-64.
FRTL-5 rat	CN	- less-responsive to TSH stimulation in terms of cAMP	Meli et al. Acta Astronaut. 1998; 42: 465-72.
FRTL-5 rat	low-speed centrifuge 5*g* and 9*g*	- response to the variable gravity force in a dose-dependent manner in terms of cAMP production following TSH-stimulation	Meli et al. Biochemie. 1999; 81: 281-285.
Thyroid gland mouse	Spaceflight 91 d	- increase in average follicle size - increase in sphingomyelinase - increase in sphingomyelin-synthase1	Albi et al. Astrobiology. 2012; 12: 1035-10341.

Table 1 (continued)

Cell line	Device and duration of exposure	Findings in microgravity (μg)	Reference
Thyroid gland mouse	Spaceflight 91 d hypergravity 2*g* centrifuge	Both conditions induce: - loss of C cells - reduction of calcitonin production - over-expression of pleiotrophin	Albi et al. PLoS One. 2012; 7: e48518.
Thyroid gland mouse	Spaceflight 3 months	- thyroid follicles appeared more organized - over-expression of caveolin-1 - over-expression of TSH-R	Masini et al. PLoS One. 2012; 7: e35418.
Thyroid gland mouse	Spaceflight 90 d	- over-expression of HBME-1 - over-expression of Galectin-3	Albi et al. Biomed. Res. Int. 2014: 652863
Thyroid gland mouse	hypergravity 2*g* centrifuge	- up-regulation of TSH-R - up-regulation of caveolin-1 - down-regulation of STAT3 - cholesterol level strongly reduced - no changes of cAMP	Albi et al. PLoS One. 2014; 9: e98250

AD adherent cells, *ACTB* Actin Beta, *cAMP* cyclic adenosine monophosphate, *CAV* Caveolin, *CN* 2D clinostat, *CTGF* Connective Tissue Growth Factor, *3D* three-dimensional; *EGF* Epidermal Growth Factor, *HBME-1* Anti-Mesothelioma antibody, *IL* Interleukin, *ITGB1* Integrin Beta-1, *MCP-1* Monocyte chemotactic protein, *MCS* multicellular spheroids, *MYO9B* Myosin, *OPN* osteopontin, *PFC* Parabolic Flight Campaign, *RCCS* rotary cell culture system, *RDX* Radixin, *RPM* random positioning machine, r-µ*g* real microgravity, *SAHC* short-arm human centrifuge; s-µ*g* simulated microgravity, *TLN-1* Talin-1, *TSH* Thyroid-stimulating hormone, *TSH-R* Thyroid-stimulating hormone receptor, *VIM* Vimentin

HTU-5

The normal thyroid cell line HTU-5 was derived from healthy human thyroid tissue. HTU-5 thyroid cells produce thyroglobulin constitutively and exert normal diploid chromosome numbers (Curcio et al. 1994). The cells were cultured in Coon's F-12 medium containing a mixture of growth factors as described earlier (Curcio et al. 1994).

FTC-133

The FTC-133 is classified as a poorly differentiated follicular thyroid cancer cell line. It was derived from a lymph node metastasis of a 42-year-old male patient (Goretzki et al. 1990). Nevertheless, the cells show thyroglobulin immunoreactivity, response to thyroid-stimulating hormone and epidermal growth factor receptors in the membrane (Goretzki et al. 1990).

ML-1

The human thyroid carcinoma cell line ML-1 originates from a dedifferentiated follicular thyroid carcinoma relapse of a 50-year-old female patient (Schönberger et al. 2000). The tumour progressed despite previous surgery and two radioiodine therapies. The cells are able to take up iodine and/or glucose *in vitro* and *in vivo*. Furthermore, they express and secrete thyroglobulin. Xenotransplantation in NMRI nude mice showed tumourigenic capacity, with the formation of tumours with follicular structures, *in vivo* (Schönberger et al. 2000).

Biological Responses to Simulated Microgravity

RPM- and CN-Exposure Induced Spheroid Formation in Thyroid Cancer Cell Lines and Normal Thyrocytes

When cultured under normal 1*g*-conditions on Earth, thyroid carcinoma cells grew in form of an adherent monolayer. Already in 2000, Martin et al. have demonstrated that normal thyrocytes grow three-dimensionally in form of thyroid follicles, when they were cultured in a rotary cell culture system (RCCS). The cells produced thyroglobulin, when they were grown in the RCCS (Martin et al. 2000). The authors showed that these artificial human thyroid organoids generated in the RCCS and in the presence of keratinocyte growth factor structurally resembled natural thyroid tissue. Interestingly, several types of cells undergo a transition when exposed to simulated microgravity. It was shown, that

Table 2 Differential gene expression and protein content of different thyroid cell lines on the RPM, the 2D Clinostat and in Space

Cell Line	Device and condition	Investigated gene expression and protein content	AD	MCS	References
ML-1	RPM 24 h	Protein content:			Grimm et al. FASEB J.
	and 72 h	Collagen 1/3	↑	↑	2002; 16: 604-6.
		Laminin	↑	↑	
		Fibronectin	↑	↑	
		Fas	↑	↑	
		p53	↑	↑	
		Bax	↑	↑	
		Bcl-2	↓	↓	
ML-1	RPM	Protein content:			Kossmehl et al. J Gravit Physiol.
		Fas	↑	↑	2002; 9: P295-6.
		p53	↑	↑	
		Bax	↑	↑	
		Bcl-2	↓	↓	
FTC-133	RPM 24 h	Gene expression:			Grosse et al. FASEB J.
		IL6	↑	↓	2012; 26: 5124-40.
		Erk1	↓	-	
		Erk2	↓	↓	
		Cav1	-	-	
		Cav2	↓	↓	
		OPN	↑	-	
		CTGF	↓	↓	
		IL8	↑	-	
FTC-133	RPM 10 d	Gene expression:			Pietsch et al. Biomaterials
		CTGF	↑	↑	2013; 34: 7694-7670.
		EGF	↑	↑	
	Space 10 d	Gene expression:			
		CTGF	(↑)	(↑)	
		EGF	(↑)	(↑)	
FTC-133	RPM 10 d	Gene expression:			Ma et al. FASEB J.
		IL6	-	-	2014; 28: 813-35.
		IL8	↓	↓	
		OPN	↑	↑	
		VEGFA	↓	↓	
		VEGFD	↑	↑	
	Space 10 d	Gene expression:			
		IL6	(-)	(-)	
		IL8	↓	↓	
		OPN	(↓)	(↓)	
		VEGFA	(↓)	(↓)	
		VEGFD	(↑)	(↑)	
FTC-133	CN 4 h	Gene expression:			Warnke et al. Cell Commun Signal.
		CTGF	↑	/	2014; 12:32.
		CAV2	↑		
		ERK1	↓		

Table 2 (continued)

Cell Line	Device and condition	Investigated gene expression and protein content	AD	MCS	References
	RPM 4 h	Gene expression:			
		CTGF	↑	/	
		CAV2	-		
		ERK1	-		
	CN 72 h	Gene expression:			
		CAV1	-	↓	
		CAV2	↓	↓	
		CTGF	-	↓	
		EGF	-	-	
		ERK1	-	↓	
		IL8	↓	↓	
		ITGB1	-	↓	
		PRKCA	-	↓	
	RPM 72 h	Gene expression:			
		CAV1	-	↓	
		CAV2	-	-	
		CTGF	↑	↓	
		EGF	-	↑	
		ERK1	-	↑	
		IL8	-	-	
		ITGB1	-	-	
		PRKCA	-	-	
FRTL-5	Texus-44	Protein content:			Albi et al. Astrobiology.
	6 min 19 s	Bax	↑	/	2011;11:57-64.
		Sphingomyelin-synthase	↑		

AD Adherent cells RPM, *Bax* Bcl-2-Associated X Protein, *Bcl-2* B-Cell Lymphoma 2, *Cav1/2* Caveolin 1/2, *CN* 2D-Clinostat, *CTGF* Connective Tissue Growth Factor, *EGF* Epidermal Growth Factor, *ERK1/2* Extracellular Signal-Regulated Kinases, *IL6* Interleukin-6, *IL8* Interleukin-8, *ITGB1* Integrin Beta-1, *MCS* Multicellular Spheroids, *OPN* Osteopontin, *PRKCA* Protein Kinase C Alpha, *RPM* Random Positioning Machine, *VEGFA/D* Vascular Endothelial Growth Factor. ↑/↓ significantly up- or down-regulated compared to control adherent cells, (x) not significant, - no changes, / no MCS

an exposure to either RPM or CN lead to the detachment and formation of 3D aggregates, so-called multicellular spheroids (MCS) for some cells, while others remained adherent (AD). This transition from 2- to 3-dimensional growth is of high interest for tissue engineering but also for possible cancer therapy (Grimm et al. 1997, 2014). In 2002 we demonstrated for the first time that ML-1 thyroid cancer cells changed their growth behaviour and form MCS on the 3D clinostat (Grimm et al. 2002) (Table 1).

When FTC-133 thyroid carcinoma cells were cultured on the RPM for 24 h, one part of the cells started to form MCS, which increased in size up to 72 h, while another part remained adherent (Grosse et al. 2012). These changes in growth behaviour were observed in each experiment (Grosse et al. 2012), but also in normal thyrocytes, which had been cultured for 7 d on the RPM (Wuest et al. 2015).

FTC-133 investigated at early time points: 4 h, 24 h and 72 h showed an early onset of spheroid formation after 24 h but numerous and much larger spheroids after 72 h (Warnke et al. 2014). No spheroids were visible in 1*g* control cultures.

This spheroid formation is of special interest, as it occurs in a scaffold-free manner and is therefore a very promising approach for tissue engineering. The 3D structures

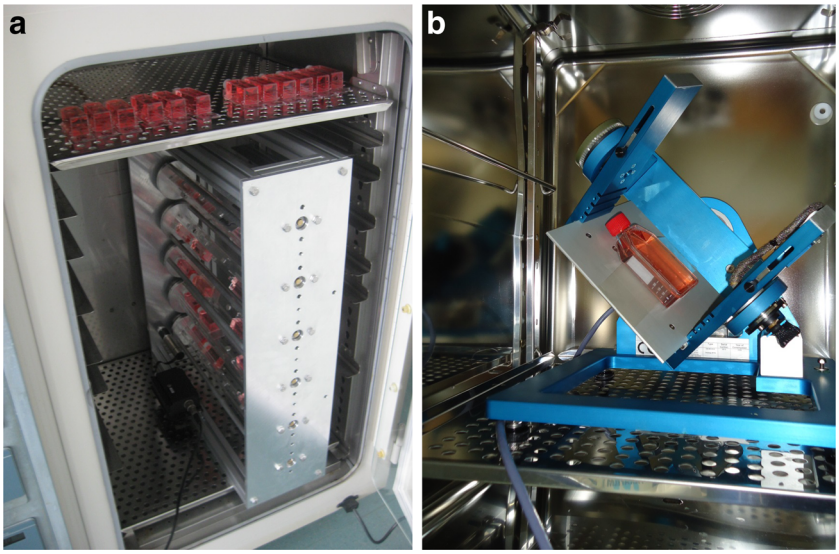

Fig. 1 **a** Fast rotating 2D clinostat and **b** Desktop Random Positioning Machine in an incubator

resemble the *in vivo* situation much better than conventional cell culture in 2D cell monolayer. Studies on molecular mechanisms, tumor cell apoptosis and the angiogenesis process in co-cultures will be of high interest in future studies (Grimm et al. 2014, Grimm et al. 1997). In a proteomic study to analyse the spheroid formation of two human thyroid cell lines cultured on a RPM, Pietsch et al. found that FTC-133 cells express surface proteins that bind fibronectin, strengthening the 3D cell cohesion (Pietsch et al. 2011).

The Cytoskeleton as a Possible Gravisensor

The cytoskeleton is a dynamic structure, which gives shape and mechanical strength to cells but also enables the adaption to external stimuli. This phenomenon can be nicely visualized by the transformation from 2D to 3D growth as observed under real and simulated microgravity conditions (Ma et al. 2014). The underlying biological and molecular mechanisms remain mostly unclear, while it is obvious, that the physical force of gravity needs to be translated into a biochemical signal. The cytoskeleton is therefore suggested to play a role as "gravisensor" in cells lacking a distinct and so far known mechanism for gravity perception (Vorselen et al. 2014).

When follicular thyroid cancer cells were investigated during parabolic flight manoeuvres (Ulbrich et al. 2011), it was shown that the response to altered gravity conditions of ML-1 cells occurred very early, within the first few seconds. After 22 s of microgravity, the F-actin and cytokeratin cytoskeleton was altered, and in parallel *ACTB* and *KRT80* mRNAs were significantly up-regulated after the first parabola (Ulbrich et al. 2011). Studies performed on sounding rockets revealed that the F-actin content increased in A431 epidermoid carcinoma cells after 7 min under microgravity (Boonstra 1999), leading to the suggestion that the actin microfilament system is sensitive to changes in gravity and that remodelling of actin microfilaments may affect signal transduction. Another interesting finding was the detection of septin-11 (SEPT11) in HTU-5 cells (Pietsch et al. 2010). The proteomic discovery of SEPT11 accumulation in HTU-5 cells indicates a role for this cytoskeleton-associated protein in thyrocyte biology. The impact of microgravity on SEPT11 will be studied in detail in future studies.

A 7-day-exposure of Nthy-ori-3-1 cells induced a clear elevation of β-actin protein in AD and MCS cells as measured by Western blot analysis (Fig. 2a). In addition, we detected a significant increase in β-tubulin protein in AD and MCS after a 7-day-culture on the RPM (Fig. 2b). In contrast, β-actin remained unchanged in FTC-133 cells cultured for 7 d on the RPM and β-tubulin was significantly elevated in MCS compared with corresponding $1g-$controls (Fig. 2c, d).

Expression of Growth Factors in Microgravity

Measurements of Vascular Endothelial Growth Factor (VEGF) in the supernatants after a 3-day-exposure of FTC-133 to either CN or RPM showed a reduced (but not significant) secretion of VEGF (Warnke et al. 2014) (Table 2). In contrast, in Space after 10 d no change in the VEGF release was measured, whereas after 10 d on the RPM the cells released a significantly decreased amount of the cytokine (Ma et al. 2014). In general, VEGF is known to promote neoangiogenesis and is therefore an important player for

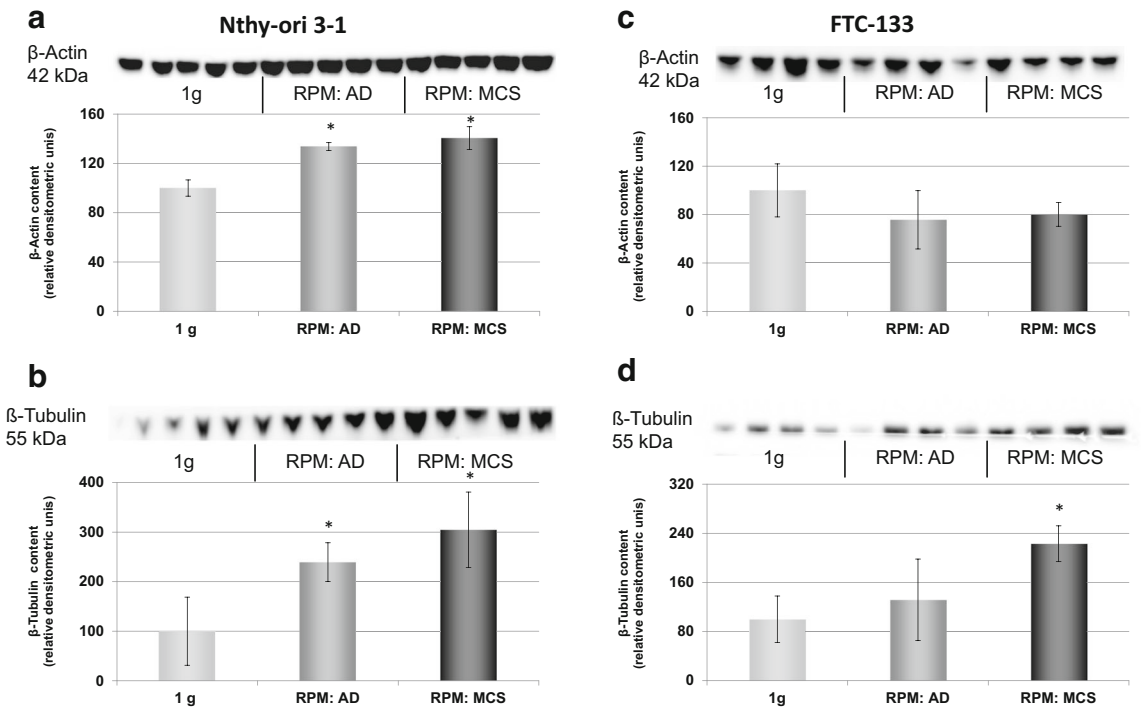

Fig. 2 Western blot analyses of β-Actin **(a)** and β-tubulin **(b)** in Nthy-ori 3-1 cells. β-actin **(c)** and β-tubulin **(d)** in FTC-133 cells

growth and metastasis of tumours (Grimm et al. 2009). A target-based therapy is already of special interest in tumour therapy (Wehland et al. 2012).

No MCS had been detected on both ground-based facilities, CN and RPM, after 4 h, but a change in the gene expression of several cytokines was expected. The Connective Tissue Growth Factor (*CTGF*) mRNA was significantly enhanced on both devices (Warnke et al. 2014). After 72 h, *CTGF* mRNA was still elevated in AD cells on the RPM, but normalized in MCS (Warnke et al. 2014). On the CN there was only a moderate, but not significant elevation, whereas the *CTGF* mRNA was significantly down-regulated in MCS (Warnke et al. 2014). In Space, the *CTGF* gene expression was up-regulated in AD and MCS, whereas the *CTGF* elevation was more pronounced in AD (Pietsch et al. 2013). A clear up-regulation of Epidermal Growth Factor (*EGF*) mRNA in AD and MCS was found in Space and on the RPM compared with controls (Pietsch et al. 2013). Interestingly, *EGF* remained static in FTC-133 cells grown on the CN, whereas *EGF* was up-regulated in MCS on the RPM after a time-period of 72 h (Warnke et al. 2014). These data suggest that EGF and CTGF play a key role in the 3D formation of thyroid cancer cells when they are grown in Space and on the RPM.

Martin et al. have demonstrated in 2000 that recombinant human keratinocyte growth factor facilitated 3D growth of human thyrocytes.

Caveolins are integral membrane proteins and components of caveolae membranes. A higher caveolin expression results in an inhibition of cancer-related pathways (growth factor signaling). We have shown that in MCS engineered in the CN or RPM the *CAV1* gene expression is down-regulated in FTC-133 thyroid cancer cells after a 72-hour-exposure (Warnke et al. 2014; Table 2). An up-regulation of caveolin-1 was found in mouse thyroid glands after a three-month-spaceflight (Masini et al. 2012), a similar result was found when mice were exposed to hypergravity (Albi et al. 2014, Table 1).

Involvement of Il-6 and Il-8 During Gravisensitive Signalling

Since the discovery of IL-6 in 1986, the knowledge on this cytokine for immune homeostasis and its pathophysiology has rapidly increased (Rath et al. 2015). IL-6 is a key cytokine for linking chronic inflammation to cancer development (Rath et al. 2015). IL-6 is a multifunctional cytokine and is expressed by human thyrocytes (Grubeck-Loebenstein et al. 1989; Aust and Scherbaum 1996). It induces the production of VEGF and is involved in neoangiogenesis (Tartour et al. 2011) and thus, may be involved in 3D formation in Space or in simulated microgravity using a RPM or 2D CN. IL-6 plays an important role in modifying various tumour characteristics, such as proliferation,

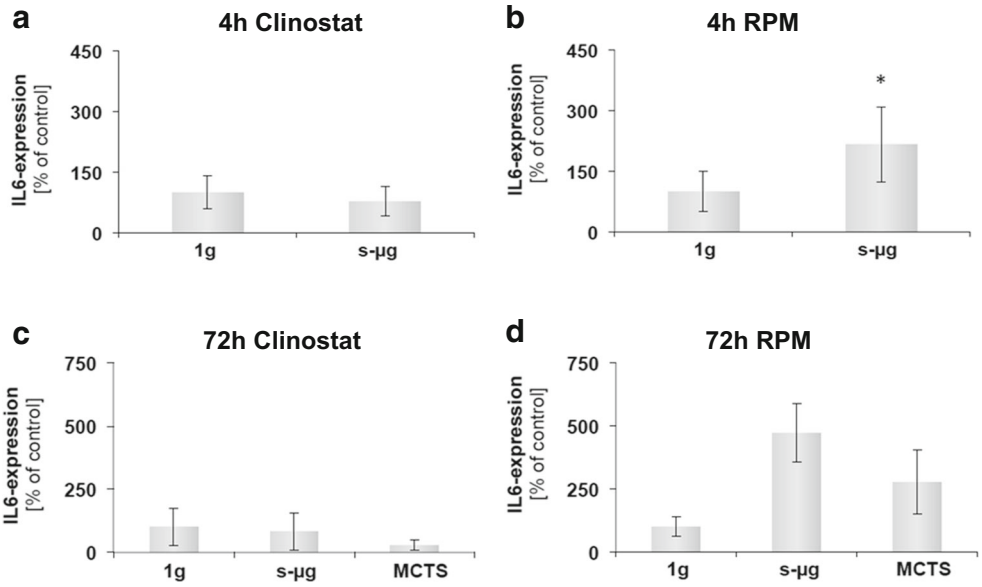

Fig. 3 Expression of the *IL6* gene after 4 h **(a)** and 72 h **(c)** on the CN and after 4 h **(b)** and 72h **(d)** on the RPM in thyroid cancer cells. *P<0.05 vs. 1g controls

migration, differentiation, apoptosis, angiogenesis, invasion and adhesion thus promoting tumour growth and metastasis (reviewed by Tartour et al. 2011). Mechanical stress or stretching enhances IL-6 production in human lung epithelial cells and smooth muscle cells via NF-κB (Copland and Post 2007, Zampetaki et al. 2005). FTC-133 cells showed an enhanced *IL6* gene expression in AD cells and no change in MCS when they were cultured on the RPM for 24 h (Grosse et al. 2012). A similar finding was observed after a 4-hour- and 72-hour-exposure of FTC-133 cells on the RPM, but no change was found for the *IL6* gene expression on the 2D CN (Fig. 3a-d) (Warnke et al. 2014). Using MAP technology, a significantly reduced release of IL-6 protein in the supernatant was found in CN, but an increase in RPM samples (Warnke et al. 2014). We recently showed that a PKCa-independent mechanism of *IL6* gene activation is very sensitive to physical forces in thyroid cells cultured *in vitro* as monolayers under conditions of vibration or hypergravity (Ma et al. 2013).

These findings nicely correspond to earlier data, suggesting an involvement of IL-6 in gravity-sensitive signalling for spheroid formation (Ma et al. 2013, 2014). In a new study we could show for the first time that both cytokines IL-6 and IL-8 induced the formation of MCS in ML-1 and UCLA RO82-W-1 cells using the liquid-overlay technique under 1*g*-conditions (Svejgaard et al. 2015). These investigations support the hypothesis that IL-6 is one of the key factors inducing spheroid formation in Space and on the RPM and CN.

Earlier studies with FTC-133 cells suggest that gravitational unloading leads to an initiation of an early phase of apoptosis. An escape from the late phase then leads to the transition from 2D to 3D growth (Grosse et al. 2012; Grimm et al. 2014).

Interleukin-8 is a chemokine produced by a variety of cell types. In humans the interleukin-8 protein is encoded by the *IL8* gene. This cytokine is a known strong promoter of angiogenesis. A recent study demonstrated that NF-κB signalling is a key regulator of angiogenesis and growth in thyroid cancer, and that IL-8 may be an important downstream mediator of NF-κB signalling in advanced thyroid cancer growth and progression (Bauerle et al. 2014). FTC-133 cells cultured for 72 h on the CN showed a significant reduction of the *IL8* gene expression in AD cells and MCS (Warnke et al. 2014). Interestingly, we did not observe significant changes of the *IL*8 mRNA after RPM exposure of the FTC-133 cells (Warnke et al. 2014). The secretion of IL-8 protein in the medium of FTC-133 cells cultured on the CN was significantly reduced, whereas a different result was found in the RPM cultures, which exerted an increase (Warnke et al. 2014, Table 2). Interestingly, a different gene expression of *IL8* and differences in the IL-8 secretion behaviour of the cells were found. Reasons for this may be the different culture chambers, which had to be used due to the geometry of the devices. We have used slide flasks on the CN and T 75 cm^2 cell culture flasks on the RPM (Warnke et al. 2014). In a planned future study we will use slide flasks for both devices. Another aspect may be the impact of vibrations, which are critical for the release of cytokines by human cells. The controls were stored next to the device in the same incubator so that the influence should be minimal but this has to be investigated in the future in more detail.

Eiermann et al. (2013) had also found significant differences in the gene expression in cells located at a further distance from the CN rotation axis. These cells are exposed to higher accelerations. Therefore, only cells within the inner 6 mm of the slide flasks were collected. A problem is

that the supernatant consists of released proteins from all cells. This means that also the release of cells exposed to higher accelerations (though still less than 0.036*g*) was measured. This problem might explain some of the differences.

Conclusions and Recommendations

Taken these data together, microgravity induces a variety of changes in thyroid cells. The thyroid cancer cells revealed signs of apoptosis (Grimm et al. 2002; Kossmehl et al. 2003), changed their growth behaviour, differentiation, migration and cell adhesion. Interestingly, already after a short-term sounding rocket flight rat FRTL-5 thyrocytes showed an increase in Bax as well as an irregular shape (Albi et al. 2011).

Spheroid formation was detected in several cell lines in ground-based facilities and also in real microgravity. It demonstrated the good practicability of ground-based devices like RPM and CN for scaffold-free tissue engineering of multicellular spheroids.

It is important to keep in mind that each device affects the cells not only by randomization of the gravity vector but also by device-specific artefacts like vibration, centrifugal accelerations and shearing forces. The susceptibility of cells to gravity alterations but also to these artefacts might vary broadly between different cell lines. A careful and conscious handling of ground-based devices is therefore suggested, with real microgravity experiments as an indispensable tool for validation to identify gravity-related effects (Herranz et al. 2013).

Changes in cytoskeletal proteins were found very early in real and simulated microgravity (Ulbrich et al. 2011; Grosse et al 2012; Pietsch et al. 2011). These observations nicely fit to early studies, reporting a cytoskeletal involvement in the transition from 2D to 3D growth behaviour (Grimm et al. 2014). So far all investigations had been made after termination of the experiments. The cells were fixed with paraformaldehyde and then stained by immunofluorescence. Great new insights are expected by the German national DLR project FLUMIAS in which a Fluorescence Microscopic Analysis System for biological and biomedical research in Space has been developed, enabling in-vivo 3D fluorescence analyses of biological samples in microgravity. FLUMIAS developed by ADS, Bremen, Germany had been successfully flown on TEXUS 52 sounding rocket in April 2015, launch site Esrange, Kiruna, Sweden. Here, FTC-133 poorly differentiated follicular thyroid cancer cells together with other cells were investigated online during a 6-min-exposure to real microgravity allowing visualization of dynamics and adaption of the cytoskeleton. These data will be published soon.

The fast rotating 2D Clinostat and the Random Positioning Machine are important ground-based devices for tissue engineering of spheroids which can be used in cancer research to study drug effects and to spare animal tests. In addition, these devices can be applied for the preparation of a future spaceflight. It is important to know when and how spheroid formation occurs and the mechanisms behind 3D growth. We become able to answer questions like, how big are the spheroids, how many are formed, do they have an impact on the operational capability of the hardware, are filters necessary to avoid that the spheroids block the tubes of the hardware, what happens to the cells when the launch is delayed, or simply to test a newly constructed hardware container under simulated microgravity conditions or check the influence of temperature changes on the cells. The ESA-CORA-Ground-based facility program has supported us to answer these questions and to prepare the SIMBOX/Shenzhou-8 in 2011 and the Cellbox-1 Space missions in 2014 (Pietsch et al. 2013, Ma et al. 2014, Riwaldt et al. 2015).

Abbreviations

° /s:	Degrees per Second
2D:	Two-dimensional
3D:	Three-dimensional
ACTB:	β-actin gene
AD:	adherent cells in simulated microgravity samples
ADS:	Airbus Defence and Space
Bax:	Bcl-2-associated X protein gene
Bcl-2:	B-cell Lymphoma 2 gene
Cav1/2:	Caveolin 1/2 genes
cm:	centimetre
CN:	Clinostat
CORA:	Continuously Open Research Announcement
CTGF:	Connective Tissue Growth Factor
DLR:	Deutsches Zentrum für Luft- und Raumfahrt
EGF:	Epidermal Growth Factor
ERK1/2:	Extracellular Signal-Regulated Kinases 1/2 genes
ESA:	European Space Agency
f-actin:	filamentous actin
FCS:	Fetal Calf Serum
FLUMIAS:	Fluorescence Microscopic Analysis System
FTC:	Follicular Thyroid Carcinoma
g:	Gravity
GBF:	Ground-based facilities
h:	hour
IL:	Interleukin
ITGB1:	Integrin Beta-1 gene
KRT80:	Keratin 80 gene
MAP:	Multi-Analyte Profiling
MCP1:	Monocyte Chemotactic Protein 1

MCS:	Multicellular Spheroids
min:	minute
mm:	millimetre
NF-κB:	Nuclear Factor 'kappa-light-chain-enhancer' of Activated B-cells
NMRI:	Naval Medical Research Institute mice
OPN:	Osteopontin gene
PCR:	Polymerase Chain Reaction
PFC:	Parabolic Flight Campaign
PKCa:	Protein kinase Ca
PRKCA:	Protein Kinase C alpha gene
RBM:	Rules-Based Medicine
RPM:	Random Positioning Machine
rpm:	revolutions per minute
PCR:	Polymerase Chain Reaction
s-μ g:	Simulated Microgravity
SD:	Standard Deviation
SV40:	Simian Virus 40
VEGF:	Vascular Endothelial Growth Factor

Acknowledgments The authors would like to thank the European Space Agency (ESA-CORA-GBF-PROJECT-2011-005 (ACRONYM DEVICE COMPARISON), ESA-CORA-GBF-PROJECT-2013-001 (ACRONYM THYROID III), D.G.) and the German Space Administration (DLR; BMWi grants 50WB1124/50WB1524; D.G.). Elisabeth Warnke is a doctoral candidate of the Helmholtz Space Life Sciences Research School, German Aerospace Center Cologne, Germany and was further funded by the German only one space Aviation and Space Medicine (DGLRM; Young Fellow Program).

Author Contributions This review is based on data of the the ESA-CORA-GBF-PROJECT-2011-005 (ACRONYM DEVICE COMPARISON) and ESA-CORA-GBF-PROJECT-2013-001 (ACRONYM THYROID III).

Conflict of interests The authors declare that they have no conflict of interest.

References

Albi, E., Curcio, F., Lazzarini, A., Floridi, A., Cataldi, S., Lazzarini, R., Loreti, E., Ferri, I., Ambesi-Impiombato, F.S.: How microgravity changes galectin-3 in thyroid follicles. Biomed. Res. Int. **2014**, 652863 (2014)

Albi, E., Curcio, F., Lazzarini, A., Floridi, A., Cataldi, S., Lazzarini, R., Loreti, E., Ferri, I., Ambesi-Impiombato, F.S.: A firmer understanding of the effect of hypergravity on thyroid tissue: cholesterol and thyrotropin receptor. PLoS One **9**, e98250 (2014b)

Albi, E., Curcio, F., Spelat, R., Lazzarini, A., Lazzarini, R., Cataldi, S., Loreti, E., Ferri, I., Ambesi-Impiombato, F.S.: Loss of parafollicular cells during gravitational changes (microgravity, hypergravity) and the secret effect of pleiotrophin. PLoS One **7**, e48518 (2012)

Albi, E., Curcio, F., Spelat, R., Lazzarini, A., Lazzarini, R., Loreti, E., Ferri, I., Ambesi-Impiombato, F.S.: Observing the mouse thyroid sphingomyelin under space conditions: a case study from the MDS mission in comparison with hypergravity conditions. Astrobiology **12**, 1035–41 (2012)

Albi, E., Ambesi-Impiombato, F.S., Peverini, M., Damaskopoulou, E., Fontanini, E., Lazzarini, R., Curcio, F., Perrella, G.: Thyrotropin receptor and membrane interactions in FRTL-5 thyroid cell strain in microgravity. Astrobiology **11**, 57–64 (2011)

Aust, G., Scherbaum, W.A.: Expression of cytokines in the thyroid: thyrocytes as potential cytokine producers. Exp. Clin. Endocrinol. Diabetes **104**, 64–67 (1996)

Bauerle, K.T., Schweppe, R.E., Lund, G., Kotnis, G., Deep, G., Agarwal, R., Pozdeyev, N., Wood, W.M., Haugen, B.R.: Nuclear factor κB-dependent regulation of angiogenesis, and metastasis in an in vivo model of thyroid cancer is associated with secreted interleukin-8. J. Clin. Endocrinol. Metab **99**, E1436–E1444 (2014)

Becker, J.L., Souza, G.R.: Using space-based investigations to inform cancer research on Earth. Nat. Rev. Cancer **13**, 315–327 (2013)

Boonstra, J.: Growth factor-induced signal transduction in adherent mammalian cells is sensitive to gravity. FASEB J. **13**, 35–42 (1999)

Briegleb, W.: Some qualitative and quantitative aspects of the fast-rotating clinostat as a research tool. ASGSB Bull. **5**, 23–30 (1992)

Copland, I.B., Post, M.: Stretch-activated signaling pathways responsible for early response gene expression in fetal lung epithelial cells. J. Cell Physiol. **10**, 133–143 (2007)

Curcio, F., Ambesi-Impiombato, F.S., Perrella, G., Coon, H.G.: Long-term culture and functional characterization of follicular cells from adult normal human thyroids. Proc. Natl. Acad. Sci. **91**, 9004–9008 (1994)

Eiermann, P., Kopp, S., Hauslage, J., Hemmersbach, R., Gerzer, R., Ivanova, K.: Adaptation of a 2D clinostat for simulated microgravity experiments with adherent cells. Microgravity Sci. Tech. **25**, 153–159 (2013)

Freed, L.E., Langer, R., Martin, I., Pellis, N.R., Vunjak-Novakovic, G.: Tissue engineering of cartilage in space. Proc. Natl. Acad. Sci. USA **94**, 13885–13890 (1997)

Goretzki, P.E., Frilling, A., Simon, D., Roeher, H.D.: Growth regulation of normal thyroids and thyroid tumors in man. Recent Results Cancer Res. **118**, 48–63 (1990)

Grimm, D., Bauer, J., Hofstädter, F., Riegger, G.A., Kromer, E.P.: Characteristics of multicellular spheroids formed by primary cultures of human thyroid tumor cells. Thyroid **7**, 859–865 (1997)

Grimm, D., Bauer, J., Kossmehl, P., Shakibaei, M., Schönberger, J., Pickenhahn, H., Schulze-Tanzil, G., Vetter, R., Eilles, C., Paul, M., Cogoli, A.: Simulated microgravity alters differentiation and increases apoptosis in human follicular thyroid carcinoma cells. FASEB J. **16**, 604–606 (2002)

Grimm, D., Bauer, J., Infanger, M., Cogoli, A.: The use of the random positioning machine for the study of gravitational effects on signal transduction in mammalian cells. Signal Transduct. **6**, 388–396 (2006)

Grimm, D., Bauer, J., Schoenberger, J.: Blockade of neoangiogenesis, a new and promising technique to control the growth of malignant tumors and their metastases. Curr. Vasc. Pharmacol. **7**, 347–357 (2009)

Grimm, D., Wehland, M., Pietsch, J., Aleshcheva, G., Wise, P., van Loon, J., Ulbrich, C., Magnusson, N.E., Infanger, M., Bauer, J.: Growing tissues, in real and simulated microgravity: new methods for tissue engineering. Tissue Eng. Part B Rev. **20**, 555–566 (2014)

Grosse, J., Wehland, M., Pietsch, J., Schulz, H., Saar, K., Hübner, N., Eilles, C., Bauer, J., Abou-El-Ardat, K., Baatout, S., Ma, X., Infanger, M., Hemmersbach, R., Grimm, D.: Gravity-sensitive

signaling drives 3-dimensional formation of multicellular thyroid cancer spheroids. FASEB J. **26**, 5124–5140 (2012)

Grubeck-Loebenstein, B., Buchan, G., Chantry, D., Londei, M., Turner, M., Pirich, K., Roka, R., Niederle, B., Kassal, H.: Analysis of intrathyroidal cytokine production in thyroid autoimmune disease: thyroid follicular cells produce interleukin-1 alpha and interleukin-6. Clin. Exp. Immunol. **77**, 324–330 (1989)

Häder, D., Hemmersbach, R., Lebert, M.: Gravity and the behaviour of unicellular organisms. Cambridge University Press, New York (2005)

Herranz, R., Anken, R., Boonstra, J., Braun, M., Christianen, P.C., de Geest, M., Hauslage, J., Hilbig, R., Hill, R.J., Lebert, M., Medina, F.J., Vagt, N., Ullrich, O., van Loon, J.J., Hemmersbach, R.: Ground-based facilities for simulation of microgravity: organism-specific recommend-dations for their use, and recommended terminology. Astrobiology **13**, 1–17 (2013)

Infanger, M., Ulbrich, C., Baatout, S., Wehland, M., Kreutz, R., Bauer, J., Grosse, J., Vadrucci, S., Cogoli, A., Derradji, H., Neefs, M., Küsters, S., Spain, M., Grimm, D.: Modeled gravitational unloading induced downregulation of endothelin-1 in human endothelial cells. J. Cell. Biochem. **101**, 1439–1455 (2007)

Klaus, D.M., Todd, P., Schatz, A.: Functional weightlessness during clinorotation of cell suspensions. Adv. Space Res. **21**(8-9), 1315–1318 (1998)

Kossmehl, P., Cogoli, A., Shakibaei, M., Pickenhahn, H., Paul, M., Grimm, D.: Simulated microgravity induces programmed cell death in human thyroid carcinoma cells. J. Gravit. Physiol. **9**, 295–296 (2002)

Kossmehl, P., Shakibaei, M., Cogoli, A., Infanger, M., Curcio, F., Schönberger, J., Eilles, C., Bauer, J., Pickenhahn, H., Schulze-Tanzil, G., Paul, M., Grimm, D.: Weightlessness induced apoptosis in normal thyroid cells and papillary thyroid carcinoma cells via extrinsic and intrinsic pathways. Endocrinology **144**(9), 4172–4179 (2003)

Kossmehl, P., Kurth, E., Faramarzi, S., Habighorst, B., Shakibaei, M., Wehland, M., Kreutz, R., Infanger, M., Danser, A.H., Grosse, J., Paul, M., Grimm, D.: Mechanisms of apoptosis after ischemia and reperfusion: role of the renin angiotensin system. Apoptosis **11**, 347–358 (2006)

Lemoine, N.R., Mayall, E.S., Jones, T., Sheer, D., Mcdermid, S., Kendalltaylor, P., Wynfordthomas, D.: Characterisation of human thyroid epithelial-cells immortalised in vitro by simian-virus 40-DNA transfection. Br. J. Cancer **60**, 897–903 (1989)

Ma, X., Wehland, M., Aleshcheva, G., Hauslage, J., Wasser, K., Hemmersbach, R., Infanger, M., Bauer, J., Grimm, D.: Interleukin-6 expression under gravitational stress due to vibration and hypergravity in follicular thyroid cancer cells. PLoS One **8**, e68140 (2013)

Ma, X., Pietsch, J., Wehland, M., Schulz, H., Saar, K., Hübner, N., Bauer, J., Braun, M., Schwarzwälder, A., Segerer, J., Birlem, M., Horn, A., Hemmersbach, R., Wasser, K., Grosse, J., Infanger, M., Grimm, D.: Differential gene expression profile and altered cytokine secretion of thyroid cancer cells in space. FASEB J. **28**, 813–835 (2014)

Martin, A., Zhou, A., Gordon, R.E., Henderson, S.C., Schwartz, A.E., Schwartz, A.E., Friedman, E.W., Davies, T.F.: Thyroid organoid formation in simulated microgravity: influence of keratinocyte growth factor. Thyroid **10**, 481–7 (2000)

Masini, M.A., Albi, E., Barmo, C., Bonfiglio, T., Bruni, L., Canesi, L., Cataldi, S., Curcio, F., D'Amora, M., Ferri, I., Goto, K., Kawano, F., Lazzarini, R., Loreti, E., Nakai, N., Ohira, T., Ohira, Y., Palmero, S., Prato, P., Ricci, F., Scarabelli, L., Shibaguchi, T., Spelat, R., Strollo, F., Ambesi-Impiombato, F.S.: The impact of long-term exposure to space environment on adult mammalian organisms: a study on mouse thyroid and testis. PLoS One **7**, e35418 (2012)

Meli, A., Perrella, G., Curcio, F., Hemmersbach, R., Neubert, J., Impiombato, F.A.: Response to thyrotropin of normal thyroid follicular cell strain FRTL5 in hypergravity. Biochimie **81**, 281–5 (1999)

Meli, A., Perrella, G., Curcio, F., Ambesi-Impiombato, F.S.: Response to hypogravity of normal in vitro cultured follicular cells from thyroid. Acta Astronaut **42**, 465–72 (1998)

Pietsch, J., Kussian, R., Sickmann, A., Bauer, J., Weber, G., Nissum, M., Westphal, K., Egli, M., Grosse, J., Schönberger, J., Wildgruber, R., Infanger, M., Grimm, D.: Application of free-flow IEF to identify protein candidates changing under microgravity conditions. Proteomics **10**, 904–13 (2010)

Pietsch, J., Sickmann, A., Weber, G., Bauer, J., Egli, M., Wildgruber, R., Infanger, M., Grimm, D.: A proteomic approach to analysing spheroid formation of two human thyroid cell lines cultured on a random positioning machine. Proteomics **11**, 2095–2104 (2011)

Pietsch, J., Sickmann, A., Bauer, J., Weber, G., Nissum, M., Westphal, K., Egli, M., Grosse, J., Schönberger, J., Eilles, C., Infanger, M., Grimm, D.: Proteome analysis of thyroid cancer cells after long-term exposure to simulated microgravity. Microgravity Sci. Technol. **23**, 381–390 (2011)

Pietsch, J., Ma, X., Wehland, M., Aleshcheva, G., Schwarzwälder, A., Segerer, J., Birlem, M., Horn, A., Bauer, J., Infanger, M., Grimm, D.: Spheroid formation of human thyroid cancer cells in an automated culturing system during the Shenzhou-8 Space mission. Biomaterials **34**, 7694–7670 (2013)

Pietsch, J., Riwaldt, S., Bauer, J., Sickmann, A., Weber, G., Grosse, J., Infanger, M., Eilles, C., Grimm, D.: Interaction of proteins identified in human thyroid cells. Int. J. Mol. Sci. **14**, 1164–1178 (2013)

Rath, T., Billmeier, U., Waldner, M.J., Atreya, R., Neurath, M.F.: From physiology to disease and targeted therapy: interleukin-6 in inflammation and inflammation-associated carcinogenesis. Arch. Toxicol. **89**, 541–554 (2015)

Riwaldt, S., Pietsch, J., Sickmann, A., Bauer, J., Braun, M., Segerer, J., Schwarzwälder, A., Aleshcheva, G., Corydon, T.J., Infanger, M., Grimm, D.: Identification of proteins involved in inhibition of spheroid formation under microgravity. Proteomics **15**, 2945–2952 (2015)

Rothermund, L., Kreutz, R., Kossmehl, P., Fredersdorf, S., Shakibaei, M., Schulze-Tanzil, G., Paul, M., Grimm, D.: Early onset of chondroitin sulfate and OPN expression in angiotensin II-dependent left ventricular hypertrophy. Am. J. Hypertens. **15**, 644–652 (2002)

Schönberger, J., Bauer, J., Spruß, T., Weber, G., Chahoud, I., Eilles, C., Grimm, D.: Establishment and characterization of the follicular thyroid carcinoma cell line ML-1. J. Mol. Med. **78**, 102–110 (2000)

Stamenković, V., Keller, G., Nesic, D., Cogoli, A., Grogan, S.P.: Neocartilage formation in 1 g, simulated, and microgravity environments: implications for tissue engineering. Tissue Eng. Part A **16**, 1729–1736 (2010)

Svejgaard, B., Wehland, M., Ma, X., Kopp, S., Sahana, J., Warnke, E., Aleshcheva, G., Hemmersbach, R., Hauslage, J., Grosse, J., Bauer, J., Corydon, T.J., Islam, T., Infanger, M., Grimm, D.: Common effects on cancer cells exerted by a Random Positioning Machine and a 2D clinostat. PLoS One **10**, e0135157 (2015)

Tartour, E., Pere, H., Maillere, B., Terme, M., Merillon, N., Taieb, J., Sandoval, F., Quintin-Colonna, F., Lacerda, K., Karadimou, A., Badoual, C., Tedgui, A., Fridman, W.H., Oudard, S.: Angiogenesis and immunity: a bidirectional link potentially relevant for the mon-

itoring of antiangiogenic therapy and the development of novel therapeutic combination with immunotherapy. Cancer Metastasis Rev. **30**, 83–95 (2011)

Ulbrich, C., Pietsch, J., Grosse, J., Schulz, H., Saar, K., Hübner, N., Hemmersbach, R., Braun, M., van Loon, J.J.W.A., Vagt, N., Egli, M., Richter, P., Einspanier, R.: Differential gene regulation under altered gravity conditions in follicular thyroid cancer cells: relationship between the extracellular matrix and the cytoskeleton. Cell Physiol. Biochem. **28**, 185–198 (2011)

Van Loon, J.J.: Some history and use of the random positioning machine, RPM, in gravity related research. Adv. Space Res. **39**, 1161–1165 (2007)

Vorselen, D., Roos, W.H., MacKintosh, F.C., Wuite, G.J., van Loon, J.J.: The role of the cytoskeleton in sensing changes in gravity by non-specialised cells. FASEB J **28**, 536–547 (2014)

Warnke, E., Pietsch, J., Wehland, M., Bauer, J., Infanger, M., Görög, M., Hemmersbach, R., Braun, M., Ma, X., Sahana, J., Grimm, D.: Spheroid formation of human thyroid cancer cells under simulated microgravity: a possible role of CTGF and CAV1. Cell Commun. Signal **12**, 32 (2014)

Wehland, M., Bauer, J., Infanger, M., Grimm, D.: Target-based anti-angiogenic therapy in breast cancer. Curr. Pharm. Des. **18**, 4244–4257 (2012)

Wuest, S.L., Richard, S., Kopp, S., Grimm, D., Egli, M.: Simulated microgravity: critical review on the use of Random Positioning Machines for mammalian cell culture. BioMed Res. Int. **2015**, 971474 (2015)

Zampetaki, A., Zhang, Z., Hu, Y., Xu, Q.: Biomechanical stress induces IL-6 expression in smooth muscle cells via Ras/Rac1-p38 MAPK-NF-kappaB signaling pathways. Am. J. Physiol. Heart Circ. Physiol. **288**, H2946–H2954 (2005)

15.4 Publikation 4

Warnke E, Pietsch J, Kopp S, Bauer J, Sahana J, Wehland M, Krüger M, Hemmersbach R, Infanger M, Lützenberg R, Grimm D: Cytokine release and focal adhesion proteins in normal thyroid cells cultured on the random positioning machine“ Cell. Physiol. Biochem.43. 257-270 (2017)

Cellular Physiology and Biochemistry

Cell Physiol Biochem 2017;43:257-270
DOI: 10.1159/000480368
Published online: August 30, 2017
Accepted: Juni 23, 2017

Original Paper

Cytokine Release and Focal Adhesion Proteins in Normal Thyroid Cells Cultured on the Random Positioning Machine

Elisabeth Warnke[a] Jessica Pietsch[a] Sascha Kopp[a] Johann Bauer[b] Jayashree Sahana[c] Markus Wehland[a] Marcus Krüger[a] Ruth Hemmersbach[d] Manfred Infanger[a] Ronald Lützenberg[a] Daniela Grimm[a,c]

[a]Clinic for Plastic, Aesthetic and Hand Surgery, Otto-von-Guericke-University Magdeburg, Magdeburg, Germany; [b]Max-Planck Institute of Biochemistry, Martinsried, Germany; [c]Institute of Biomedicine, Pharmacology, Aarhus University, Aarhus, Denmark; [d]DLR, German Aerospace Centre, Institute of Aerospace Medicine, Gravitational Biology, Cologne, Germany

Key Words
Thyroid • Multicellular spheroids • Cytokines • Focal adhesion • Extracellular matrix proteins • Pathway analyses

Abstract
Background/Aims: Spaceflight impacts on the function of the thyroid gland *in vivo*. *In vitro* normal and malignant thyrocytes assemble in part to multicellular spheroids (MCS) after exposure to the random positioning machine (RPM), while a number of cells remain adherent (AD). We aim to elucidate possible differences between AD and MCS cells compared to 1*g*-controls of normal human thyroid cells. ***Methods:*** Cells of the human follicular epithelial thyroid cell line Nthy-ori 3-1 were incubated for up to 72 h on the RPM. Afterwards, they were investigated by phase-contrast microscopy, quantitative real-time PCR and by determination of cytokines released in their supernatants. ***Results:*** A significant up-regulation of *IL6*, *IL8* and *CCL2* gene expression was found after a 4h RPM-exposure, when the whole population was still growing adherently. MCS and AD cells were detected after 24 h on the RPM. At this time, a significantly reduced gene expression in MCS compared to 1*g*-controls was visible for *IL6*, *IL8*, *FN1*, *ITGB1*, *LAMA1*, *CCL2*, and *TLN1*. After a 72 h RPM-exposure, IL-6, IL-8, and TIMP-1 secretion rates were increased significantly. ***Conclusion:*** Normal thyrocytes form MCS within 24 h. Cytokines seem to be involved in the initiation of MCS formation via focal adhesion proteins.

Introduction

Long-term space missions are a challenge for the health of crewmembers. There are reports about various health concerns such as dysfunctions of the musculoskeletal and cardiovascular system, a down-regulation of the immune system, and visual problems [1-3]. In space, the thyroid gland *in vivo* revealed a variety of changes such as follicles with

E. Warnke and J. Pietsch contributed equally to this manuscript.

Daniela Grimm
Department of Biomedicine, Space Medicine, Aarhus University, Wilhelm Meyers Allé 4, DK-8000 Aarhus C, (Denmark)
Tel. +45-871 67693, Fax +45-8612 8804, E-Mail dgg@biomed.au.dk

larger thyrocytes and increases in cAMP, thyrotropin-receptors (TSHR), and caveolin-1 [4, 5]. On the cellular level, it is known that both real (r-μ*g*) and simulated microgravity (s-μ*g*) influence growth behaviour, gene expression pattern, protein synthesis and secretion in thyroid cancer cells [6-11]. In addition, thyroid hormone production is decreased, while a TSHR up-regulation was detected in follicular thyroid cancer cells after exposure for 24 h to a random positioning machine (RPM) [12] - a device designed to simulate microgravity conditions [13, 14]. As thyroid hormones produced by the thyroid gland are influencing the function of nearly every cell and organ of the human body [15, 16], thyroid cells cultured under microgravity justify a thorough investigation. Therefore, the research was extended to normal thyrocytes.

Culturing normal thyroid cells in a rotary cell culture system (RCCS), three-dimensional (3D) cell aggregates resembling thyroid follicles were observed exhibiting the ability to produce thyroglobulin [17]. Rat FRTL-5 thyroid cells were investigated in r-μ*g* during a TEXUS rocket flight. The cells did not respond to thyrotropin (TSH) treatment and exhibited an irregular shape with condensed chromatin, shedding of the TSHR in the supernatant, and elevated protein levels of sphingomyelin-synthase and Bax [18]. Mice exposed to hypergravity treatment revealed up-regulation of the TSHR and caveolin-1 as well as a down-regulation of STAT3 without changes in cAMP [19].

Earlier experiments have shown that human thyroid cancer cells exhibit changes in the secretion of growth factors and cytokines, as well as alterations in the factors involved in 3D growth, in the cytoskeleton, and in the extracellular matrix composition when cultured in a an RPM [10, 20, 21]. Furthermore, human thyroid cells may exhibit two phenotypes in s-μ*g* either in the form of multicellular spheroids (MCS) or as adherent monolayer (AD) cells [20, 21].

For the present study, the human follicular epithelial thyroid cell line Nthy-ori 3-1 was exposed for 4 h, 24 h and 72 h to the RPM. MCS and AD cells were investigated in comparison to static 1*g*-controls. For this purpose, phase-contrast images were taken to monitor expected changes in the morphology of the thyrocytes. Furthermore, quantitative real-time PCR (qPCR) and multi-analyte profiling (MAP) analyses were performed. The chosen genes and cytokines were detected previously to have changed in cells of this cell line in s-μ*g* after RPM-exposure of 7 and 14 days [21]. The principal aim of these experiments was to close the knowledge gap concerning the impact of microgravity on the behaviour of normal thyroid cells exposed for a short time to s-μ*g* generated by an RPM.

Materials and Methods

Culture of Nthy-ori 3-1 cells

The Nthy-ori 3-1 cell line (Sigma-Aldrich, Munich, Germany) is a primary human thyroid follicular epithelial cell line. The immortalised cell line exhibits thyroid specific functions, such as iodide-trapping and thyroglobulin synthesis and reveals no signs of tumorigenesis, when transplanted into nude mice [22].

The Nthy-ori 3-1 cells were cultured under standard cell culture conditions (37°C and 5% CO_2). The cells grew in RPMI 1640 medium (Life Technologies, Naerum, Denmark), supplemented with 1 % penicillin/streptomycin (Life Technologies) and 10 % (v/v) fetal calf serum (FCS) (Biochrom, Berlin, Germany). The cells were cultured in T25 cm^2 vented cell culture flasks (Sarstedt, Newton, USA) for one day prior to RPM-exposure. Each flask was seeded with 1×10^6 cells. The culture flasks were filled completely with medium without any air bubbles. The flasks (n = 60 per time point) were assigned randomly to use as static controls (1*g*; n = 30) or as RPM-samples (n = 30). The 1*g*-controls were positioned next to the RPM in the same incubator. Supernatants and cells were harvested after 4 h, 24 h or 72 h according to the protocol.

Random positioning machine (RPM)

The Desktop RPM manufactured by Airbus Defense & Space (ADS, Leyden, The Netherlands) was used for the simulation of microgravity [23]. The device was stored in an incubator at 37°C and 5 % CO_2, operated in real random direction mode at 60 degrees/s and equipped with T25 flasks. The flasks were fixed to the ground plate, giving a maximum distance of 7.5 cm from the centre of rotation.

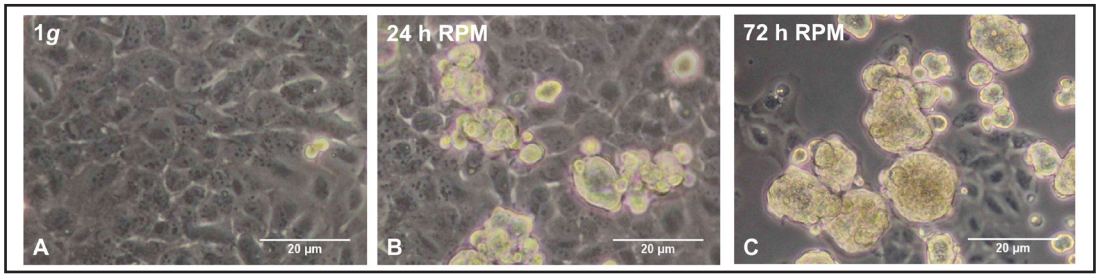

Fig. 1. Phase-contrast microscopy images of Nthy-ori 3-1 cells under 1*g*-conditions and after 24 h and 72 h of exposure to the RPM. Human thyrocytes of the cell line Nthy-ori 3-1 were exposed to the RPM for up to 72 h. Compared to 1*g*-controls (A), which showed only cells growing as adherent monolayers, cells exposed to s-µ*g* generated by the RPM showed no morphological differences after 4 h (data not shown), but started to detach and form 3D aggregates after a 24 h RPM-exposure (B). The MCS increased in number and size over time (72 h), while adherent cells decreased (C).

After the experimental run, cells and supernatants were harvested according to the protocol. The supernatants were collected and centrifuged at 4°C and 3000 rpm. Samples of 1.5 mL were transferred from the supernatants to 2 mL Eppendorf tubes (Eppendorf, Wesseling-Berzdorf, Germany) and frozen at -80°C for MAP analyses. The pellet resulting from centrifugation contained the MCS. After removal of the supernatant, the MCS pellets were snap frozen in liquid nitrogen. AD cells were washed twice with PBS on ice, scraped off the bottom surface and transferred into a tube. After a centrifugation for 10 min at 3000 rpm and 4°C, the supernatant was discarded. The pellets were resuspended in 1 mL PBS and again centrifuged for 10 min at 3000 rpm and 4°C. The remaining supernatant was discarded carefully and the pellets with AD cells snap frozen in liquid nitrogen. Finally, the cells were stored at -80°C.

Phase-contrast microscopy

Phase-contrast microscopy was performed for visual observation of the cellular morphology, using the Leica Microscope (Leica Microsystems CMS GmbH, Germany). Pictures of RPM and control samples were taken after 4 h and 24 h (Fig. 1).

Cytokine measurements by multianalyte profiling (MAP) technology

Cytokines and proteins released into the supernatant were analysed by the company Myriad RBM (Austin, Texas, USA). The MAP analysis was performed using the Human CytokineMAP A and the KidneyMAP® as described previously [24-29]. Supernatants were taken after 4 h, 24 h and 72 h from 1*g*- and RPM-samples (n = 9-10; each group) and stored at -80°C until shipment to Myriad RBM.

RNA isolation and quantitative real-time PCR (qPCR)

RNA isolation was performed using the RNeasy Mini Kit (Qiagen, Hilden, Germany), with an additional DNase digestion step (Qiagen) in order to eliminate residual DNA contaminations. Subsequently, the amount of RNA was quantified via a Photometer Ultrospec2010 (Amersham Biosciences, Freiburg, Germany). The first strand cDNA synthesis kit (Thermo Fisher Scientific, Waltham, US) was used for reverse transcription. qPCR was performed using the 7500 Real-Time PCR System (Applied Biosystems, Darmstadt, Germany) according to routine protocols [30-32]. cDNA-selective-primers were synthesized by TIB Molbiol (Berlin, Germany) and are listed in Table 1. The primers were designed using Primer Express (Applied Biosystems, Darmstadt, Germany) to have a T_m of ~ 60°C and to span exon-exon boundaries. All samples were measured in triplicate. For normalization, 18S rRNA

Table 1. Primers used for quantitative real-time PCR. All sequences are given in 5'-3' direction

Gene	Primer Name	Sequence
18S rRNA	18S-F	GGAGCCTGCGGCTTAATTT
	18S-R	GGAGCCTGCGGCTTAATTT
FN1	FN1-F	AGATCTACCTGTACACCTTGAATGACA
	FN1-R	CATGATACCAGCAAGGAATTGG
IL6	IL6-F	CGGGAACGAAAGAGAAGCTCTA
	IL6-R	GAGCAGCCCCAGGGAGAA
CXCL8	CXCL8-F	TGGCAGCCTTCCTGATTTCT
	CXCL8-R	GGGTGGAAAGGTTTGGAGTATG
CCL2	CCL2-F	GCTATAGAAGAATCACCAGCAGCAA
	CCL2-R	TGGAATCCTGAACCCACTTCTG
LAMA1	LAMA1-F	TGCTCATGGTCAATGCTAATCTG
	LAMA1-R	TCTATCAATCCTCTTCCTTGGACAA
ITGB1	ITGB1-F	GAAAACAGCGCATATCTGGAAAT
	ITGB1-R	CAGCCAATCAGTGATCCACAA
TLN1	TLN1-F	GATGGCTATTACTCAGTACAGACAACTGA
	TLN1-R	CATAGTAGACTCCTCATCTCCTTCCA

All sequences are given in 5'-3' direction

was used as a housekeeping gene. The comparative C_T ($\Delta\Delta C_T$) method was used for relative quantification of transcription levels and 1*g* was defined as 100 % for reference.

Western blot analyses

Whole cell lysates were used for Western blotting following routine protocols for gel electrophoresis and trans-blotting, as described earlier [31, 33]. Equal amounts of 10 µL lysate containing 2 µg/µL protein were loaded on precast TGX stain-free gels (Bio-Rad, Munich, Germany). Transturbo blot PVDF membranes (Bio-Rad) were used for blotting. Each Western blot contained 5 samples for each group: 4 h 1*g*, 4 h RPM-AD cells, 24 h 1*g*, 24 h RPM AD cells and 24 h RPM MCS.

The following primary antibodies were used at a dilution of 1:1000: fibronectin (F3648), laminin (L9393) and talin (T3287) (all Sigma-Aldrich) and vascular endothelial growth factor (VEGFA; ab46154, Abcam, Cambridge, United Kingdom). The corresponding secondary antibodies were used at a dilution of 1:3000: HRP-linked anti-mouse IgG (#7076) and anti-rabbit IgG (#7074, both Cell Signaling Technology, Massachusetts, USA). The analysis was performed in ChemiDoc XRS+ (Bio-Rad), and the densitometric quantification was performed using ImageLab (BioRad).

Pathway Studio analysis

The commercially available Pathway Studio v.11 (Elsevier Research Solutions, Amsterdam, The Netherlands) was applied for the investigation of mutual regulation networks. For the analysis, SwissProt numbers of the investigated proteins were entered and networks built by the software based on relationships and processes from the literature, PubMed, databases and experimental data [9, 10, 33].

Statistical evaluation

Statistical evaluation was performed with SPSS 15.0 (SPSS, Inc., Chicago, IL, USA) using the Mann-Whitney-U-Test. All data are presented as mean ± standard deviation (SD) values and differences between groups were considered significant at $p < 0.05$.

Results

Multicellular spheroid (MCS) formation

Subconfluent monolayers of the human follicular epithelial thyroid cell line Nthy-ori 3-1 were exposed to the RPM or to 1*g*-control conditions. Both groups were located in parallel in the same incubator. After 4 h, the cells of both RPM and 1*g*-controls groups showed solely adherent growth. MCS formation occurred within 24 h on the RPM (Fig. 1) while cells of the 1*g*-controls continued to grow as a 2D cell monolayer attached to the bottom of the culture flask. In RPM cultures, the mixture of AD cells and MCS remained for up to 72 h of RPM-exposure, although the number of AD cells appeared to decrease slightly. The two cell populations could be harvested separately from the RPM-samples according to the method described above.

Cytokine release of Nthy-ori 3-1 cells after RPM-exposure

Concentrations of selected cytokines within the various culture supernatants were determined by MAP analysis in order to estimate the secretion activities of the cells (Human CytokineMAP A and Human KidneyMAP®, carried out by Myriad RBM). Table 2 shows all of the cytokines of these two MAPs, which could be detected.

Interleukin 6 (IL-6; *IL6*), interleukin 8 (IL-8; *CXCL8*), cystatin-c (*CST3*), tissue inhibitor of metalloproteinase (TIMP-1; *TIMP1*) and VEGF (*VEGF*) could be detected after 4 h, whereas monocyte chemoattractant protein (MCP-1; *CCL2*) could only be detected after 24 h and 72 h and interleukin 7 (IL-7; *IL7*) could only be detected after 72 h and even then only in the RPM-samples.

Although these cytokines have been identified, only five of them revealed significant differences between 1*g* and the respective RPM sample. Cystatin-c (*CST3*) and tissue inhibitor of metalloproteinase-1 (*TIMP1*) were reduced significantly in s-µ*g* compared to 1*g* after 4 h.

Table 2. Cytokines released by Nthy-ori 3-1 cells after a 4 h-, 24 h- and 72 h-RPM-exposure, detected by Multi-Analyte Profiling using human CytokineMAP A® and human KidneyMAP®

		4h		24h		72h	
Factors	LDD (pg/mL)	1*g* (pg/mL)	RPM (pg/mL)	1*g* (pg/mL)	RPM (pg/mL)	1*g* (pg/mL)	RPM (pg/mL)
Human CytokineMAP A							
IL-6	1.0	15.72	13.00	107.78	102.70	180.00	267.22
(*IL6*)		± 9.12	± 4.31	± 39.98	± 17.06	± 26.45	± 34.13 *
IL-7	6.1	n.d.	n.d.	n.d.	n.d.	n.d.	8.54
(*IL7*)							± 0.72
IL-8	0.56	37.9	30.4	324.6	224.8	468.4	642.3
(*CXCL8*)		± 19.47	± 10.02	± 177.32	± 54.84	± 92.08	± 176.16 *
MCP-1	15	n.d.	n.d.	112.22	66.89	433.56	441.1
(*CCL2*)				± 53.42	± 20.09	± 82.27	± 67.67
Human KidneyMAP®							
Cystatin-c	20	358.00	185.56	3,022.2	2,680.0	9,755.56	11,190.00
(*CST3*)		± 87.6	± 35.00 *	± 739.04	± 727.74	± 1,101.63	± 1,781.2
TIMP-1	6.1	177.00	102.7	2,410.0	2,030.0	6,344.44	8,366.67
(*TIMP1*)		± 44.73	± 20.78 *	± 811.73	± 376.96	± 869.36	± 1,531.89*
VEGF	3.9	12.07	10.85	110.00	124.6	328.56	359.5
(*VEGFA*)		± 2.45	± 2.39	± 36.33	± 38.71	± 56.35	± 72.24

The gene names of the proteins are given in brackets. Values are given as mean ± SD; 1*g*, ground control; n.d., not detectable; *, P <0.05 vs. 1*g*; LDD (Least Detectable Dose) determined as the mean of 20 blank readings.

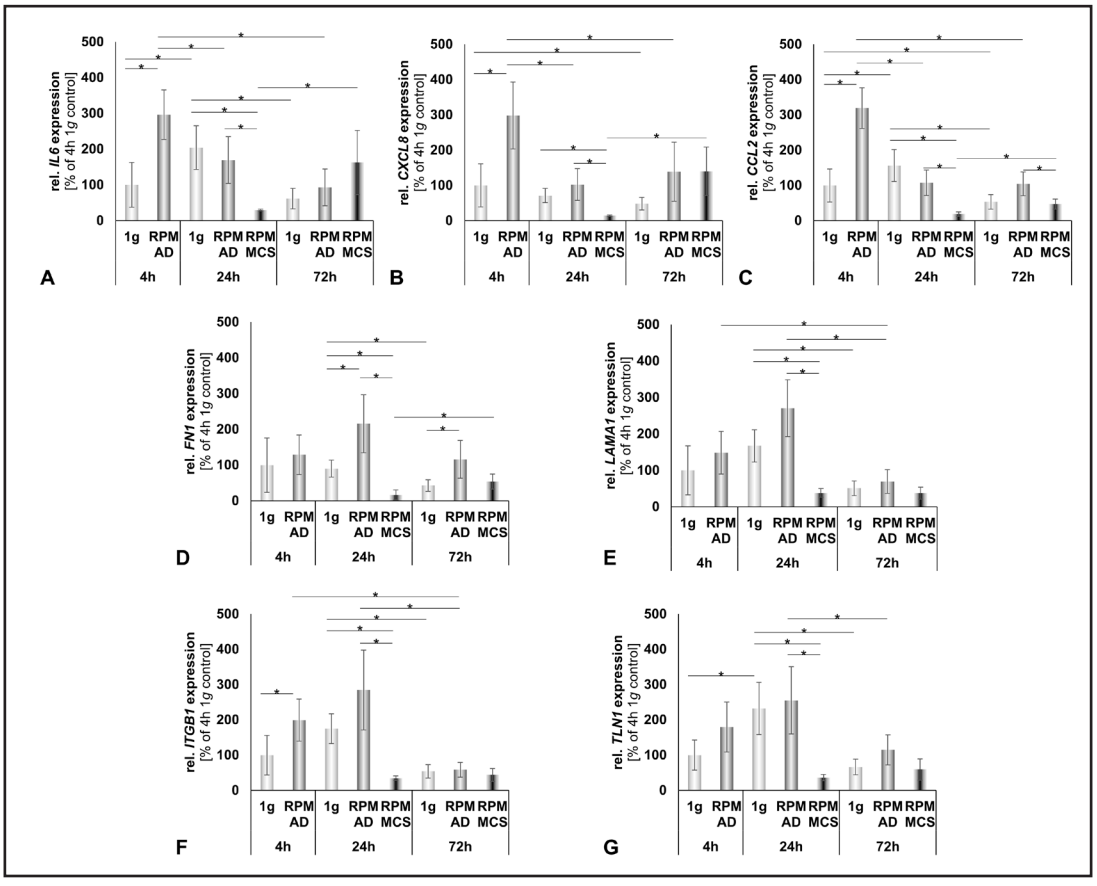

Fig. 2. Quantitative real-time PCR (qPCR) was used to determine the gene expression. The gene expression levels of *IL6* (A), *CXCL8* (B), *CCL2* (C), *FN1* (D), *LAMA1* (E), *ITGB1* (F), and *TLN1* (G) were measured after 4 h, 24 h and 72 h RPM-exposure and in corresponding 1*g*-controls. All values were expressed relative to the value for 4 h of 1*g*, which was set to 100 % and all other values are expressed relative to this value. 1*g* – static control; RPM – random positioning machine; AD – adherent cells; MCS – multicellular spheroids; n = 5-6; * - p<0.05.

After 24 h RPM-exposure, no significant changes could be observed. However, after 72 h, IL-6 (*IL6*), IL-8 (*CXCL8*) as well as TIMP-1 (*TIMP1*) were elevated significantly in s-µ*g* compared to 1*g*-controls.

Altered gene expression in Nthy-ori 3-1 cells exposed to the RPM

Changes in the mRNA expression levels of *IL6*, *CXCL8* and *CCL2* were investigated by qPCR (Fig. 2A-C). This revealed a significant increase between 1*g*- control cells and RPM-AD cells that had been exposed for 4 h. However, these increases in gene expression were already equalized after 24 h. Interestingly, the gene expression was decreased significantly after 24 h in RPM-MCS samples compared to 1*g*-controls as well as RPM-AD samples. For *IL6* and *CXCL8* no significant alterations were detectable after RPM-exposure for 72 h. *CCL2* gene expression was only reduced significantly compared to RPM-AD samples, but not compared to 1*g*-controls.

Furthermore, we focused on the genes coding for fibronectin (*FN1*), laminin (*LAMA1*), β_1-integrin (*ITGB1*), and talin (*TLN1*), as these are involved in focal adhesion processes. Only *ITGB1* showed a significantly increased gene expression in RPM-AD samples compared to 1*g*-controls after 4 h (Fig. 2F). The other three genes revealed no significant changes at this time point (Fig. 2D, E and G). However, 24 h of RPM exposure triggered a significantly elevated expression in *FN1* in RPM-AD samples compared to 1*g*-controls and MCS, while *TLN1, ITGB1* and *LAMA1* were up-regulated significantly in RPM-AD samples compared to RPM-MCS samples only, but were expressed similarly in 1*g*-control samples. After RPM-exposure for 72 h, only a significant increase in RPM-AD samples compared to 1*g* controls could be detected for *FN1* expression level (Fig. 2D).

Content of selected proteins after RPM-exposure

After focusing on gene expression changes, we studied the ECM and cell adhesion molecules laminin, fibronectin and talin-1 (Fig. 3A, B, and D). The amount of laminin was similar in cells exposed for 4 h to the RPM, but increased after 24 h. There was no significant difference in the laminin protein content after a 24 h-exposure (Fig. 3A). Also, the fibronectin accumulation was approximately equal in samples incubated for 4 h. After 24 h, both, the RPM-AD cells and the RPM-MCS cells exhibited increased amounts of fibronectin (Fig. 3B). Talin-1, which links integrins to the actin cytoskeleton has been shown to be increased slightly in MCS compared to 1*g* and AD cells after RPM-exposure for 24 h. VEGF was released into the supernatant and was unaltered in 1*g*-control cells of thyrocytes cultured for 4 h on the RPM, while RPM-AD cells that had been exposed for 24 h exhibited a lower VEGF content. There was no difference in VEGF content between MCS and 1*g*-control cells (Fig. 3C).

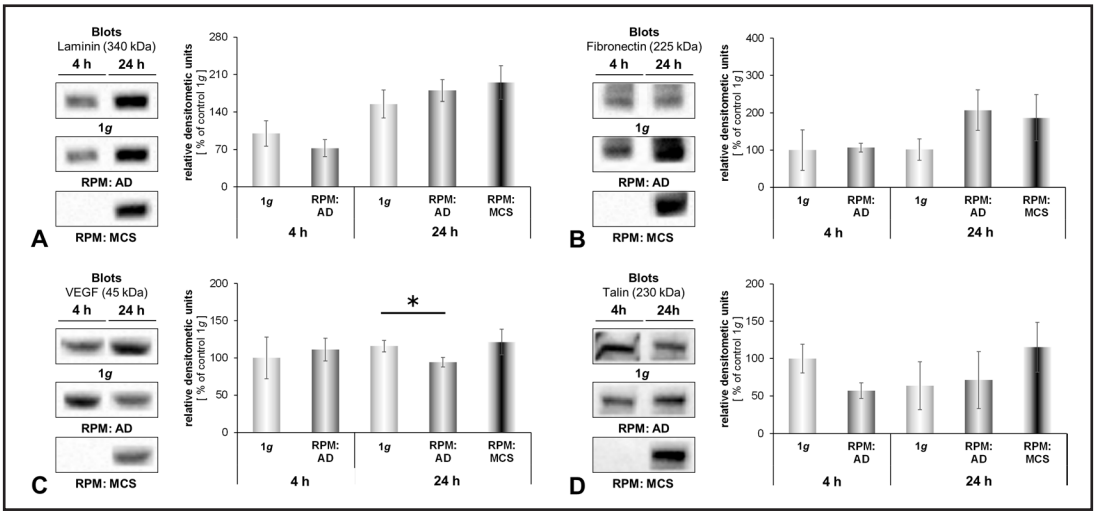

Fig. 3. Content of cell adhesion proteins, VEGF and talin. Nthy-ori 3-1 cells were harvested after 4 h and 24 h of exposure to the RPM or as corresponding 1*g*-controls. The protein contents of laminin (A), fibronectin (B), VEGF (C) and talin (D) were detected by Western blot analyses. Static 1*g*-control (1*g*); random positioning machine (RPM); adherent cells (AD); multicellular spheroids (MCS); n =5; * $p < 0.05$ vs. 1*g*-control.

Pathway Analyses

Searching related information via Pathway Studio, proteins of differentially expressed genes and proteins detected in the supernatant of Nthy-ori 3-1 cells were investigated with respect to their cellular localization and their interaction on the protein level (Fig. 4) as well as in regard to their mutual influence on the genetic level (Fig. 5). The cohort of proteins analysed includes the extracellular proteins laminin A1 and fibronectin, the membrane proteins integrin-β_1 and talin-1. These four proteins can bind to each other as shown by the solid lines in Fig. 4 [34, 35]. Their stability is enhanced by a direct interaction with TIMP1 [36] and via an indirect positive action by IL-8 [37]. IL-7 and VEGF also have an influence on the ITGB1, LAMA1, FN1, TLN1 complex [38-40], while IL-6, MCP-1 and cystatin c do not appear to make contact with this complex.

On the gene level *LAMA1* is isolated from the genes of the other soluble and membrane-bound proteins investigated (Fig. 5). Like VEGFA, IL-6 and MCP-1 have positive regulatory effects on the genes of *ITGB1* and *FN1* [41-45]. IL-8 can up-regulate *FN1* expression [46]. *CXCL8* and *CCL2* genes are also up-regulated by VEGF and IL-6 [47, 48], while *TLN1* is down-regulated by IL-6 and IL-8 [49]. In addition, cystatin c affects turnover of fibronectin [50] and IL-7 regulates the expression of *CCL2* and *CXCL8* [51].

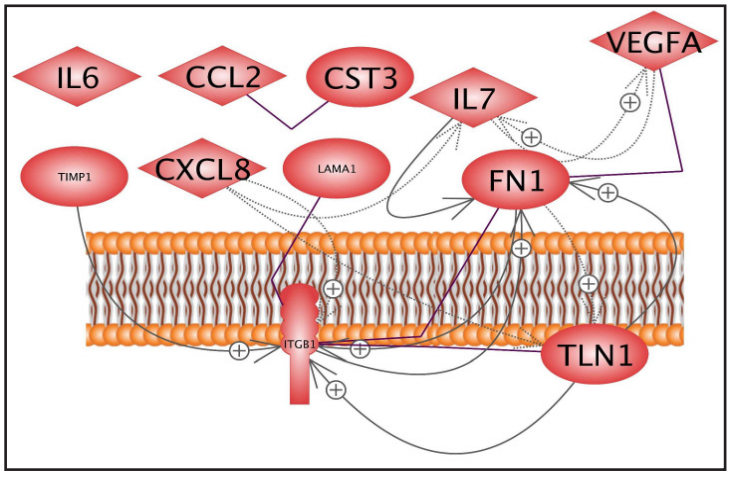

Fig. 4. Mutual interaction and localization of the 11 investigated proteins. Interaction and localization of cytokines observed in cell culture supernatants (Table 2) and of proteins whose genes were sensitive to exposure to the RPM (Fig. 2). Solid lines indicate binding, solid arrows show directed interaction, dashed arrows show influence. + signs point to an activity enhancing effect. The interaction network was built up using Pathway Studio v.11.

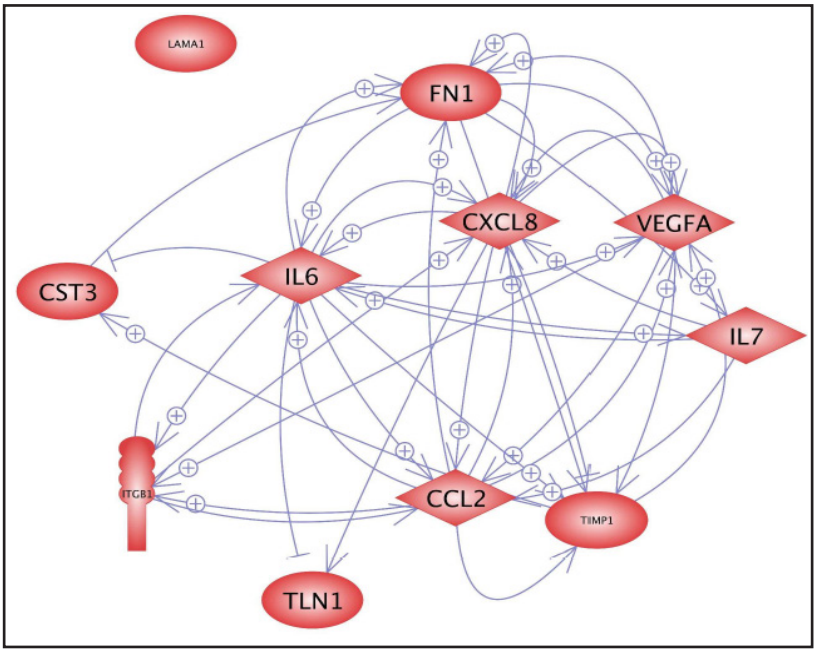

Fig. 5. Mutual interaction of selected genes at the gene expression level. Selected genes, whose up- or down-regulation were analysed by qPCR after RPM-exposure as shown in Fig. 2 together with the genes of the proteins secreted into the supernatant as shown in Table 2. The arrows indicate influence. Arrows with + sign indicate up-regulation, while lines with crossbars at the end show down-regulation. The interaction network was built up using Pathway Studio v.11.

Discussion

In this study, we investigated the morphological and molecular biological changes of normal human thyrocytes (Nthy-ori 3-1 cell line) exposed for 4 h, 24 h and 72 h to a an RPM. The objective of this project was to monitor changes occurring during short-term RPM-exposure in normal human thyrocytes with respect to the influence of soluble factors on proteins involved in focal adhesion. These findings might help to further understand the observed impact of microgravity on the formation of 3D aggregates of normal human thyrocytes and other cells [4, 5].

MCS formation

One part of the RPM-exposed normal human thyroid cells of the Nthy-ori 3-1 cell line formed MCS, while the other part continued to grow adherently. The MCS became visible after 24 h. This observation broadens the observation made by Kopp et al., who investigated MCS after 7 and 14 days [21]. This early 3D growth is in agreement with the formation of cancer MCS by the thyroid cancer cells lines ML-1, FTC-133 and RO82-W-1 [12, 21, 28, 49]. Like the thyroid cancer cells FTC-133, the normal Nthy-ori 3-1 cells required a lag time of several hours of RPM-exposure, before some of the cells started to detach from the bottom of the culture flask and to assemble to 3D aggregates [28], while others remained adherent. Hence, regarding the morphological changes triggered by s-μ*g*, a striking difference between normal and cancer cells could not be detected.

Genes and proteins altered by RPM-exposure

Investigating cytokines, we found an influence of s-μ*g* on IL-6 (*IL6*) and IL-8 (*CXCL8*) at gene and protein secretion levels (Table 2, Fig. 2). The cytokines IL-6 and IL-8 are involved in angiogenesis and progression in different cancer types [52-54]. On the RPM, their genes were up-regulated significantly after 4 h in RPM-AD cells. However, after 24 h both were un-regulated again in RPM-AD cells, but were down-regulated significantly in MCS cells (Fig. 2). During the next 48 h a slight tendency of up-regulation in AD as well as MCS cells was observed although this was not significant (Fig. 2A, B). In parallel, the secretion of IL-6 and IL-8 into the supernatant did not reveal any alteration due to s-μg until 72 h when both proteins were up-regulated significantly in RPM-exposed cells (Table 2).

IL-6 and IL-8 play a key role in angiogenesis and 3D growth in cancer [55, 56]. IL-6 induces the production of VEGF [57] and a similar function is assumed for IL-8 (Fig. 5). When secreted by U937 cells IL-8 induces the fibronectin expression by inflammatory breast cancer cells (SUM149 cell line) via interaction with IL-8 specific receptors and stimulation of the PI3K/Akt signalling pathway [46].

IL-6 and IL-8 influence the formation and growth of MCS established under 1*g*-conditions [49, 58]. Recently, we demonstrated their direct impact using the liquid-overlay technique [49]. The cytokines IL-6 and IL-8 are strong regulators controlling *FN1* and *ITGB1* expression (Fig. 5). Furthermore, both cytokines were increased significantly in space samples of human thyroid cancer FTC-133 cells cultured in r-μ*g* conditions for 12 days on the International Space Station compared with 1*g*-controls [9]. However, in this case no MCS formation could be observed whereas during another spaceflight on which FTC-133 cells were grown for 10 days in μ*g* and MCS were formed, no differences between ground and space samples could be observed for IL-6 and only a slight decrease was observed for IL-8 [7]. How these findings can be explained regarding the role of IL-6 and IL-8 in 3D growth has to be elucidated in future space experiments.

An important finding was the detection of IL-7 in the supernatant after RPM-exposure for 72 h (Table 2). Interestingly, control samples did not secrete IL-7. IL-7 is considered a powerful pro-inflammatory cytokine, which can induce tumorigenesis [59]. A variety of cells, for example intestinal epithelial cells, keratinocytes, hepatic tissue, endothelial cells, smooth muscle cells, fibroblasts, thyroid cancer cells and others, have proven to produce IL-7 [21, 60]. IL-6 interacts with IL-7 and vice versa (Fig. 5). Together they have a regulatory influence on

cell-cell adhesion of melanocytes [61], but no data exist concerning the interaction between IL-6 and IL-7 for normal thyroid cells. In our experiments the cells secreted IL-7 only after 72 h on the RPM, while the corresponding 1*g*-control cells did not secrete this cytokine at all. However, it could be shown that Nthy-ori 3-1 cells secrete IL-7 after 7 days when cultured under normal 1*g*-conditons and on the RPM [21].

In addition, IL-7 can influence ECM production and decrease fibronectin expression. This was shown in human subconjunctival fibroblasts [62]. In our experiments the *FN1* gene expression was elevated in Nthy-ori 3-1 AD cells after RPM-exposure for 24 h compared with 1*g*-control cells, while the *FN1* mRNA was down-regulated in MCS cells (Fig. 2A). After a 72 h RPM-exposure, the *FN1* expression was still down-regulated in Nthy-ori 3-1 MCS compared to AD cells. This finding was paralleled by the secretion of IL-7 by the RPM-mounted thyroid cells after 72 h and might demonstrate a regulatory interaction of IL-7 with fibronectin (Fig. 4). In addition, these data suggest that the cytokine IL-7 might be a very likely key candidate involved in regulating MCS formation [21].

Integrins are transmembrane α- and β-subunit forming receptors for distinct ECM proteins, such as fibronectin, or laminin [63]. They mediate the cell adhesion to ECM components supporting adhesion of cells grown on two-dimensional surfaces and within three-dimensional matrices [64]. Although integrins consist of α- and β-subunit, incorporated β_1-integrin seems to play a special role increasing cell migration and invasion, and decreasing sensitivity to anti-cancer drug in triple-negative breast cancer [65]. Overexpression of β_1-integrin has been demonstrated to improve the activities and functions of several benign cell types [66]. For example, r-μ*g* during a parabolic flight induced β_1-integrin expression in human chondrocytes [67].

The role that laminin plays in MCS formation remains to be elucidated. However, it is a fact that laminins interact with several integrin isoforms and are involved in migration and development [35, 68]. Moreover, since the gene expression of *LAMA1* was down-regulated in MCS cells, an impact of this gene or protein seems to be very likely. Interestingly, laminin A1 was not detected in a recent proteome study, which revealed more than 5000 proteins of thyroid cancer cells [69]. Therefore, the presence of laminin A1 could be a sign of normal cell differentiation as was shown for human mesenchymal stem cells [70].

Talin (*TLN1*) is found in high concentrations in focal adhesions and links integrins to the actin cytoskeleton [71]. Due to its direct interaction with β_1-integrin (Fig. 4), we analysed the gene expression of *TLN1*. In Nthy-ori 3-1 cells, the *TLN1* mRNA was found to be down-regulated significantly in MCS after RPM-exposure for 24 h, but without differences to normal gravity after 4 and 72 h. It has been shown that TLN1 is involved in RPM-dependent thyroid carcinoma MCS formation [8]. Regarding the findings described above, the *TLN1* gene expression might point to the time frame in which the detachment and subsequent formation of MCS occurs.

VEGF was detectable in Nthy-ori 3-1 cells and the secretion of VEGF increased over time in the supernatant (Table 2). No difference between 1*g*-controls and RPM-samples could be observed up until 72 h. VEGF plays an important role in neoangiogenesis, proliferation and migration, mainly of endothelial cells but also of various other cells types [72-74]. VEGF seems to be affected considerably in thyroid cancer cells exposed to s-μ*g* [72, 75]. Furthermore, there might be a delayed response in Nthy-ori 3-1 cells, when exposed to s-μ*g*. It could be shown that VEGF secretion was decreased after RPM-exposure for 7d [21].

The secretion of TIMP-1 was significantly lower after 4 h in RPM-samples compared with 1*g*-controls, whereas a 1.32-fold elevated amount of TIMP-1 was measured after 72 h in the supernatant of RPM-samples. TIMPs inhibit metalloproteinases, which in turn are widely known to degrade the ECM and thus participate in remodelling the shape and composition of cell aggregates and tissues [76, 77]. An overexpression of TIMP-1 was also implicated in several cancer types and correlated with a less-positive outcome for a patient after treatment [76]. A decreased expression of TIMP-1 seems to facilitate the detachment of the thyroid Nthy-ori 3-1 cells from the bottom of cell culture flasks in the early hours of RPM-exposure (Table 2) due to a failure to stabilize integrin-β_1 activity [36]. The later increase might be a

facilitator of cell-cell contacts during the rearrangement of the focal adhesion complex for 3D cell aggregate formation [69]. A similar influence could be observed in endothelial cells. Even after 7 d and 14 d of RPM-exposure, the amount of TIMP-1 was reduced significantly in s-μ*g* [24]. These data indicate the involvement of TIMP-1 in 3D formation of MCS, which contain a high amount of ECM proteins.

Cystatin-c is secreted as an extracellular polypeptide and functions biologically as a protease inhibitor. Dysregulated cystatin-c levels are implicated in various clinical diseases [78]. The secretion of cystatin-c was decreased significantly after 4 h of RPM-exposure. Later on, no differences between the different groups were evident. As cystatin-c was down-regulated together with TIMP-1 a general inhibition of ECM degradation seems to be a result of microgravity. Further experiments should be conducted to verify this hypothesis.

MCP-1 is a key member of the large family of chemokines which regulate mainly cell trafficking. MCP-1 itself is associated with regulating migration and infiltration of monocytes/macrophages [79]. Many experiments were conducted focusing on MCP-1 and its involvement in various diseases like hypertension, inflammatory or neuronal diseases and cancer. A high or constitutive expression level of *CCL2* is often observed [80-82]. The human thyroid Nthy-ori 3-1 cells secrete MCP-1 after 24 h in a continually increasing amount of MCP-1 although no differences could be observed between normal gravity and s-μ*g*. These findings are in accordance with the earlier results regarding MCP-1 in the supernatant of Nthy-ori 3-1 cells cultivated on the RPM for 7 d [21]. Whether this expression has an impact on the signal transduction or if the MCP-1 specific receptor CCR2 [83] is even expressed, remains to be elucidated.

Conclusion

The normal human thyroid cell line Nthy-ori 3-1 was shown to form MCS as early as 24 h after RPM-exposure. The secretion of several cytokines in connection with focal adhesion proteins paint a picture of entangled and positively or negatively interacting proteins which might strengthen the onset of the MCS formation. Further analyses will have to be performed to elucidate in more detail how these cytokines exert their effect. Though MCS formation is induced by exposing cells to an RPM, which is comparable to their behaviour in r-μ*g*, our results indicate what might happen during a spaceflight. However, they have to be verified under this condition.

Acknowledgements

The authors would like to thank the German Space Agency (DLR; (DG) BMWi projects 50WB1124 and 50WB1524), Aarhus University, Denmark, and DGLRM (Young Fellow Program for EW). We would like to thank the team of PRS & EJE Hertfordshire, UK, for academic proofreading of the manuscript. The funders had no role in study design, data collection and analysis, decision to publish, or preparation of the manuscript. EW is a doctoral candidate of the Helmholtz Space Life Sciences Research School, German Aerospace Centre Cologne, Germany. We like to thank the PhD school for support.

Disclosure Statement

The authors declare no competing financial interest.

References

1 White RJ, Averner M: Humans in space. Nature 2001;409:1115-1118.
2 Grimm D, Wise P, Lebert M, Richter P, Baatout S: How and why does the proteome respond to microgravity? Expert Rev Proteomics 2011;8:13-27.

3 Rea G, Cristofaro F, Pani G, Pascucci B, Ghuge SA, Corsetto PA, Imbriani M, Visai L, Rizzo AM: Microgravity-driven remodeling of the proteome reveals insights into molecular mechanisms and signal networks involved in response to the space flight environment. J Proteomics 2016;137:3-18.
4 Albi E, Curcio F, Lazzarini A, Floridi A, Cataldi S, Lazzarini R, Loreti E, Ferri I, Ambesi-Impiombato FS: How microgravity changes galectin-3 in thyroid follicles. Biomed Res Int 2014;2014:652863.
5 Masini MA, Albi E, Barmo C, Bonfiglio T, Bruni L, Canesi L, Cataldi S, Curcio F, D'Amora M, Ferri I, Goto K, Kawano F, Lazzarini R, Loreti E, Nakai N, Ohira T, Ohira Y, Palmero S, Prato P, Ricci F, Scarabelli L, Shibaguchi T, Spelat R, Strollo F, Ambesi-Impiombato FS: The impact of long-term exposure to space environment on adult mammalian organisms: a study on mouse thyroid and testis. PLoS One 2012;7:e35418.
6 Pietsch J, Ma X, Wehland M, Aleshcheva G, Schwarzwalder A, Segerer J, Birlem M, Horn A, Bauer J, Infanger M, Grimm D: Spheroid formation of human thyroid cancer cells in an automated culturing system during the Shenzhou-8 Space mission. Biomaterials 2013;34:7694-7705.
7 Ma X, Pietsch J, Wehland M, Schulz H, Saar K, Hubner N, Bauer J, Braun M, Schwarzwalder A, Segerer J, Birlem M, Horn A, Hemmersbach R, Wasser K, Grosse J, Infanger M, Grimm D: Differential gene expression profile and altered cytokine secretion of thyroid cancer cells in space. FASEB J 2014;28:813-835.
8 Grosse J, Wehland M, Pietsch J, Schulz H, Saar K, Hubner N, Eilles C, Bauer J, Abou-El-Ardat K, Baatout S, Ma X, Infanger M, Hemmersbach R, Grimm D: Gravity-sensitive signaling drives 3-dimensional formation of multicellular thyroid cancer spheroids. FASEB J 2012;26:5124-5140.
9 Riwaldt S, Pietsch J, Sickmann A, Bauer J, Braun M, Segerer J, Schwarzwalder A, Aleshcheva G, Corydon TJ, Infanger M, Grimm D: Identification of proteins involved in inhibition of spheroid formation under microgravity. Proteomics 2015;15:2945-2952.
10 Riwaldt S, Bauer J, Pietsch J, Braun M, Segerer J, Schwarzwalder A, Corydon TJ, Infanger M, Grimm D: The Importance of Caveolin-1 as Key-Regulator of Three-Dimensional Growth in Thyroid Cancer Cells Cultured under Real and Simulated Microgravity Conditions. Int J Mol Sci 2015;16:28296-28310.
11 Bauer J, Wehland M, Pietsch J, Sickmann A, Weber G, Grimm D: Annotated Gene and Proteome Data Support Recognition of Interconnections Between the Results of Different Experiments in Space Research. Microgravity Sci Technol 2016;28:357-365.
12 Grimm D, Bauer J, Kossmehl P, Shakibaei M, Schoberger J, Pickenhahn H, Schulze-Tanzil G, Vetter R, Eilles C, Paul M, Cogoli A: Simulated microgravity alters differentiation and increases apoptosis in human follicular thyroid carcinoma cells. FASEB J 2002;16:604-606.
13 Brungs S, Egli M, Wuest SL, M. Christianen PC, W. A. van Loon JJ, Ngo Anh TJ, Hemmersbach R: Facilities for Simulation of Microgravity in the ESA Ground-Based Facility Programme. Microgravity Sci Technol 2016;28:191-203.
14 Warnke E, Kopp S, Wehland M, Hemmersbach R, Bauer J, Pietsch J, Infanger M, Grimm D: Thyroid Cells Exposed to Simulated Microgravity Conditions – Comparison of the Fast Rotating Clinostat and the Random Positioning Machine. Microgravity Sci Technol 2016;28:247-260.
15 Hanley P, Lord K, Bauer AJ: Thyroid Disorders in Children and Adolescents: A Review. JAMA Pediatr 2016;170:1008-1019.
16 Ito K, Kagaya Y, Shimokawa H: Thyroid hormone and chronically unloaded hearts. Vascul Pharmacol 2010;52:138-141.
17 Martin A, Zhou A, Gordon RE, Henderson SC, Schwartz AE, Schwartz AE, Friedman EW, Davies TF: Thyroid organoid formation in simulated microgravity: influence of keratinocyte growth factor. Thyroid 2000;10:481-487.
18 Albi E, Ambesi-Impiombato FS, Peverini M, Damaskopoulou E, Fontanini E, Lazzarini R, Curcio F, Perrella G: Thyrotropin receptor and membrane interactions in FRTL-5 thyroid cell strain in microgravity. Astrobiology 2011;11:57-64.
19 Albi E, Curcio F, Lazzarini A, Floridi A, Cataldi S, Lazzarini R, Loreti E, Ferri I, Ambesi-Impiombato FS: A firmer understanding of the effect of hypergravity on thyroid tissue: cholesterol and thyrotropin receptor. PLoS One 2014;9:e98250.
20 Pietsch J, Sickmann A, Weber G, Bauer J, Egli M, Wildgruber R, Infanger M, Grimm D: A proteomic approach to analysing spheroid formation of two human thyroid cell lines cultured on a random positioning machine. Proteomics 2011;11:2095-2104.

21 Kopp S, Warnke E, Wehland M, Aleshcheva G, Magnusson NE, Hemmersbach R, Corydon TJ, Bauer J, Infanger M, Grimm D: Mechanisms of three-dimensional growth of thyroid cells during long-term simulated microgravity. Sci Rep 2015;5:16691.
22 Lemoine NR, Mayall ES, Jones T, Sheer D, McDermid S, Kendall-Taylor P, Wynford-Thomas D: Characterisation of human thyroid epithelial cells immortalised *in vitro* by simian virus 40 DNA transfection. Br J Cancer 1989;60:897-903.
23 Borst AG, van Loon JJWA: Technology and Developments for the Random Positioning Machine, RPM. Microgravity Sci Technol 2008;21:287-292.
24 Grimm D, Infanger M, Westphal K, Ulbrich C, Pietsch J, Kossmehl P, Vadrucci S, Baatout S, Flick B, Paul M, Bauer J: A delayed type of three-dimensional growth of human endothelial cells under simulated weightlessness. Tissue Eng Part A 2009;15:2267-2275.
25 Grimm D, Bauer J, Ulbrich C, Westphal K, Wehland M, Infanger M, Aleshcheva G, Pietsch J, Ghardi M, Beck M, El-Saghire H, de Saint-Georges L, Baatout S: Different responsiveness of endothelial cells to vascular endothelial growth factor and basic fibroblast growth factor added to culture media under gravity and simulated microgravity. Tissue Eng Part A 2010;16:1559-1573.
26 Grosse J, Warnke E, Pohl F, Magnusson NE, Wehland M, Infanger M, Eilles C, Grimm D: Impact of sunitinib on human thyroid cancer cells. Cell Physiol Biochem 2013;32:154-170.
27 Infanger M, Ulbrich C, Baatout S, Wehland M, Kreutz R, Bauer J, Grosse J, Vadrucci S, Cogoli A, Derradji H, Neefs M, Kusters S, Spain M, Paul M, Grimm D: Modeled gravitational unloading induced downregulation of endothelin-1 in human endothelial cells. J Cell Biochem 2007;101:1439-1455.
28 Warnke E, Pietsch J, Wehland M, Bauer J, Infanger M, Gorog M, Hemmersbach R, Braun M, Ma X, Sahana J, Grimm D: Spheroid formation of human thyroid cancer cells under simulated microgravity: a possible role of CTGF and CAV1. Cell Commun Signal 2014;12:32.
29 Grosse J, Warnke E, Wehland M, Pietsch J, Pohl F, Wise P, Magnusson NE, Eilles C, Grimm D: Mechanisms of apoptosis in irradiated and sunitinib-treated follicular thyroid cancer cells. Apoptosis 2014;19:480-490.
30 Infanger M, Faramarzi S, Grosse J, Kurth E, Ulbrich C, Bauer J, Wehland M, Kreutz R, Kossmehl P, Paul M, Grimm D: Expression of vascular endothelial growth factor and receptor tyrosine kinases in cardiac ischemia/reperfusion injury. Cardiovasc Pathol 2007;16:291-299.
31 Kossmehl P, Kurth E, Faramarzi S, Habighorst B, Shakibaei M, Wehland M, Kreutz R, Infanger M, AH JD, Grosse J, Paul M, Grimm D: Mechanisms of apoptosis after ischemia and reperfusion: role of the renin-angiotensin system. Apoptosis 2006;11:347-358.
32 Rothermund L, Kreutz R, Kossmehl P, Fredersdorf S, Shakibaei M, Schulze-Tanzil G, Paul M, Grimm D: Early onset of chondroitin sulfate and osteopontin expression in angiotensin II-dependent left ventricular hypertrophy. Am J Hypertens 2002;15:644-652.
33 Kopp S, Slumstrup L, Corydon TJ, Sahana J, Aleshcheva G, Islam T, Magnusson NE, Wehland M, Bauer J, Infanger M, Grimm D: Identifications of novel mechanisms in breast cancer cells involving duct-like multicellular spheroid formation after exposure to the Random Positioning Machine. Sci Rep 2016;6:26887.
34 Green JA, Berrier AL, Pankov R, Yamada KM: beta1 integrin cytoplasmic domain residues selectively modulate fibronectin matrix assembly and cell spreading through talin and Akt-1. J Biol Chem 2009;284:8148-8159.
35 Ichikawa-Tomikawa N, Ogawa J, Douet V, Xu Z, Kamikubo Y, Sakurai T, Kohsaka S, Chiba H, Hattori N, Yamada Y, Arikawa-Hirasawa E: Laminin alpha1 is essential for mouse cerebellar development. Matrix Biol 2012;31:17-28.
36 Jung KK, Liu XW, Chirco R, Fridman R, Kim HR: Identification of CD63 as a tissue inhibitor of metalloproteinase-1 interacting cell surface protein. EMBO J 2006;25:3934-3942.
37 Xie K: Interleukin-8 and human cancer biology. Cytokine Growth Factor Rev 2001;12:375-391.
38 Shao B, Yago T, Coghill PA, Klopocki AG, Mehta-D'souza P, Schmidtke DW, Rodgers W, McEver RP: Signal-dependent slow leukocyte rolling does not require cytoskeletal anchorage of P-selectin glycoprotein ligand-1 (PSGL-1) or integrin alphaLbeta2. J Biol Chem 2012;287:19585-19598.
39 Ariel A, Hershkoviz R, Cahalon L, Williams DE, Akiyama SK, Yamada KM, Chen C, Alon R, Lapidot T, Lider O: Induction of T cell adhesion to extracellular matrix or endothelial cell ligands by soluble or matrix-bound interleukin-7. Eur J Immunol 1997;27:2562-2570.

40 Mitsi M, Hong Z, Costello CE, Nugent MA: Heparin-mediated conformational changes in fibronectin expose vascular endothelial growth factor binding sites. Biochemistry 2006;45:10319-10328.
41 Zhang GJ, Crist SA, McKerrow AK, Xu Y, Ladehoff DC, See WA: Autocrine IL-6 production by human transitional carcinoma cells upregulates expression of the alpha5beta1 firbonectin receptor. J Urol 2000;163:1553-1559.
42 Suhr KB, Tsuboi R, Seo EY, Piao YJ, Lee JH, Park JK, Ogawa H: Sphingosylphosphorylcholine stimulates cellular fibronectin expression through upregulation of IL-6 in cultured human dermal fibroblasts. Arch Dermatol Res 2003;294:433-437.
43 Giunti S, Tesch GH, Pinach S, Burt DJ, Cooper ME, Cavallo-Perin P, Camussi G, Gruden G: Monocyte chemoattractant protein-1 has prosclerotic effects both in a mouse model of experimental diabetes and *in vitro* in human mesangial cells. Diabetologia 2008;51:198-207.
44 Ashida N, Arai H, Yamasaki M, Kita T: Distinct signaling pathways for MCP-1-dependent integrin activation and chemotaxis. J Biol Chem 2001;276:16555-16560.
45 Ancelin M, Chollet-Martin S, Herve MA, Legrand C, El Benna J, Perrot-Applanat M: Vascular endothelial growth factor VEGF189 induces human neutrophil chemotaxis in extravascular tissue via an autocrine amplification mechanism. Lab Invest 2004;84:502-512.
46 Mohamed MM: Monocytes conditioned media stimulate fibronectin expression and spreading of inflammatory breast cancer cells in three-dimensional culture: A mechanism mediated by IL-8 signaling pathway. Cell Commun Signal 2012;10:3.
47 Lee TH, Avraham H, Lee SH, Avraham S: Vascular endothelial growth factor modulates neutrophil transendothelial migration via up-regulation of interleukin-8 in human brain microvascular endothelial cells. J Biol Chem 2002;277:10445-10451.
48 Heinrich PC, Behrmann I, Haan S, Hermanns HM, Muller-Newen G, Schaper F: Principles of interleukin (IL)-6-type cytokine signalling and its regulation. Biochem J 2003;374:1-20.
49 Svejgaard B, Wehland M, Ma X, Kopp S, Sahana J, Warnke E, Aleshcheva G, Hemmersbach R, Hauslage J, Grosse J, Bauer J, Corydon TJ, Islam T, Infanger M, Grimm D: Common Effects on Cancer Cells Exerted by a Random Positioning Machine and a 2D Clinostat. PLoS One 2015;10:e0135157.
50 Nikitovic D, Juranek I, Wilks MF, Tzardi M, Tsatsakis A, Tzanakakis GN: Anthracycline-dependent cardiotoxicity and extracellular matrix remodeling. Chest 2014;146:1123-1130.
51 Damas JK, Waehre T, Yndestad A, Otterdal K, Hognestad A, Solum NO, Gullestad L, Froland SS, Aukrust P: Interleukin-7-mediated inflammation in unstable angina: possible role of chemokines and platelets. Circulation 2003;107:2670-2676.
52 Kobawala TP, Trivedi TI, Gajjar KK, Patel DH, Patel GH, Ghosh NR: Significance of Interleukin-6 in Papillary Thyroid Carcinoma. J Thyroid Res 2016;2016:6178921.
53 Kumari N, Dwarakanath BS, Das A, Bhatt AN: Role of interleukin-6 in cancer progression and therapeutic resistance. Tumour Biol 2016;9: 11553-11572.
54 Shi J, Wei PK: Interleukin-8: A potent promoter of angiogenesis in gastric cancer. Oncol Lett 2016;11:1043-1050.
55 Mihara M, Hashizume M, Yoshida H, Suzuki M, Shiina M: IL-6/IL-6 receptor system and its role in physiological and pathological conditions. Clin Sci (Lond) 2012;122:143-159.
56 Singh JK, Simoes BM, Howell SJ, Farnie G, Clarke RB: Recent advances reveal IL-8 signaling as a potential key to targeting breast cancer stem cells. Breast Cancer Res 2013;15:210.
57 Tartour E, Pere H, Maillere B, Terme M, Merillon N, Taieb J, Sandoval F, Quintin-Colonna F, Lacerda K, Karadimou A, Badoual C, Tedgui A, Fridman WH, Oudard S: Angiogenesis and immunity: a bidirectional link potentially relevant for the monitoring of antiangiogenic therapy and the development of novel therapeutic combination with immunotherapy. Cancer Metastasis Rev 2011;30:83-95.
58 Provatopoulou X, Georgiadou D, Sergentanis TN, Kalogera E, Spyridakis J, Gounaris A, Zografos GN: Interleukins as markers of inflammation in malignant and benign thyroid disease. Inflamm Res 2014;63:667-674.
59 Zarogoulidis P, Lampaki S, Yarmus L, Kioumis I, Pitsiou G, Katsikogiannis N, Hohenforst-Schmidt W, Li Q, Huang H, Sakkas A, Organtzis J, Sakkas L, Mpoukovinas I, Tsakiridis K, Lazaridis G, Syrigos K, Zarogoulidis K: Interleukin-7 and interleukin-15 for cancer. J Cancer 2014;5:765-773.
60 Jiang Q, Li WQ, Aiello FB, Mazzucchelli R, Asefa B, Khaled AR, Durum SK: Cell biology of IL-7, a key lymphotrophin. Cytokine Growth Factor Rev 2005;16:513-533.

61 Kirnbauer R, Charvat B, Schauer E, Kock A, Urbanski A, Forster E, Neuner P, Assmann I, Luger TA, Schwarz T: Modulation of intercellular adhesion molecule-1 expression on human melanocytes and melanoma cells: evidence for a regulatory role of IL-6, IL-7, TNF beta, and UVB light. J Invest Dermatol 1992;98:320-326.
62 Yamanaka O, Saika S, Ikeda K, Miyazaki K, Ohnishi Y, Ooshima A: Interleukin-7 modulates extracellular matrix production and TGF-beta signaling in cultured human subconjunctival fibroblasts. Curr Eye Res 2006;31:491-499.
63 Hynes RO: Integrins: bidirectional, allosteric signaling machines. Cell 2002;110:673-687.
64 Kubow KE, Horwitz AR: Reducing background fluorescence reveals adhesions in 3D matrices. Nat Cell Biol 2011;13:3-5.
65 Yin HL, Wu CC, Lin CH, Chai CY, Hou MF, Chang SJ, Tsai HP, Hung WC, Pan MR, Luo CW: beta1 Integrin as a Prognostic and Predictive Marker in Triple-Negative Breast Cancer. Int J Mol Sci 2016;17: 1432.
66 Liang W, Zhu C, Liu F, Cui W, Wang Q, Chen Z, Zhou Q, Xu S, Zhai C, Fan W: Integrin beta1 Gene Therapy Enhances *in Vitro* Creation of Tissue-Engineered Cartilage Under Periodic Mechanical Stress. Cell Physiol Biochem 2015;37:1301-1314.
67 Aleshcheva G, Wehland M, Sahana J, Bauer J, Corydon TJ, Hemmersbach R, Frett T, Egli M, Infanger M, Grosse J, Grimm D: Moderate alterations of the cytoskeleton in human chondrocytes after short-term microgravity produced by parabolic flight maneuvers could be prevented by up-regulation of BMP-2 and SOX-9. FASEB J 2015;29:2303-2314.
68 Savino W, Mendes-da-Cruz DA, Golbert DC, Riederer I, Cotta-de-Almeida V: Laminin-Mediated Interactions in Thymocyte Migration and Development. Front Immunol 2015;6:579.
69 Bauer J, Kopp S, Schlagberger EM, Grosse J, Sahana J, Riwaldt S, Wehland M, Luetzenberg R, Infanger M, Grimm D: Proteome Analysis of Human Follicular Thyroid Cancer Cells Exposed to the Random Positioning Machine. Int J Mol Sci 2017;18: 546.
70 Kim TO, Park SH, Kim HS, Ahuja N, Yi JM: DNA methylation changes in extracellular remodeling pathway genes during the transformation of human mesenchymal stem cells. Genes Genomics 2016;38:611-619.
71 Vignoud L, Albiges-Rizo C, Frachet P, Block MR: NPXY motifs control the recruitment of the alpha5beta1 integrin in focal adhesions independently of the association of talin with the beta1 chain. J Cell Sci 1997;110:1421-1430.
72 Grimm D, Bauer J, Schoenberger J: Blockade of neoangiogenesis, a new and promising technique to control the growth of malignant tumors and their metastases. Curr Vasc Pharmacol 2009;7:347-357.
73 Hu K, Olsen BR: Vascular endothelial growth factor control mechanisms in skeletal growth and repair. Dev Dyn 2017;246:227-234.
74 Pożarowska D, Pożarowski P: The era of anti-vascular endothelial growth factor (VEGF) drugs in ophthalmology, VEGF and anti-VEGF therapy. Cent Eur J Immunol 2016;41:311-316.
75 Wehland M, Bauer J, Magnusson NE, Infanger M, Grimm D: Biomarkers for anti-angiogenic therapy in cancer. Int J Mol Sci 2013;14:9338-9364.
76 Jackson HW, Defamie V, Waterhouse P, Khokha R: TIMPs: versatile extracellular regulators in cancer. Nat Rev Cancer 2017;17:38-53.
77 Verma RP, Hansch C: Matrix metalloproteinases (MMPs): Chemical–biological functions and (Q)SARs. Bioorg Med Chem 2007;15:2223-2268.
78 Jurczak P, Groves P, Szymanska A, Rodziewicz-Motowidlo S: Human cystatin C monomer, dimer, oligomer, and amyloid structures are related to health and disease. FEBS Lett 2016;590:4192-4201.
79 Deshmane SL, Kremlev S, Amini S, Sawaya BE: Monocyte Chemoattractant Protein-1 (MCP-1): An Overview. J Interferon Cytokine Res 2009;29:313-326.
80 Gerard C, Rollins BJ: Chemokines and disease. Nat Immunol 2001;2:108-115.
81 Rudemiller NP, Crowley SD: The role of chemokines in hypertension and consequent target organ damage. Pharmacol Res 2017;119:404-411.
82 Yoshimura T: The production of monocyte chemoattractant protein-1 (MCP-1)/CCL2 in tumor microenvironments. Cytokine DOI:10.1016/j.cyto.2017.02.001.
83 Vakilian A, Khorramdelazad H, Heidari P, Sheikh Rezaei Z, Hassanshahi G: CCL2/CCR2 signaling pathway in glioblastoma multiforme. Neurochem Int 2017;103:1-7.

15.5 Liste weiterer Publikationen

Folgende weitere Publikationen sind während der Doktorarbeit entstanden:

5) Wehland M, **Warnke E**, Frett T, Hemmersbach R, Hauslage J, Ma X, Alehcheva G, Pietsch J, Bauer J, Grimm D: The impact of microgravity and vibration on gene and protein expression of thyroid cells. Microgravity Sci. Technol. 28. 261-274 (2016)

6) Riwaldt S, Bauer J, Wehland M, Slumstrup L, Kopp S, **Warnke E**, Dittrich A, Magnusson NE, Pietsch J, Corydon TJ, Infanger M, Grimm D: Pathways Regulating Spheroid Formation of Human Follicular Thyroid Cancer Cells under Simulated Microgravity Conditions: A Genetic Approach. Int. J. Mol. Sci. 17. 528 (2016)

7) Kopp S, **Warnke E**, Wehland M, Aleshcheva G, Magnusson NE, Hemmersbach R, Juhl Corydon T, Bauer J, Infanger M, Grimm D: Mechanisms of three-dimensional growth of thyroid cells during long-term simulated microgravity. Sci Rep. 5. 16691 (2015)

8) Wehland M, Aleshcheva G, Schulz H, Saar K, Hübner N, Hemmersbach R, Braun M, Ma X, Frett T, **Warnke E**, Riwaldt S, Pietsch J, Corydon TJ, Infanger M, Grimm D: Differential gene expression of human chondrocytes cultured under short-term altered gravity conditions during parabolic flight maneuvers. Cell Commun Signal. 13. 18 (2015)